TEXTILE RESEARCH JOURNAL

Publication of

TEXTILE RESEARCH INSTITUTE

VOLUME 31 FEBRUARY 1961 NUMBER 2

One of a series

FORMALDEHYDE, METHACRYLAMIDE AND OXTAIL SOUP made their appearance in the Applications Lab each noon. The first two were used in filling free space in Lincoln fibers, the last in filling space elsewhere. Steaks were out of the question — Petty Cash was pinched, and no one had heard of upgrading thrifty meat cuts with Tona® enzyme-balanced meat tenderizers.

By which devious path we come to our advertising message: Did you know that Wallerstein has as good a name in meats as in textiles? Wallerstein enzymes are used to tenderize meats in packing houses, restaurants and homes — Wallerstein antioxidants to guard the flavor and color of franks, hams and luncheon meats.

This has more than noon-hour significance for you! Constant searching for enzymes to be used in many fields — meat, beer, pharmaceuticals, to name a few besides textiles — fills our shelves with scores of commercial, development and experimental enzymes of all descriptions. Purity ranges from AR grade on down. The probability is good that some of these enzymes could be put to use by enterprising textile researchers. Perhaps you? If you were to tell us about your requirements, we might be able to pick you out a few interesting numbers. And, remember, please, we make Rapidase® and Serizyme®, too!

WALLERSTEIN COMPANY
Division of Baxter Laboratories, Inc.
Staten Island 3, N.Y.

If you haven't investigated Cellase™, a new high potency cellulase, write Dept. R-2 for a free sample.

TEXTILE RESEARCH JOURNAL

Volume 31 *February 1961* Number 2

IN THIS ISSUE

Mechanical Properties of Textile Fabrics.

Part I: Shearing. *Bengt Behre* 87

Part II: Buckling. *Bengt Dahlberg* 94

Part III: Shearing and Buckling of Various Commercial Fabrics. *Joel Lindberg, Bengt Behre, and Bengt Dahlberg* 99

Response of Cottons to Chemical Treatments. Part I: Fiber Mercerization and Urea Treatments. *L. Rebenfeld* 123

Physical Properties of Wool Fibers at Various Regains. *A. R. Haly and M. Feughelman*

Part I: Stresses Developed at Constant Strain Due to Regain Change by Absorption or Desorption 131

Part II: Recovery from Extension 135

Studies in Adsorption. Part XIV: The Mechanism of Adsorption of Disperse Dyes by Cellulose Acetates and other Hydrophobic Fibers. *Charles H. Giles* 141

The Geometry and Properties of Two-Bar Tricot Fabrics of Acetate, Viscose, and Cotton. *Hazel M. Fletcher and S. Helen Roberts* 151

Some Theoretical Considerations of Cellulose Cross-Linking. *John L. Gardon and Richard Steele* 160

On Changes in the Weight Distribution Function of Artificial Fibers Due to Random Fiber Breakage. *W. J. Byatt* .. 171

LETTERS TO THE EDITOR

Cotton Fiber Weight Distribution (Four Letters)

Tel. Chytiris 175

Edward W. S. Calkins 176

R. L. N. Iyengar 177

Louis A. Fiori, Jack E. Sands, Gain L. Louis, John D. Tallant 178

Acid Hydrolysis of Dimethylol Urea Polymerized in Cotton. *K. C. Eapen, J. R. Modi, and P. C. Mehta* 181

Cuprammonium Insolubility as a Test for Covalent Cross-Linking of Cellulose. *R. D. Mehta and P. C. Mehta* 182

REPRINT REQUESTS SHOULD BE DIRECTED TO THE AUTHORS

SEE ARTICLES FOR ADDRESSES

Editor:
Richard K. Toner

Production Editor:
Dorothy Dana Hollmann

Advisory Board

Herbert J. Ball
Earl E. Berkley
John Boulton
C. H. Fisher
Walter J. Hamburger
Milton Harris
R. M. Hoffman
Harold P. Lundgren
Herman Mark
Edward R. Schwarz
George Switlyk
Helmut Zahn

TEXTILE RESEARCH JOURNAL, published monthly at Prince and Lemon Streets, Lancaster, Pa., is devoted to the interest of research in textile and allied industries. It is published by Textile Research Institute.

Manuscripts and communications should be sent to the Publications Department, P.O. Box 625, Princeton, N. J.

Second-class postage paid at Lancaster, Pa.

Subscription rates: $25.00 per year; additional for postage, 50 cents to Canada, $1.00 to all other countries. Single copies, $2.50 each.

Contents copyright © 1961 by Textile Research Institute. Advertising rates supplied on request.

ABRASION

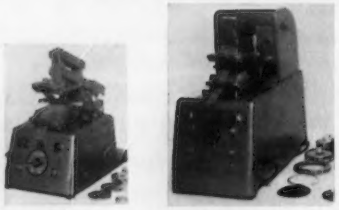

Flex Tester | **CSI Stoll QM Univ. Wear Tester** | **Surface Abrader**

Both the Flex Tester and the Surface Abrader have incorporated a single feature of the Univ. Wear Tester into smaller units at a reduced price. These units retain the sample size, abrasion head dimensions and automatic elect. end points of the Univ. Wear Tester.

References: ASTM D1175, D1375 & D1379
Fed. Spec. CCC-191b Method 5300 & 5302

Brochure and prices upon request.

CUSTOM SCIENTIFIC INSTRUMENTS, INC.
541 Devon St. Kearny, N. J.

FEBRUARY 1961
VOL. 31 NO. 2

TEXTILE RESEARCH JOURNAL

Mechanical Properties of Textile Fabrics

Part I: Shearing

Bengt Behre

Swedish Institute for Textile Research, Gothenburg, Sweden

Abstract

In this part, two alternative methods for measuring shear properties of fabrics are described. One method is recording and consists of an attachment to the Instron Tensile Tester. Complete load–deformation curves are obtained. The stress distribution in a fabric sample subjected to shear is analyzed and the results used to construct a non-recording shear tester for routine testing.

Introduction

A piece of fabric may be regarded as a thin plate having certain specific dimensions. A thin plate can be deformed only in a limited number of ways which are independent of each other, and only four are of interest in connection with textile fabrics (Figure 1). They are compression and bending perpendicular to the plane of the plate, extension–compression in the directions of the threads, and shearing in the plane of the plate.

Part I deals exclusively with shear, although there is some evidence that shear is related to extension–compression in the bias direction of a woven fabric [3].

A device for measurement of shear, the Planoflex, is described by Dreby [1], who measured the angle between the two opposite shear limits where the sample wrinkles. The same limits have been used with a device by Mörner and Eeg-Olofsson [4], the measurement being made by means of an attachment to the Instron Tensile Tester. A force–deformation diagram between the two limits can be obtained. Similar diagrams have also been obtained with a device by Go et al. [2] in which the sample is mounted between two parallel bars of a frame. Common to all devices is that a tensile force is applied to the samples in one direction. In the following description that tensile force is called the preload.

The stress distribution in a sample sheared in Mörner's device was studied and, as a result of this investigation, two different apparatuses were constructed. One of them is a modification of Mörner's apparatus, particular attention being given to variability of preloading, accuracy, need of care, speed, and independence of shear deformation of preloading. The second one is a non-recording shear tester for routine testing in industry.

Stress Distribution in a Sheared Sample

A sample subjected to shear can be regarded as a cantilever (Figure 1) where the height is much larger than the width. The stress distribution in any section of the cantilever of Figure 2 can be studied. The force T acts perpendicularly to the cantilever at the free end. The weight of the cantilever is assumed to be small and is disregarded.

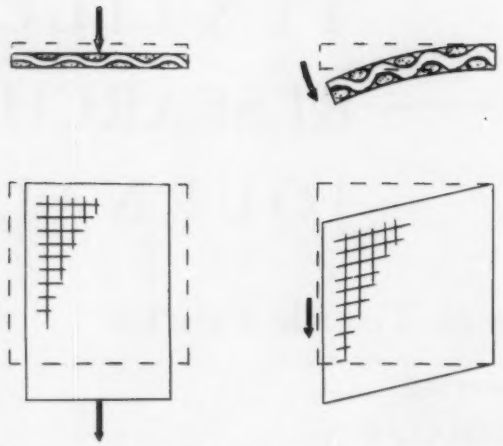

Fig. 1. Length and angle deformation in, and perpendicular to, the plane of a plate.

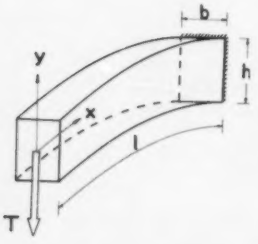

Fig. 2. Bending of a cantilever, showing symbols used.

In such a cantilever the shear stresses are parabolically distributed,

$$\tau_{xy} = \frac{3}{2} \cdot \frac{T}{bh} \cdot \left(1 - \frac{4y^2}{h^2}\right) \qquad (1)$$

and the tensile stresses are linearly distributed

$$\sigma_{xx} = \frac{12T}{bh^3} \cdot xy \qquad (2)$$

A tensile force P (preload) superimposed in the x-direction gives a total tensile stress

$$\sigma_x = \frac{1}{bh} \cdot \left(\frac{12}{h^2} \cdot T \cdot xy + P\right) \qquad (3)$$

This equation was applied to some measurements in Mörner's apparatus. The difference between the forces at the two end-values where wrinkles appeared was obtained from the Instron diagrams. Because of the construction of the apparatus [4], the difference between these forces was $1.67\ T \cos \gamma$, where γ is the mean angle of the two end-values of the deformation, while the preload in the x-direction was $P \cos \gamma$. In the investigation, nine samples were tested with alternately the warp and the weft preloaded. All tests were made at three levels of $P \cos \gamma$. Thirty-six values of $1.67\ T \cos \gamma$ have been arranged in groups for each level and plotted against $P \cos \gamma$ in Figure 3. A wide scatter is obtained because it is difficult to observe when wrinkles appear in the sample.

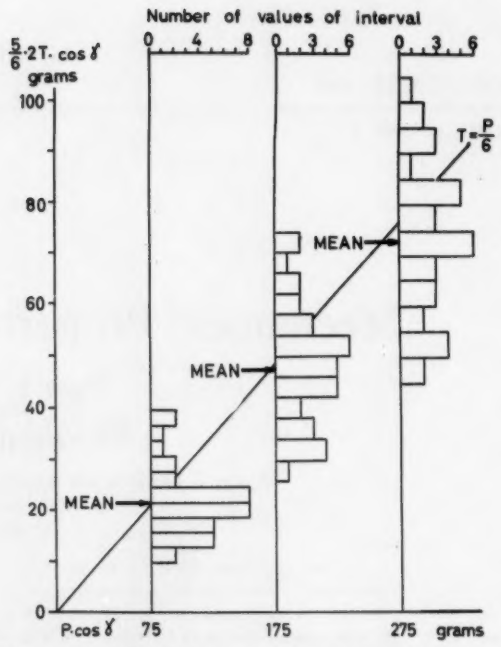

Fig. 3. Relation between preload and shear force when wrinkles are formed in a limp fabric.

The fabric tested was a limp filament rayon fabric. The dimensions of the specimen were 10 cm. square. This fabric can take up only very small compressional stresses which occur just as the sign of the smallest value of σ_x is changed. $x = l = h$ and $y = -h/2$ give the smallest value of xy in Equation 3. Thus $\sigma_x = 0$ when the value of T is

$$T_0 = \frac{P}{6} \qquad (4)$$

The straight line in Figure 3 corresponds to this theoretical result. Because of the close agreement between this line and the means of measured values, the given equations were considered to hold for fabrics subjected to shear measurements.

Apparatus and Results

Recording Shear Tester

The device in Figure 4 was built as an attachment to the Instron Tensile Tester. The linear motion of

the cross-head 1 is converted to rotation by means of a heavy weight 2 and a 1-mm. diameter steel wire 3, fixed by the screw 38 to a grooved wheel 4. The diameter of the wheel at the bottom of the groove is $90/\pi$ cm., so that 0.25 cm. of cross-head motion corresponds to 1° of rotation. Two small screws 40 fix the wheel to a bar 6, which is connected with the two vertical bars, 7 and 30, by means of the bearings 36 and 42. A fourth bar 15, connected with the vertical ones by means of the bearings 16 and 31, completes a movable frame. The lower and upper bars, 6 and 15, of this frame are mounted on the bolts 43 and 46 of a cross-frame, 25 and 35, by means of bearings 39 and 24. The cross-frame is attached to the main support columns of the Instron machine. (If wide column separation is not available, the lengths of 6 and 15 have to be reduced.) Lowering of the cross-head gives a clockwise motion of the movable frame. The opposite motion may require a small weight 37 on the bar 30 to avoid buckling of the wire 3.

A separate device is used to keep the clamps 12 and 18 parallel and 10 cm. apart while the sample 10 is being mounted. The upper and lower edges of the sample are parallel to the threads in the fabric, but the clamps are always placed perpendicular to these edges, independent of fabric skewness. Each clamp consists of jaws, articulating at the bottom and clasped at the top by a pin. One of the jaws has a smooth edge, while the other is fitted with a strip of leathering. The bars 6 and 15 are kept horizontal while the right-hand clamp is mounted in the two apertures, 8 and 13, of the bar 7. The clamp is fastened by means of the clasps 9 and 11. The left clamp is hung on the double hook 19, connected with the Instron cell by means of a thin wire 20 and a flexible but inextensible chain 21. An adjustment nut 22 with corresponding screw fits in the Instron coupling by means of a pin 23.

Two wire hooks 27 can move in apertures in the left jaw, so that they act symmetrically on two center points of the left clamp. By means of conically shaped heads to the right of those hooks, the force acts at the same points during the tests. The wire hooks 26, which are placed in the eyes 28 when not in use, are attached to 27. Their other

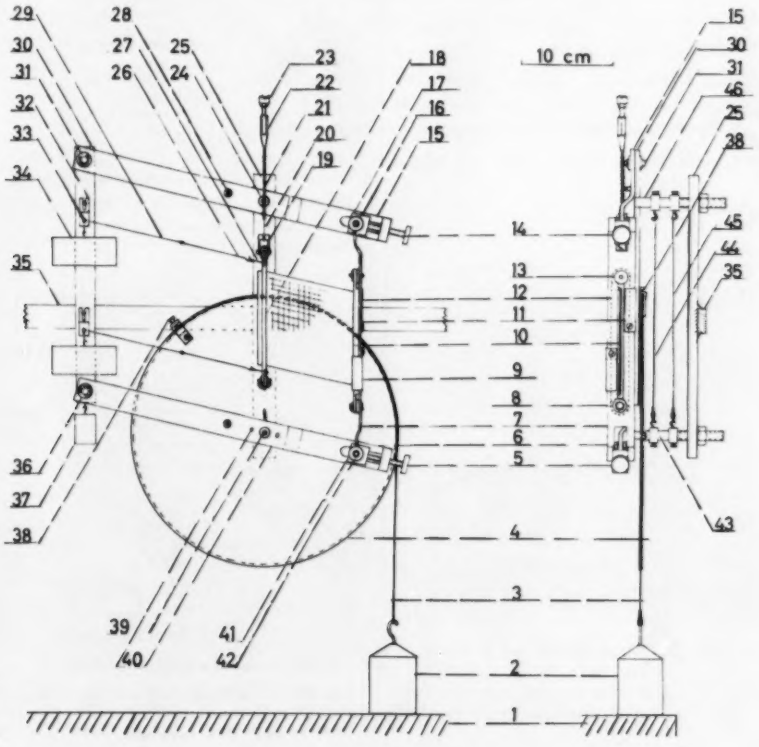

Fig. 4. Recording shear apparatus.

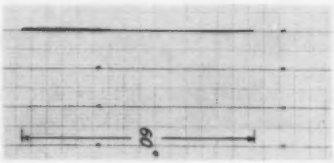

Fig. 5. Accuracy test with a 3-ply cotton thread of 20 m./g. mounted in place of cloth sample.

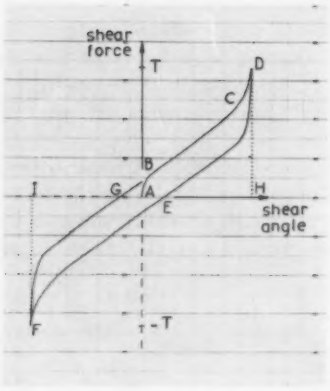

Fig. 6. Example of shear curve.

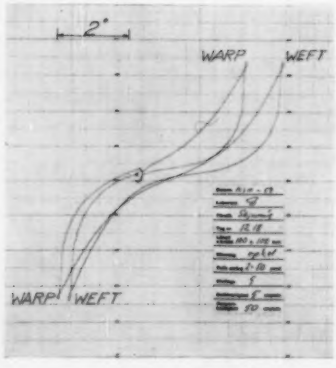

Fig. 7. Shear curves for a nylon/rayon/Dacron* blend (320 g./m.²), preloaded in warp and weft direction. (* DuPont polyester fiber)

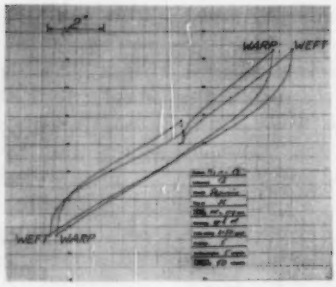

Fig. 8. Shear curves for a worsted (341 g./m.²), preloaded in warp and weft direction.

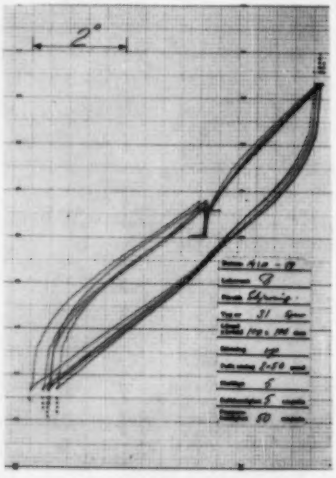

Fig. 9. Reproducibility test. Shear curves for five samples from a worsted fabric (350 g./m.²).

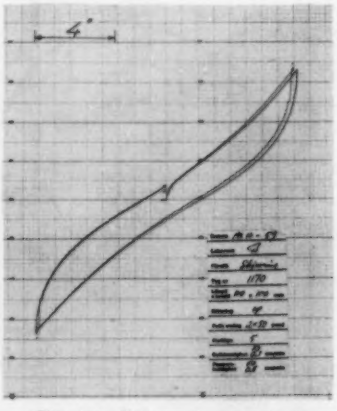

Fig. 10. Effect of rate of deformation. Worsted fabric (329 g./m.²) at 0.4°/min. and 40°/min.

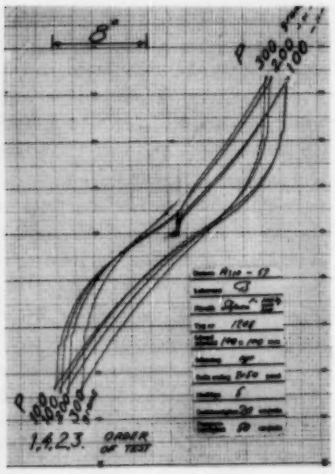

Fig. 11. Variation of the preload P at constant h = 10 cm. and $T_r = \pm$ 33.3 g. Worsted fabric (206 g./m.²).

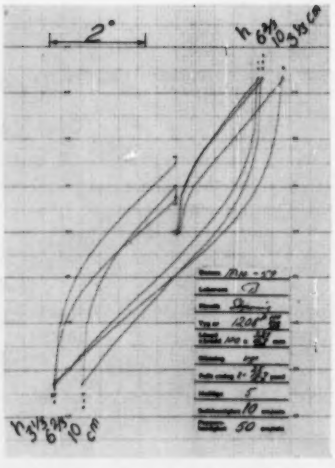

Fig. 12. Variation of the sample width h at constant P/h = 30 g./cm. and $T_r/h = \pm$ 1.67 g./cm. Worsted fabric (206 g./m.²).

ends are connected with the weights 34 by means of textile thread 29. In the gaps 32 in the bar 30 there are pins with needle bearings at each end, and the pins are grooved to a small diameter where the threads 29 pass over them. This arrangement gives an evenly distributed tensile force (the preload) on the specimen.

The wire 20 and the middle bottom point of clamp 18 are put in line with the wires 44 and 45 by means of the screws 5 and 14. The entire guide blocks 17 and 41 move when those screws are used.

Systematic Errors of the Device

By means of the adjustment nut 22 the systematic errors can be made very small. If a textile thread is mounted between the middle points of the two clamps, the test curve in Figure 5 is recorded. The angle deflection between the end points is 60° and the full-scale load is 100 g.

Shear Force–Angle Diagrams

The preload for standard measurements is $P = 200$ g. The maximum shear force used is $T_0 = \pm 33$ g., according to Equation 4. A chart speed of 50 cm./min. is used in all tests, and the cross-head speed is chosen to give diagrams of a suitable size. The angle motion is 4°/cm. of cross-head motion.

A typical shear curve is shown in Figure 6. Here the force and the deformation are zero at A. The force is increasing to the limit of T_0 at the point D with a constant rate of deformation. The motions of cross-head and chart are then automatically reversed and the force decreases to $-T_0$ at the point F, passing zero at E. After the second reversal the force again passes zero at the point G. The shear angle γ through which the sample has been deformed by the application of the force $-T_0$ after T_0 is measured from the diagram. It is proportional to the distance I-H. The deformation energy A_s is also measured from the diagram. Although not quite correct, it has been represented by the area G-D-H-E-F-I-G. Finally, the recovered energy C_s in one cycle is measured by the sum of the areas I-G-F-I and D-H-E-D.

The preload P can be applied to the sample in the warp or the weft direction of the fabric, and the result can to some extent be influenced by this choice (Figures 7 and 8).

The reproducibility of the measurements is very good, as can be seen from Figure 9. The curves are for five different samples taken from the same fabric.

The rate of deformation seems to have very little effect on the results. The ratio between the rates of deformation in Figure 10 is 1:100.

The influence of the preload P is normally not very great. In Figure 11 the preload was changed while the points of reversal were kept at constant shear force, i.e., independent of T_0.

The mean tensile stress P/h and the mean shear stress T_r/h at the points of reversal were both kept constant in Figure 12. This test shows that the influence of specimen width is also not very great.

Non-Recording Shear Tester

Equation 4 shows that $T_0 = P/6$ where T_0 is the shear force when the smallest tensile stress in the sample is $\sigma_x = 0$, and P is the preload on the sample. Figure 13 shows how this theoretical relation can be utilized to construct a simple non-recording shear tester[1]. The sample is clamped along two edges so that an evenly-distributed load Q is acting vertically at the lower edge A by gravity; the upper edge B is supported at a point C. The distance between this point C and the middle of the edge B is equal to one-sixth of the length of the edge. The system is in equilibrium when the center of the lower edge A is vertically below the point C. The load Q is then resolved into the pre-

[1] Patent pending.

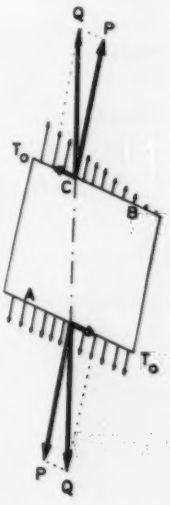

Fig. 13. Forces on the sample in the non-recording shear tester.

load P and the shear force T_0 at each edge. The small arrows indicate the distribution of the force P at the two edges.

The shear tester (Figure 14) consists of a frame 2 incorporating two uprights 3, the top ends being in the form of edges 23 which are set exactly horizontal by means of the water levels 1. Secured to the frame is a transverse arm 14 which carries a vertically-mounted micrometer 6 at each end. The micrometer screws are provided with horizontal reading arms 18 including white sighting wires 20 and guided by the columns 19. A balance beam in the form of a clamp 10 is placed upon the metal edges 23 by means of a pair of pins 12. This pair and another pair of pins 11 are mounted equidistant from the geometrical center of the clamp. According to Equation 4 the distance between the axes of the two pair of pins 11 and 12 should be 3.33 cm.; the distance chosen was 3.00 cm. In this way there will be tension in all parts of the sample, the size of which is 10 cm. square. The weight of the plug 22 makes the center of gravity of the total beam coincide with the axis of the pins 12. The nail 13 of the plug is fitted to the clamp when that condition is fulfilled. Suspended from the sample 7 is a weight 16 which is in the form of a clamp similar to the beam 10.

The sample is cut as a rectangle 10.0 × 11 cm., one system of threads being parallel to the longer edges. The two clamps are fitted to a locating block by means of conical pins inserted through the holes 5 and 15. The sample is placed on one leg of each of the clamps which are then closed by means of the pins 4 and 9. The left counterbalance 22 is fitted to the left side of the clamp 10 and the clamped sample is moved from the locating block to its position in the apparatus. When the right reading arm 18 is above a certain level, the bottom of the clamp 10 is resting on a plate 17. This plate is lowered simultaneously with the arm 18 by means of the micrometer 6. Just after the contact between the plate 17 and clamp 10 is broken, the right sighting wire 20 will be seen on a level with two black sighting points 8 at the right part of beam 10. These sighting points are made in the front and the back sides of the tubes where the plugs 22 are intended to be attached to the ends of the beam 10. The sighting wire and points can be best seen simul-

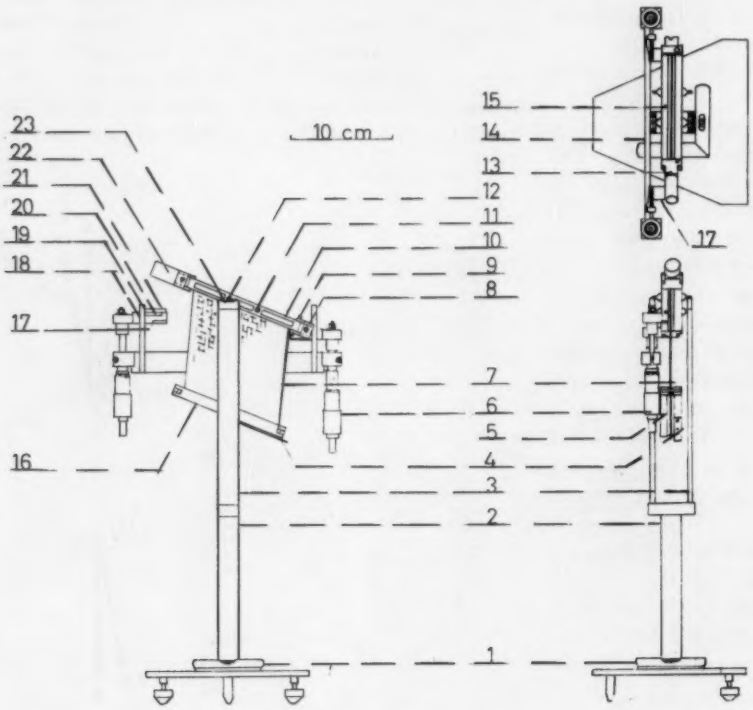

Fig. 14. Non-recording shear tester.

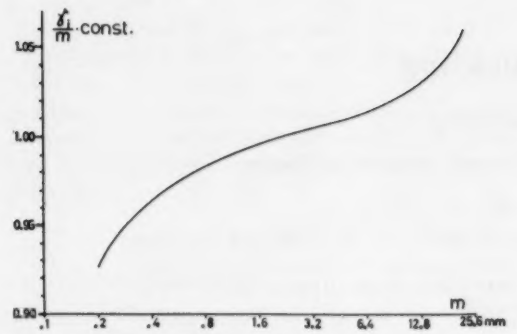

Fig. 15. Deviation from proportionality between the value of m read off and the shear angle.

taneously when a red paper 21 is used as a background. The displacement m of the micrometer screw from the zero position is now determined.

From the geometry of the device the following equations can be derived.

$$m + n = t \sin \alpha$$
$$l \sin (\alpha - \gamma_{right}) = u \cos \alpha$$

where m = the displacement of the micrometer screw from the zero position, n = the vertical distance between the axis of the pins 12 and the initial position of the sighting wire 20 at zero positions of corresponding micrometer 6, α = the dip of the beam 10, l = the width of the square-shaped sample in the clamps, t = the distance between the axis of the pins 12 and the right sighting points 8, and u = half the distance between the axes of the pins 11 and the pins 12.

The deviation from proportionality between the shear angle γ_{right} in degrees and the measured value m in millimeters is given in Figure 15.

Before measurement of the complementary shear angle γ_{left}, the beam 10 is moved so that the pins 11 will rest upon the edges 23. The plug 22 is removed and a similar plug is inserted in the right end of the beam 10. The left arm 18 is then lowered and the operation continued as before. The sum γ of γ_{right} and γ_{left} is called the shear angle of the fabric tested with this device. Both the preload and balancing point can be changed to give shear angles for different values of P and T_0 according to what is required.

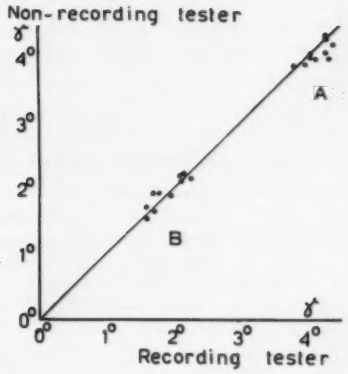

Fig. 16. Shear angles of ten samples from each of (A) a cotton shirt poplin (126 g./m.²) and (B) a Sanforized cotton fabric (169 g./m.²).

The reproducibility of the non-recording device is tested by comparison with the recording device. In our experience, it is difficult to get reproducible results on cotton fabrics. Therefore we have measured the shear angle of ten samples from each of two different types of cotton fabric. The samples were first tested in the recording device and then in the non-recording device. Before each reading, the sheared samples were allowed to creep for half a minute. As seen in Figure 16, for each fabric the scatter of values around the symmetry axis is less than that in the coordinate directions. Thus the values of the non-recording device correspond well with those of the recording device: the variation caused by handling the samples between measurements and by reading error is less than that due to unevenness in the piece.

Literature Cited

1. Dreby, E. C., *Am. Dyestuff Reptr.* **30**, 651 (1941).
2. Go, Y., Shinohara, A., and Matsuhashi, F., *J. Soc. Text. Cell. Ind. Japan* **12**, 563–568 (1956).
3. Lindberg, J., Waesterberg, L., and Svenson, R., *J. Textile Inst.*, **51**, T1475–T1492 (1960).
4. Mörner, B. and Eeg-Olofsson, T., TEXTILE RESEARCH JOURNAL **27**, 611–615 (1957).

Manuscript received June 7, 1960.

Part II: Buckling

Bengt Dahlberg

Swedish Institute for Textile Research, Gothenburg, Sweden

Abstract

In this part, a method for measuring plate and shell buckling of fabrics is described. The same instrument can also be used to measure extension–compression in the plane of the fabric. The instrument consists of an attachment to the Instron Tensile Tester, and complete load–deformation curves are obtained.

Introduction

In the introduction to Part I a fabric was regarded as a thin plate. It was shown that such a plate could be deformed only in four main ways: compression and bending perpendicular to the plane of the plate and extension–compression and shearing in the plane of the plate. In this part we will deal with extension–compression in the plane of the plate and pay particular attention to the compression part of the deformation.

It is a well-known fact that if the compression load exceeds a certain value, the plate will buckle (Figure 1) [1, 2]. The load at which this happens is called the buckling load. Before buckling occurs, however, the plate or the fabric is compressed a certain distance. The total compression at the buckling load is called buckling compression and is shown to be of special importance in determining the formability of a fabric [3]. Very often a textile fabric is not in the form of a plane plate when it is subjected to compressive forces. For instance, when a sleeve is buckled, the fabric already has a curvature perpendicular to the direction of the compressive force. The same phenomenon will occur in most complex deformations. One good example is testing handle by squeezing the fabric in the hand.

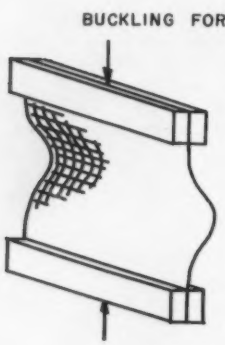

Fig. 1. Principle of plate buckling.

Buckling of cylinders, spheres, etc. is usually called shell buckling.

A method for measuring plate buckling has been described [1, 2] in the literature and results given for a number of filament rayon fabrics. In this paper an apparatus is described which can be used for both plate buckling and shell buckling and also for registering the compression of the fabric before buckling.

Apparatus

The apparatus is made as an attachment to the Instron Tensile Tester; the principal construction is shown in Figure 2. The clamps, 21 and 22, are exchangeable and could have any desired form. They are straight for plate buckling and corrugated for shell buckling. The corrugations can vary in form and radius of curvature. There are two clamps, one fixed and one movable, 5 and 6, and the rectangular sample 7 is mounted between them. The fixed clamp is screwed to the arm 9, which can be fitted to the cross-head of the Instron. In the upper end of the arm there is a point bearing, 12. The movable clamp is kept in position by two rods 3, which are fixed into the point-bearing. The movable system is loaded by the weight 1 and hangs on the wires 2 from the Instron load-cell. The clamps consist of two jaws, 21 and 22 (the corrugated ones are shown in Figure 2), the screw, 19, and the springs 14 which open the jaws when the screw is loosened. Figure 3 shows the apparatus mounted in the Instron. The clamps, 5 and 6, are pressed against each other when the cross-head

moves upward. The force between the clamps reduces the load on the load-cell. This force can be registered on the Instron recorder. Frictional losses due to the system itself can be reduced to small values. Figure 4 shows a curve of a load–deformation cycle without any sample mounted. The maximum force due to friction in the system is about 1 g.

Results

Load–Deformation Curve

The sample length normally used is 2.5 cm. and the width 10 cm. The total linear deformation is 1 cm., or 40%. The radius of curvature of the corrugated clamps is normally 0.8 cm. and the rate of cross-head motion 1 cm./min. Figure 5 shows some examples of the deformation pattern obtained with corrugated clamps. Different materials give different deformation patterns.

The load–deformation curves have approximately the same form, independent of the form of the clamps. The most characteristic feature is a much higher buckling load for shell buckling than for plate buckling, which could be expected from the theory of elasticity. In Part III we will discuss the different forms of buckling curves that are obtained for different fabrics.

Figure 6 shows a typical buckling curve which begins at A. From A to B the fabric is compressed in the plane, and at B buckling occurs. After passing through B, the curve for an ideal isotropic material should rise slowly up to the point C. At this point, which corresponds to 40% linear deformation, the motion of the cross-head is reversed and a recovery curve C-D is obtained.

In the discussions which follow in Part III, the buckling load at B is denoted by P_1 and the load at 20% linear deformation is denoted by P_2.

The area under the curve A-B-C-K-A represents the buckling energy A and the area under the curve D-C-K-D represents the recovered buckling energy C. The distance A-D represents the permanent linear deformation.

From point D a new buckling cycle up to E and back to F can be obtained. The buckling energy, B, for the second cycle is the area under the curve D-E-K-D. The difference between the buckling

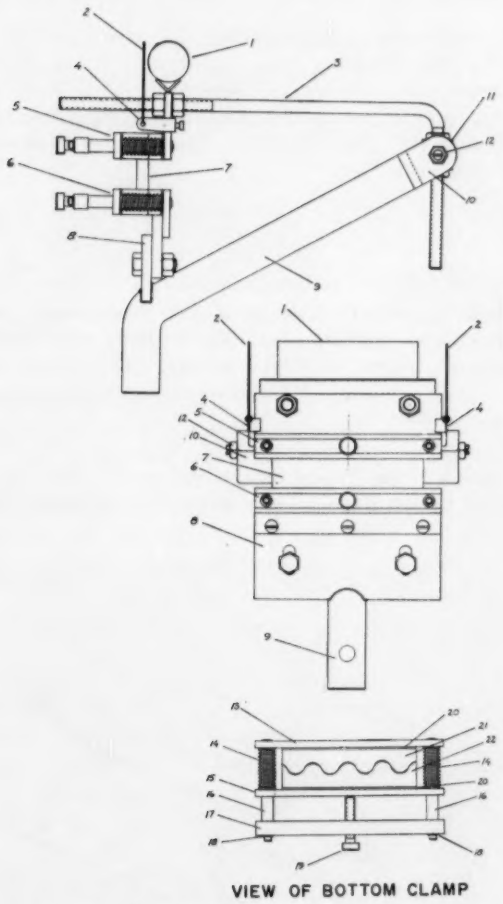

Fig. 2. Buckling apparatus.

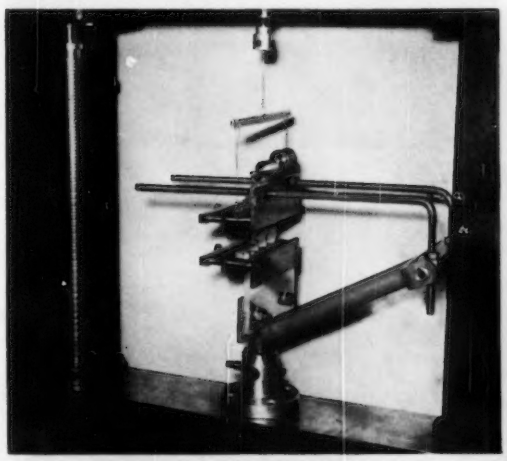

Fig. 3. Buckling apparatus.

energy in the first and second cycles ($A - B$) is the non-cyclical buckling energy loss. The sample can be cut in any fabric direction. Figures 7 and 8 show shell buckling curves for two fabrics cut in warp, weft, 45° and 135° directions. There is practically no difference in buckling load between the thread and the bias directions, but the compressibility is much higher in the latter.

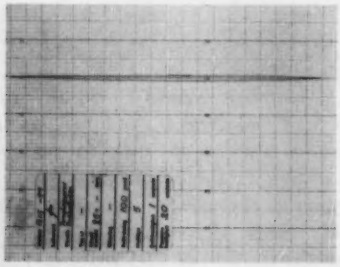

Fig. 4. Accuracy test of apparatus without sample. Full scale load is 100 g.

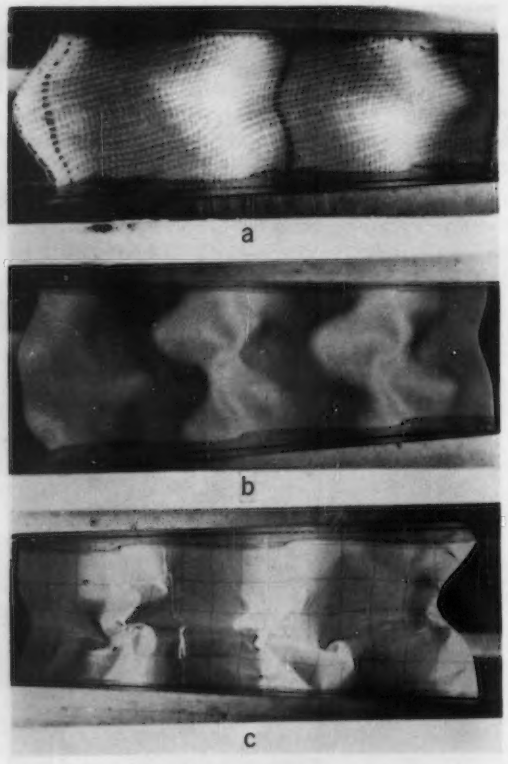

Fig. 5. Shell buckling patterns of (a) wool sateen, (b) cotton sheeting, and (c) notebook paper.

Reproducibility of Results

The reproducibility for shell buckling was tested by cutting five different samples from the same wool fabric. Figure 9 shows the buckling curves obtained. The variation is very small, probably due to true variations between the samples rather than errors in measurement.

Influence of Rate of Deformation

The influence of rate of linear deformation is rather small, as can be seen from Figure 10. The time for a complete cycle is 10 min. in the left curve and 24 sec. in the right one. The curves relate to shell buckling.

Influence of Sample Length and Corrugation Radius

In the case of plate buckling, it can be shown [1] that the buckling load varies with the sample length in approximate agreement with Euler's equation for buckling of bars rigidly supported at both ends. That is, the buckling load P_1 follows the equation

$$P_1 = \frac{4\pi^2 b}{l^2} \qquad (1)$$

where b is the bending stiffness and l the sample length. Experiments have also been made to study the relation between buckling load and sample length for shell buckling. The radius of the half-circles which make up the corrugations was also altered.

Figure 11 shows the results. The values for the buckling load P_1 and for the load at 20% deformation P_2 are given. Three values for the radius of

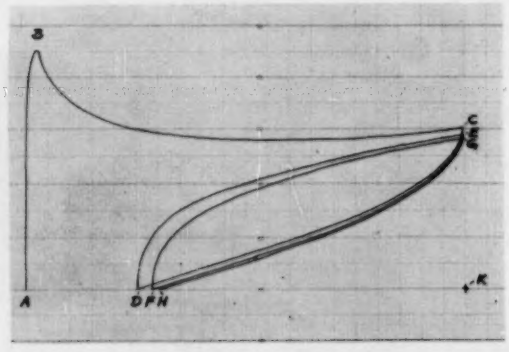

Fig. 6. Example of shell buckling curve.

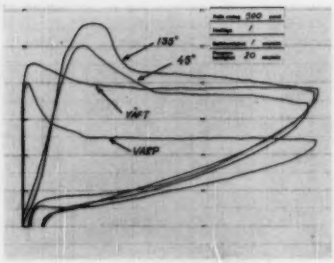

Fig. 7. Diagrams of shell buckling in different fabric directions. Nylon/rayon/Dacron blend (320 g./m.²); full scale load, 200 g.

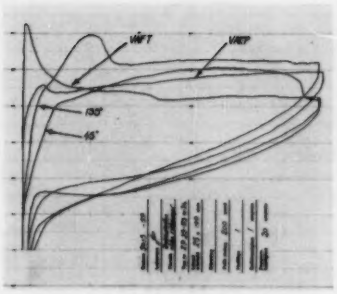

Fig. 8. Diagrams of shell buckling in different fabric directions. Wool fabric (341 g./m.²); full scale load, 200 g.

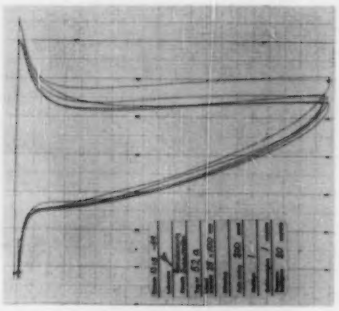

Fig. 9. Reproducibility test. Diagrams of five samples from a worsted fabric (350 g./m.²); full scale load, 200 g.

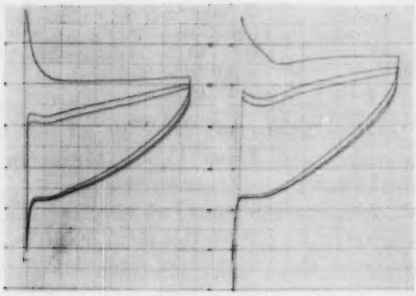

Fig. 10. Effect of rate of deformation. Worsted fabric (329 g./m.²); 0.8% and 20%/min.; full scale load, 200 g.

curvature were chosen; 0.25, 0.5, and 0.8 cm. Only the values for 0.25 and 0.8 are shown in Figure 11. These values are compared with the results obtained with plane clamps. The fabric used for Figure 11 was a plain weave cotton fabric, weight 206 g./m.² It was observed that different sample lengths gave different forms of buckling curve. To the right of the line A-A, at approximately 0.5 cm. sample length, the curves have a pronounced maximum at the buckling point (Type 1). To the left of line A-A there is no buckling point at all (Type 3). At the line A-A, curves of Type 2 are obtained. The type of curve can be characterized by the ratio P_2/P_1. The ratio gradually decreases with decreasing sample length. This gradual change in type of buckling curve is probably due to a change in deformation conditions. In shell buckling, both bending and compression occur in different directions. When the sample length is decreased, it can be assumed that the compression

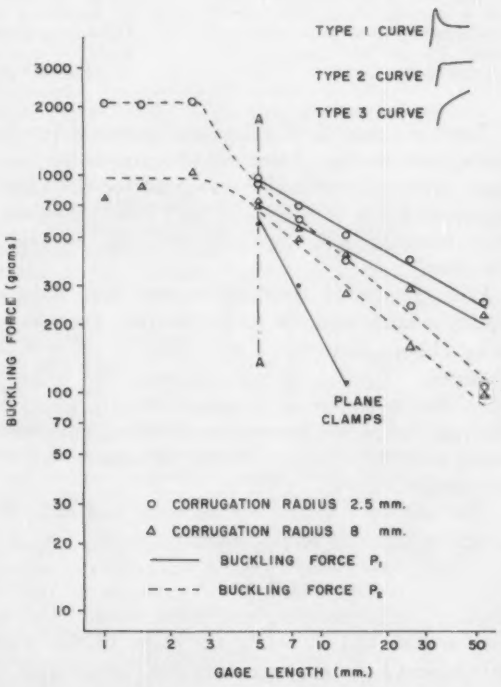

Fig. 11. Effect of sample length on buckling load.

will predominate more and more over bending until a point is reached where there is only compression and no bending; this will occur around the line A-A. A further decrease in sample length will obviously have no effect on the deformation load, which then becomes constant for a constant relative compression.

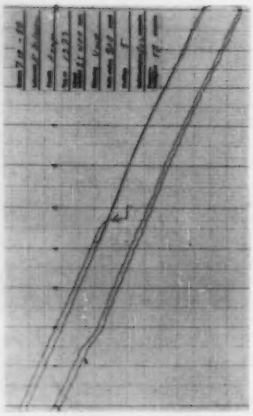

Fig. 12. Extension–compression of a cotton fabric (146 g./m.²). Deformation 0.18% at full scale load 200 g., i.e., compressibility = 0.9×10^{-4} cm./g.

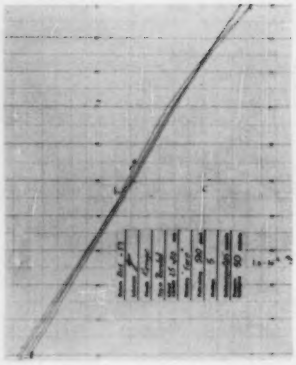

Fig. 13. Extension–compression of nonwoven fabric (85 g./m.²). Deformation 0.60% at full scale load 500 g., i.e., compressibility = 1.2×10^{-4} cm./g.

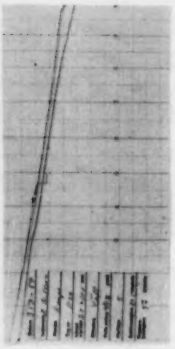

Fig. 14. Extension–compression of wool gabardine (332 g./m.²). Deformation 0.16% at full scale load 40 g., i.e., compressibility = 4.0×10^{-4} cm./g.

There is a very small difference between different corrugated clamps. There will of course be limiting cases, when the radius of curvature for the same sample width is very large or very small; then the shell buckling will approach the case of plate buckling.

From Figure 11 it could be seen that Euler's equation holds well for plane clamps. For corrugated clamps, however, a very different relation is obtained. Instead of varying with the inverse value for the square of the sample length, which is the case for plane clamps, the buckling load here varies with the inverse value of the square root of the sample length.

The relation between the buckling load and the sample length can be written as

$$P_1 = P_0 \cdot l^{-n} \qquad (2)$$

where P_0 is the buckling load when $l = 1$.

If $n = n_1$ and $P_0 = P_{01}$ for plane clamps and $n = n_2$ and $P_0 = P_{02}$ for corrugated clamps with a certain radius of curvature, the point of intersection between the equations

$$P_1 = P_{01} \cdot l^{-n_1}$$
$$P_2 = P_{02} \cdot l^{-n_2}$$

will be

$$l_A = \left(\frac{P_{01}}{P_{02}}\right)^{1/n_1 - n_2}$$

and

$$P_A = \left(\frac{P_{02}{}^{n_1}}{P_{01}{}^{n_2}}\right)^{1/n_1 - n_2}$$

This point of intersection may be an interesting fabric parameter. From Figure 11 is obtained $l_A = 0.41$ cm.; $P_A = 80$ g./cm.

If we know the thickness t we may also calculate a slenderness ratio l_A/t for this point of intersection. The value of this slenderness ratio should be dependent on the compressibility.

By measuring the buckling load for plane and corrugated clamps at selected sample lengths, it is possible to calculate a number of parameters which will be characteristic for the fabric.

Compressibility

It was mentioned in the introduction that the buckling compression determines the formability of a fabric [3]. The buckling compression can either be measured directly by enlarging the first part of the buckling curve or calculated from the compressibility in the plane of the fabric and the bending stiffness. The latter procedure is better because it gives a specific value for the fabric, independent of the sample length. The compressibility is the inversed slope of the first portion of the buckling curve.

It is better to use the corrugated clamps rather than the plane clamps when determining compressibility. The buckling load is much higher and therefore the compression can be recorded over larger loads, which improves the accuracy. The sample is mounted as before. It was found advantageous to subject the sample to both extension

and compression. The extension load was the same as the compression load, which was usually chosen as ⅓ of the buckling load, and the whole cycle between extension and compression was recorded. Typical curves are given in Figures 12–14. The compressibility is calculated as the inverse value of the average slope through the origin.

Literature Cited

1. Dahlberg, B. and Eeg-Olofsson, T., *Off. medd. fr. TEFO*, 11 (1958).
2. Eeg-Olofsson, T., *J. Textile Inst.* **50**, T112–T132 (1959).
3. Lindberg, J., Waesterberg, L., and Svenson, R., *J. Textile Inst.*, **51**, T1475–T1491 (1960).

Part III: Shearing and Buckling of Various Commercial Fabrics

Joel Lindberg, Bengt Behre, and Bengt Dahlberg

Swedish Institute for Textile Research, Gothenburg, Sweden

Abstract

Load–deformation curves obtained by the methods for shearing and buckling described in Part I and II are analyzed and discussed. Parameters obtained from these curves are given for 66 commercial fabrics covering an extreme range. Different fabrics show widely different values for the parameters obtained from both shearing and buckling curves. It is further shown that there exist close relationships between simple deformations like shearing and plane buckling and complex deformations like buckling of corrugated fabric shells. The formability of a fabric is defined as the maximum compression a fabric can take up before it buckles, given a certain geometric arrangement. The formability partly determines the tailorability and the crease pattern of fabrics. The formability is dependent on fabric direction, and it is shown that the integrated formability should be related to the product of buckling load and shear angle. A theoretical analysis of formability is given, and it is shown that it can be expressed as the product of an anisotropy ratio and the square of the fabric thickness.

It is further shown that the shell buckling load depends on both the plane buckling load and the shear angle, in such a way that increasing shear angle leads to decreasing shell buckling load. It is shown that combination of high formability and low shell buckling load generally is attained by combining relatively high thickness with low bending modulus. It is also shown that wool fabrics generally have this combination of properties. A fabric map is given for all the commercial fabrics. Each fabric has a certain position on the map dependent on bending stiffness (which is closely related to buckling load) and shear angle.

Attention is given to the relation between creasing behavior of fabrics and fabric properties. There is a certain relation between crease recovery angle and formability and a good relation between this angle and the noncyclical energy loss in shell buckling. The hypothesis that recovery properties depend mainly on the interaction within the fabric between frictional forces and elastic forces of the fibers is put forward. The energy loss following any fabric deformation depends mainly on friction. The permanent deformation is probably due to the fact that the elastic forces of the fibers cannot overcome the friction. By means of a rheological model it is shown how friction and fiber stiffness may interact in a fabric. It is shown that the stiffness value should be that obtained at infinitely slow loading of the fiber.

Introduction

A number of different commercial fabrics, selected to cover the largest possible range of normal fabric types, were measured by the methods for shearing and buckling described in Parts I and II. Other fabric properties measured were weight, thickness, bending stiffness, and crease recovery angle. Several other materials such as sheet

rubber, plastic films, and paper were also measured for comparison. Examples of full load–deformation curves are given for some of the materials; the rest of the data is given in tables.

In this paper are discussed the characteristic features of both the loading and the recovery part of shearing and buckling curves, the relation between simple and complex deformation, and the relation between recovery curves and crease recovery properties of fabrics.

Shearing

Different Shear Curves

From Figure 1a to Figure 16a it is seen that widely different types of curves can be obtained for different materials. The curves are more or less completely linear with very little hysteresis for a rubber sheet (Figure 16a), water repellent cotton fabric (Figure 2a), nonwoven fabric (Figure 9a), and paper (Figure 15a). These materials are homogeneous; all woven fabrics showing such curves are very tightly woven or have a high frictional resistance at yarn intersections.

There are obviously two factors which determine the shear curve. Frictional forces are produced when the intersecting yarns move relative to each other. Elastic forces are produced when the two yarn systems approach jamming. If we have a tightly woven fabric, the systems will already be jammed. The elastic forces are then very rapidly built up, and there will be no sliding of yarns over each other at the intersections.

If the friction is very low and the fabric loosely woven (low cover factor), curves of the type shown in Figures 5a, 10a, and 13a are obtained. Here the load rapidly increases as jamming is approached.

If friction is increased while the same cover factor is maintained, an S-shaped loading curve is obtained. The load at first increases rapidly due to static friction, then the systems slide, and finally the load rapidly increases due to jamming (Figures 6a and 7a).

If the friction continues to increase, the curves shown in Figures 1a and 11a are obtained. Most light cotton fabrics are of this type. Slipping begins just before the maximum force is obtained. An extreme case is the glass fabric in Figure 12a. A maximum hysteresis effect is obtained with this curve.

In Table I the values for the shear angle as well as for shear energy and the recovered shear energy are given. It is also possible to calculate an index showing whether the curve is concave, convex, or S-shaped, by taking the ratio between the measured shear energy and the shear energy calculated from the shear angle on the assumption that the curve is linear. If this index is larger than one, the curve is mostly convex upwards; if it is smaller than one the curve is mostly concave upwards; if it is equal to one the curve is linear. The index is given in Table I.

The shear angle for various fabrics varies over a large range from 0.1° to 50°. This is not a function of weight or thickness, as can be seen from Figures 13a and 14a or fabric numbers 57 and 58 in Table I. These fabrics are at the extremes of the range, but have about the same weight. The relation between shear angle and fabric properties will be discussed later.

Recovered Energy

In most cases the recovered energy in shearing is very small. It is reasonable to assume that this is due to the loss of frictional energy when the intersecting yarns slide over each other. The fiber deformations must be extremely small for the shear deformations obtained, so it seems very unlikely that the energy losses occur in the fibers themselves. This is further borne out by the fact that fabrics such as nonwoven and tightly woven fabrics, although they may be very light, show little or no energy loss. The percentage recovered energy is given in Table I and in Figure 17. Most fabrics show less than 35%. The glass fabric in Figure 12a has practically no recovered energy at all; since glass fibers are very elastic, all the energy loss must be due to friction.

Buckling

Buckling Curve

From Figures 1 to 16, b and c, it is seen that the buckling curves for shell buckling and plate buckling are in most cases similar to each other. Both these curves will therefore be discussed simultaneously.

The curves consists of three parts: the compression part, the buckling curve, and the recovery curve.

The compression part of the curve will not be discussed here, although a method for measuring it has been given in Part II.

The buckling curve can have different forms. From the curves given in Figures 1 to 16, b and c,

it is evident that they can rise, fall, or be horizontal from the buckling point. Very often a pronounced maximum is obtained just at the buckling point. Such a maximum is usually more pronounced in shell buckling than in plate buckling. Exactly how differences in the form of the curve should be interpreted is not very clear. A plausible explanation for plate buckling is that the bending stiffness changes with the radius of curvature due to a change in the moment of inertia.

This is consistent with the Euler equation

$$P = \frac{4\pi^2 \cdot EI}{l^2}$$

where P is the buckling load, E the modulus of elasticity, I the moment of inertia, and l the sample length.

Obviously both increases and decreases of the moment of inertia can occur. Reduction in thickness decreases the moment of inertia, but increased internal compression reduces fiber slippage and increases the moment of inertia.

Sometimes the maximum obtained in plate buckling may be an artifact. This may happen if the clamps are not exactly parallel or if the sample is not properly mounted. Different parts of the sample may then buckle in two directions simultaneously, giving, in effect, shell buckling and a much higher buckling load. The sample may very quickly snap over to plate buckling with a consequent very rapid reduction in the buckling load.

The ratio P_2/P_1 is an index showing whether the buckling curve rises or falls. When $P_2/P_1 < 1$ the curve falls and when $P_2/P_1 > 1$ the curve rises.

Plate buckling is denoted by index p, P_p and shell buckling with index d, P_d. Both P_{p2}/P_{p1} and P_{d2}/P_{d1} are given in Table I. For plate buckling, thin fabrics give more rapidly rising curves than thick fabrics. For shell buckling only thick and porous fabrics give rising curves.

Plate Buckling and Bending Stiffness

Bending stiffness is most commonly measured by means of the cantilever method [8]. All fabrics in Table I have been measured by this method. It is interesting to compare the plate buckling load P_{p1} or P_{p2} with the bending stiffness, b. In Figures 18 and 19, P_{p1} and P_{p2} are plotted against the bending stiffness (log–log scale). The 45° line in Figure 18 shows that there is a good linear relationship between b and P_{p1}. The relationship between b and P_{p2} seems to follow the relation $b = k \cdot P^2_{p2}$ (equation for the line in Figure 19). The variation around the line in Figure 18 is still very large. For one and the same value of b, P_{p1} can vary by a factor of 4. It is not clear whether this is a true difference, or whether it depends on the method of measurement. The problem should be studied more thoroughly.

Recovered Energy

In all cases the recovery curve commences at 40% buckling. It can be seen from Figures 1b and 1c to 16b and 16c that the difference in recovered energy is very large among different fabrics and also between plate buckling and shell buckling. From Figure 20 and Table I is seen that the recovered energy for plate buckling varies between 80 and 30% and that most fabrics lie between 65 and 50%. The radius of curvature for 40% buckling is approximately 0.5 cm. This is a very slight deformation, and it seems highly unlikely that the high loss of energy is due to fiber deformation. As in the case of shearing, it seems reasonable to assume that the loss of energy largely depends on frictional energy developed when fibers are slipping over each other.

Shell buckling gives still lower values for the recovered energy. As seen from Figure 20, there is a marked difference between plate buckling and shell buckling.

Wool fabrics generally have high values for the recovered energy. Of the 18 fabrics showing a recovered energy of more than 40% for shell buckling, 13 are wool fabrics. For a rubber sheet there is very little difference in recovered energy between plate and shell buckling, but for paper the difference is very large (Figures 15 b and c, and 16 b and c).

The low values generally obtained for the recovered energy must have a great influence on the dynamic properties of fabrics. The fabric in a garment will be subjected to repeated and different complex deformations. The crease pattern will change with the movements of the wearer. The speed of change from one crease pattern to another will depend on stiffness, mass damping, and frictional damping; i.e., the lost energy. Even if the methods given are not suitable for evaluating the dynamic properties of fabrics, it is at least possible to conclude that the difference in recovered energy shown to exist must have a great influence on these properties.

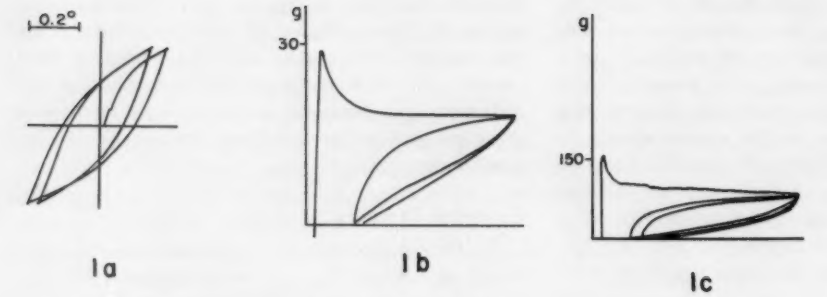

Fig. 1. Fabric 5. Cotton, 160 g./m.².

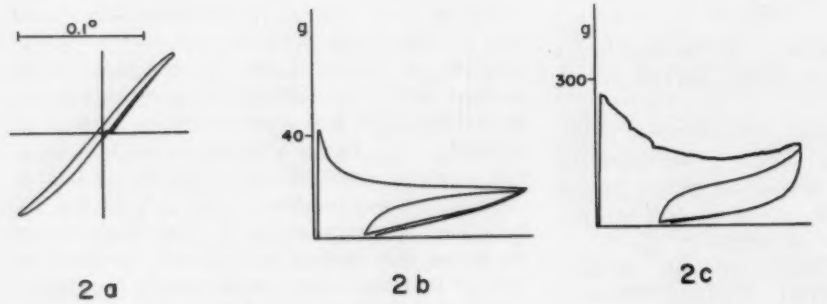

Fig. 2. Fabric 9. Cotton, 97 g./m.².

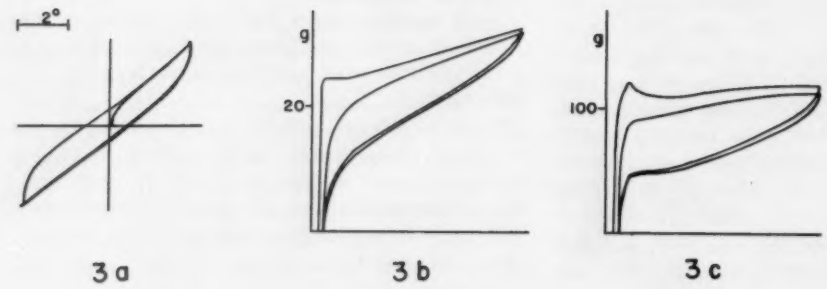

Fig. 3. Fabric 35. Wool, 376 g./m.².

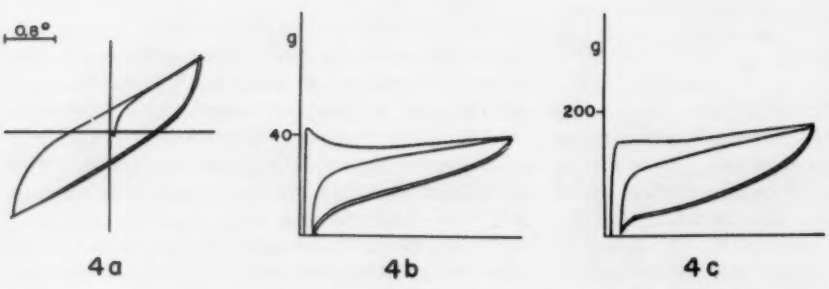

Fig. 4. Fabric 36. Wool/rayon, 401 g./m.².

a = Shearing, b = Plate Buckling, c = Shell Buckling

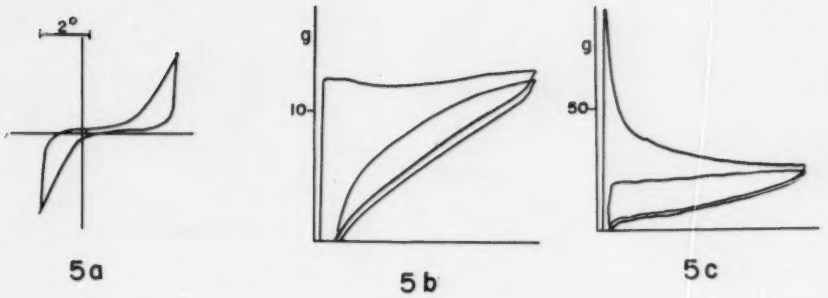

Fig. 5. Fabric 45. Cell. acetate, 97 g./m.².

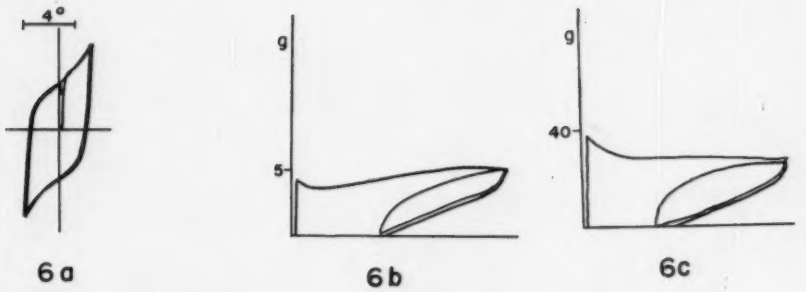

Fig. 6. Fabric 48. Nylon, 149 g./m.².

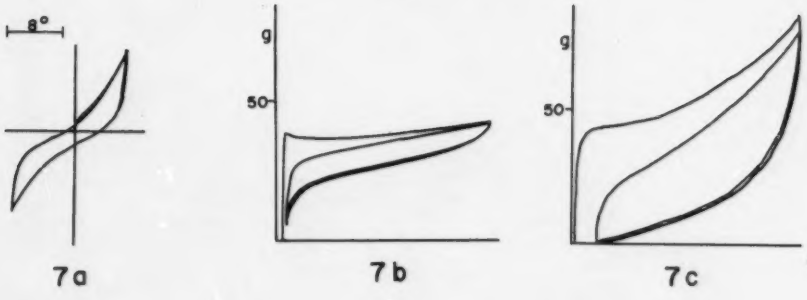

Fig. 7. Fabric 53. Cotton, 343 g./m.².

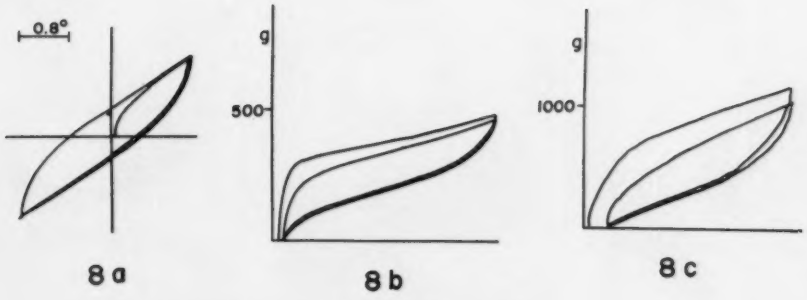

Fig. 8. Fabric 55. Wool, 691 g./m.².

a = Shearing, b = Plate Buckling, c = Shell Buckling

9a

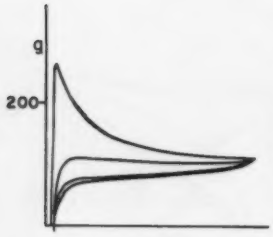

9b

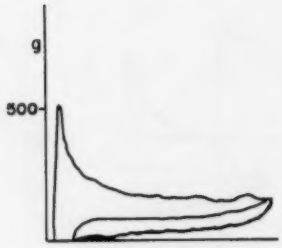

9c

Fig. 9. Fabric 58. Nonwoven, 85 g./m.².

10a

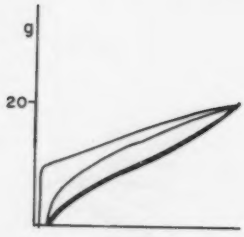

10b

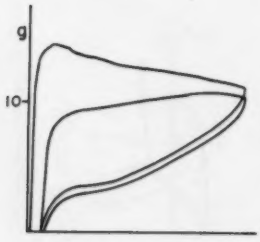

10c

Fig. 10. Fabric 57. Cotton, 79 g./m.².

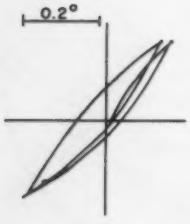

11a

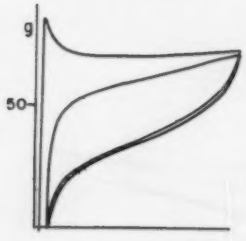

11b

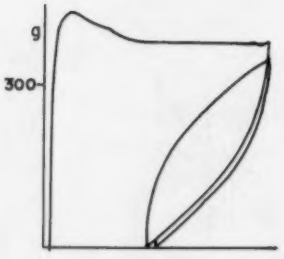

11c

Fig. 11. Fabric 66. Wool/rayon/cotton, 392 g./m.².

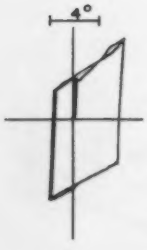

12c

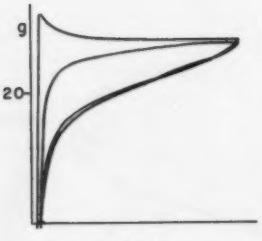

12b

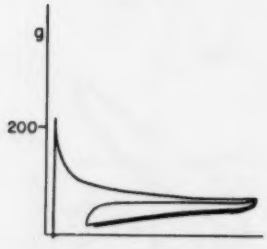

12c

Fig. 12. Glass fabric, 135 g./m.².

a = Shearing, b = Plate Buckling, c = Shell Buckling

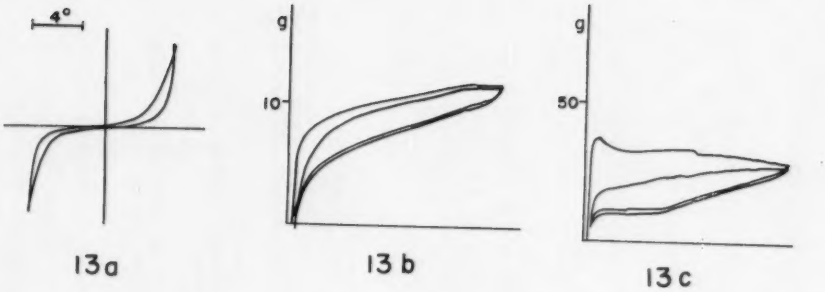

Fig. 13. Set filament nylon fabric, 74 g./m.².

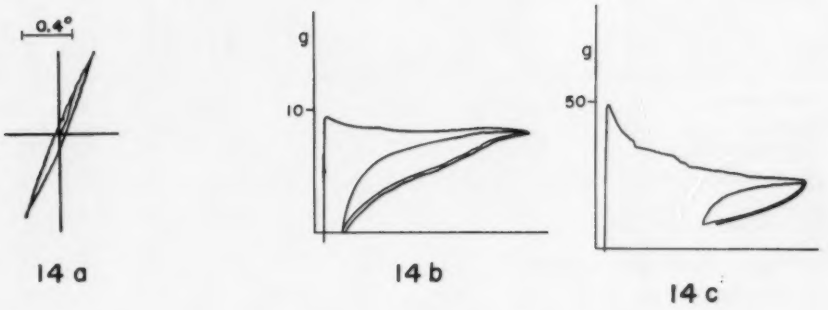

Fig. 14. Untreated fabric of Figure 13, 66 g./m.².

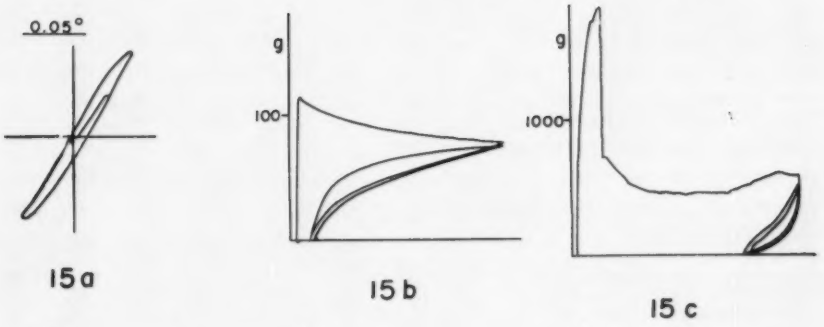

Fig. 15. Paper, 78 g./m.².

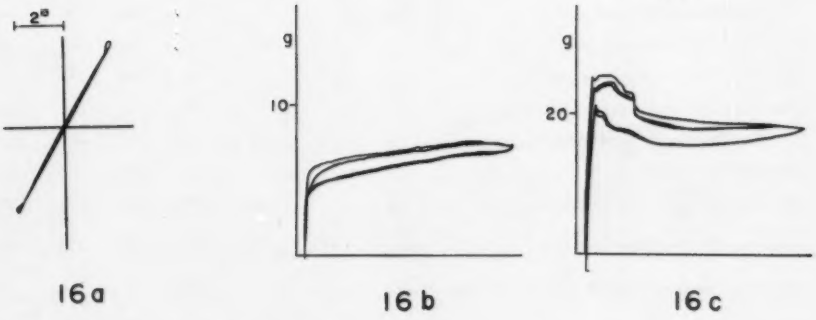

Fig. 16. Sheet rubber, 282 g./m.².

a = Shearing, b = Plate Buckling, c = Shell Buckling

TABLE I

	Cotton. Five-harness sateen. Fire-protecting fabric	Cotton. 3/1 twill. waterproof treated. Pillowcase fabric	Cotton. Plain and rib weave combination 3 harness. Dress fabric	Cotton. Plain weave. Poplin fabric	Cotton. Plain weave. Sheeting	Cotton. Plain weave. Shirting fabric	Cotton. Plain and weft rib combined weave. Dress fabric	Cotton. Plain weave. Shirting fabric	Cotton. Plain weave. Pillowcase fabric
Fabric number	1	2	3	4	5	6	7	8	9
Weight, W, g./m.^{2}	403	248	205	164	160	136	116	112	97
Thickness, t, mm.	.63	.48	.58	.35	.26	.28	.28	.22	.18
Volume weight, $\frac{W}{t}\cdot 10^{-3}$, g./cm.^{3}	.64	.52	.35	.47	.62	.49	.41	.51	.54
Shear angle, γ, degrees	.11	.18	4.4	1.3	.18	5.5	10	4.7	.98
Shape index of shear curve	1.03	1.11	1.15	1.94	1.21	1.32	1.24	1.38	1.68
Shear energy, A_s, g. degrees	1.8	3.2	83	40	3.5	120	110	200	27
Recovered shear energy, C_s, g. degrees	1.8	2.6	45	6.6	2.8	38	30	40	7
Recovered shear energy, $\frac{C_s}{A_s}\cdot 100$	100	81	54	17	80	32	20	28	26
Bending stiffness, cantilever method, b, g. cm.^{2}/cm.	1.8	1.2	.22	.36	.17	.10	.10	.09	.16
Plate buckling force, P_{p1}, g.	81	42	13	18	8.0	10	6.1	3.0	—
Plate buckling force, P_{p2}, g.	88	36	20	17	10	10	11	8.6	5.7
Shape index of plate buckling curve, $\frac{P_{p2}}{P_{p1}}$	1.08	.86	1.52	.96	1.30	1.00	1.75	2.86	—
Plate buckling energy, A_p, g. cm.	92	39	22	19	11	11	11	8.5	6.0
Plate buckling energy, B_p, g. cm.	72	25	16	14	7.5	8.5	8.0	7.0	4.2
Plate buckling noncyclical energy loss, $\frac{A_p - B_p}{A_p}\cdot 100$	27	36	27	29	14	19	27	18	30
Recovered plate buckling energy, C_p, g. cm.	36	15	10	7.5	5.0	6.5	6.0	5.5	3.3
Recovered plate buckling energy, $\frac{C_p}{A_p}\cdot 100$	39	39	45	41	48	62	55	65	55
Shell buckling force, P_{d1}, g.	810	620	120	220	140	92	50	44	84
Shell buckling force, P_{d2}, g.	560	290	100	68	69	28	33	29	33
Shape index of shell buckling curve	.70	.46	.90	.31	.49	.30	.50	.66	.39
Shell buckling energy, A_d, g. cm.	590	310	110	80	80	38	34	30	36
Shell buckling energy, B_d, g. cm.	300	110	76	36	35	29	25	15	15
Shell buckling, noncyclical energy loss, $\frac{A_d - B_d}{A_d}\cdot 100$	41	65	28	55	56	24	25	52	60
Recovered shell buckling energy, C_d, g. cm.	140	50	31	25	13	13	9.5	7.0	5.0
Recovered shell buckling energy, $\frac{C_d}{A_d}\cdot 100$	24	16	29	34	16	33	28	23	16
Permanent deformation, shell buckling	32	35	4	25	30	2	10	28	30
Shell buckling force/plate buckling force, $\frac{P_{d2}}{P_{p2}}$	6.4	7.8	5.3	4.0	6.6	2.8	3.1	3.4	5.8
Formability, $P_{p2}\cdot\gamma$	9.4	6.4	87	22	1.8	55	100	40	5.6
Anisotropy, $\frac{P_{p2}\cdot\gamma}{t^2}\cdot 10^{-2} = \text{const.}\cdot\frac{E_{a1}}{E_{a2}}$	.24	.28	2.6	1.8	.27	7.0	13	8.3	1.7
Apparent shell buckling modulus, $\frac{P_{d2}}{t^{3.25}}\cdot 10^{-1} = \text{const.}\cdot E_{a1}\cdot\sqrt[4]{E_{a2}}$	260	310	61	210	550	190	220	400	870
Apparent bending modulus, $\frac{P_{p2}}{t^3}\cdot 10^{-1} = \text{const.}\cdot E_{a1}$	35	33	10	40	59	45	49	81	98
Stiffening index, $\frac{P_{p2}}{W\cdot t^2}\cdot 100 = u_1$	55	63	29	85	97	94	120	160	180
Crease recovery angle, %	63	35	57	42	32	52	35	35	37

TABLE I

Cotton. Plain weave. Shirting fabric	Cotton, number 10 crease-resistant treated. Shirting fabric	Cotton. Plain weave. Shirting fabric	Cotton, number 12 crease-resistant treated. Shirting fabric	Cotton, crease-resistant treated. Plain weave. Shirting fabric	Cotton, crease-resistant treated. Plain weave. Shirting fabric	Cotton, crease-resistant treated. Plain weave. Shirting fabric	Cotton, crease-resistant treated. Plain weave. Shirting fabric	Cotton, crease-resistant treated. Five-harness sateen. Shirting fabric	Cotton/spun rayon, 90/10, crease-resistant treated. Plain weave. Shirting fabric	Spun rayon, crease-resistant treated. Plain weave. Shirting fabric	Spun rayon, crease-resistant treated. Plain weave. Shirting fabric	Filament rayon, crease-resistant treated. Basket weave. Dress fabric	Spun rayon, crease-resistant treated. Plain weave. Dress fabric	Spun rayon, crease-resistant treated. 2/2 twill. Suiting fabric	Wool. Plain weave. Dress fabric (worsted)	Wool. Plain weave. Dress fabric (worsted)	Wool. Crepe weave. Dress fabric (worsted)	Wool. Plain-knitted. Jersey fabric
10	11	12	13	14	15	16	17	18	19	20	21	22	23	24	25	26	27	28
151	161	—	129	188	171	170	147	144	112	132	177	240	250	320	127	203	206	269
.32	.34	25	.25	.38	.29	.34	.23	.20	.20	.20	.25	.48	.47	.52	.36	.66	.64	1.10
.47	.47	—	.52	.49	.59	.50	.64	.72	.56	.66	.71	.50	.53	.62	.35	.31	.32	.24
2.7	4.6	9.0	7.4	1.6	2.2	3.2	.56	2.9	1.4	.56	4.0	20	9.7	12	27	16	18	4.6
1.75	1.32	1.08	1.22	1.89	1.79	1.55	1.74	1.33	1.95	1.42	.83	.85	.81	.92	.78	1.16	1.18	1.43
78	100	160	150	48	63	80	16	63	45	13	54	270	130	190	350	310	340	110
15	25	53	50	7	9.6	14	4.1	15	7.9	4.0	18	53	36	56	230	96	110	35
19	25	33	34	15	15	18	26	24	18	31	33	20	28	30	66	31	31	32
.081	.096	—	.039	.10	.13	.085	.15	.091	.12	.16	.067	.10	.24	.36	.021	.024	.049	.063
3.7	6.4	3.5	3.0	9.5	10.0	4.2	6.6	4.7	4.0	11	—	10	14	12	2.5	2.0	4.3	7.4
7.9	9.5	8.2	8.5	8.3	14	8.3	9.2	9.3	7.7	11	5.9	18	19	19	7.5	8.0	10	16
2.14	1.49	2.34	2.83	1.21	1.39	1.98	1.39	1.98	1.95	1.01	—	1.71	1.34	1.62	3.00	4.00	2.38	2.20
8.0	9.5	8.0	9.0	13	15	9.0	9.5	9.5	8.0	12	5.5	18	20	19	7.5	8.5	11	17
5.5	7.5	7.5	8.0	85	12	6.5	6.5	7.5	6.0	8.5	4.3	16	16	16	6.0	6.5	9.0	13
31	21	6	13	32	21	28	32	21	25	26	23	14	21	16	20	24	14	21
4.5	6.0	6.5	6.5	6.0	7.5	4.8	5.0	6.5	4.7	6.0	3.6	12	12	11	5.0	5.0	7.5	9.0
57	63	81	72	48	52	53	53	58	58	52	65	67	59	58	67	59	71	55
74	68	38	35	100	100	86	130	110	100	150	59	58	96	69	20	24	37	60
38	44	23	28	52	69	39	66	63	74	110	34	74	87	84	18	16	33	58
.51	.67	.61	.80	.50	.69	.45	.50	.60	.72	.72	.58	1.28	.91	1.62	.90	.67	.89	.97
40	43	24	28	56	70	40	69	65	73	112	35	70	85	80	18	18	33	57
30	37	19	23	42	61	34	49	49	42	72	21	65	63	66	16	14	31	46
25	15	24	18	25	13	17	29	25	43	36	42	9	27	18	7	18	9	19
9.5	15	5.5	8.5	13	23	16	15	18	13	24	7.0	39	30	30	11	5.5	19	24
24	34	23	30	23	32	24	22	28	17	21	20	34	35	37	62	32	56	42
26	40	10	2	28	3	1	26	3	28	24	42	2	3	4	1	4	1	7
4.8	4.6	2.8	3.3	4.5	5.0	4.7	7.2	6.8	9.6	9.6	5.8	4.2	4.6	4.5	2.4	2.0	3.2	3.6
22	46	72	61	21	32	27	5.0	27	12	6.0	24	346	181	220	231	133	182	75
2.2	4.0	12	9.7	1.5	3.8	2.3	.95	6.8	3.0	1.5	3.9	15	8.2	8.1	18	3.1	4.5	.62
150	150	210	250	120	290	130	780	1200	1400	2000	310	80	100	71	50	62	14	4.3
24	28	53	55	21	57	21	75	110	96	140	38	16	18	13	16	2.8	3.9	1.2
51	51	—	110	43	97	42	120	160	170	210	53	32	35	220	46	9.0	12	5.0
42	74	43	62	60	47	64	49	55	26	56	43	80	66	64	83	80	86	66

TABLE I—Continued

	Wool. 2/2 twill. Suiting fabric (worsted)	Wool. Broken 2/2 twill. Suiting fabric (woolen)	Wool. 2/2 twill. Suiting fabric (worsted)	Wool. Honeycomb weave. Suiting fabric (worsted)	Wool. 1/3 twill and basket combined weave. Suiting fabric (worsted)	Wool. 3/3 twill. Suiting fabric (worsted)	Wool. 2/2 twill. Suiting fabric (worsted)	Wool/spun rayon. Twill. Uniform fabric	Wool/spun rayon. 50/50. Plain weave. Suiting fabric
Fabric number	29	30	31	32	33	34	35	36	37
Weight, W, g./m.^{2}	273	282	283	310	329	330	376	401	164
Thickness, t, mm.	.68	1.09	.64	.75	.80	.68	.81	1.06	.40
Volume weight, $\frac{W}{t}\cdot 10^{-3}$, g./cm.^{3}	.40	.26	.43	.41	.41	.48	.46	.38	.41
Shear angle, γ, degrees	7.4	15	3.7	7.9	13	2.8	6.4	2.5	18
Shape index of shear curve	1.30	1.22	1.43	1.28	1.12	1.38	1.19	1.55	.81
Shear energy, A_s, g. degrees	160	300	87	170	230	62	130	64	250
Recovered shear energy, C_s, g. degrees	60	110	24	65	99	20	60	15	110
Recovered shear energy, $\frac{C_s}{A_s}\cdot 100$	38	38	28	39	43	32	48	23	45
Bending stiffness, cantilever method, b, g. cm.^{2}/cm.	.13	.17	.16	.18	.18	.34	.21	.43	.029
Plate buckling force, P_{p1}, g.	11	15	14	15	15	25	16	31	2.0
Plate buckling force, P_{p2}, g.	17	22	19	21	22	31	22	33	7.5
Shape index of plate buckling curve, $\frac{P_{p2}}{P_{p1}}$	1.52	1.47	1.34	1.37	1.44	1.25	1.38	1.06	3.75
Plate buckling energy, A_p, g. cm.	17	23	20	21	22	29	23	32	7.5
Plate buckling energy, B_p, g. cm.	15	20	17	19	21	25	20	25	6.5
Plate buckling noncyclical energy loss, $\frac{A_p - B_p}{A_p}\cdot 100$	12	13	15	12	7	14	13	22	13
Recovered plate buckling energy, C_p, g. cm.	11	16	13	14	16	17	15	18	5.5
Recovered plate buckling energy, $\frac{C_p}{A_p}\cdot 100$	65	67	64	67	73	60	65	56	73
Shell buckling force, P_{d1}, g.	85	81	140	94	110	170	94	240	24
Shell buckling force, P_{d2}, g.	73	72	100	88	85	120	92	150	20
Shape index of shell buckling curve	.86	.90	.75	.94	.75	.74	.98	.63	.83
Shell buckling energy, A_d, g. cm.	76	78	110	91	89	130	95	170	20
Shell buckling energy, B_d, g. cm.	72	67	94	81	78	100	81	130	17
Shell buckling, noncyclical energy loss, $\frac{A_d - B_d}{A_d}\cdot 100$	5	14	12	12	12	21	15	21	13
Recovered shell buckling energy, C_d, g. cm.	47	45	59	55	54	61	49	70	9.0
Recovered shell buckling energy, $\frac{C_d}{A_d}\cdot 100$	62	58	55	60	61	47	51	32	46
Permanent deformation, shell buckling	1	2	2	1	1	4	3	3	1
Shell buckling force/plate buckling force, $\frac{P_{d2}}{P_{p2}}$	4.4	3.3	5.5	4.3	3.9	3.4	4.2	4.7	2.7
Formability, $P_{p2}\cdot\gamma$	131	328	70	161	272	86	142	82	138
Anisotropy, $\frac{P_{p2}\cdot\gamma}{t^2}\cdot 10^{-2} = \text{const.}\cdot\frac{E_{a1}}{E_{a2}}$	2.9	2.8	1.7	2.9	4.3	1.8	2.2	.74	8.7
Apparent shell buckling modulus, $\frac{P_{d2}}{t^{3.25}}\cdot 10^{-1} = \text{const.}\cdot E_{a1}\cdot\sqrt[4]{E_{a2}}$	26	5.4	44	22	18	43	18	13	39
Apparent bending modulus, $\frac{P_{p2}}{t^3}\cdot 10^{-1} = \text{const.}\cdot E_{a1}$	5.3	1.7	7.2	4.9	4.2	9.9	4.1	2.7	12
Stiffening index, $\frac{P_{d2}}{W\cdot t^2}\cdot 100 = n_1$	13	6.6	16	12	10	20	8.9	7.3	29
Crease recovery angle, $^\circ$	86	84	81	89	90	81	87	83	75

TABLE I—Continued

Wool/spun Dacron,* 55/45. Plain weave. Suiting fabric.	Wool/spun rayon, 50/50. 2/2 twill. Suiting fabric	Spun nylon/rayon/Dacron. Plain weave. Suiting fabric	Spun nylon/rayon/Dacron. Plain weave. Dress fabric	Silk. Plain weave	Filament nylon. Plain weave	Filament Orlon.* Plain weave	Filament cell. acetate. Plain weave	Filament rayon/filament cell. acetate. Five-harness sateen. Lining fabric	Filament Perlon. Plain weave	Filament nylon. Plain weave	Filament Saran. Twill. Upholstery fabric	Cotton. Plain weave. Blanket fabric	Spun rayon. Double plain weave. Blanket fabric	Cashmere wool. 2/2 twill. Overcoat fabric	Cotton. Terry toweling fabric	Spun rayon/wool/cotton. Double plain weave. Ulster fabric	Wool. Double weave. Ulster fabric	Wool. Melton. Uniform fabric
38	39	40	41	42	43	44	45	46	47	48	49	50	51	52	53	54	55	56
218	249	320	323	31	48	84	97	122	138	149	378	291	336	341	343	646	691	697
.38	.64	.58	.60	.07	.16	.16	.16	.19	.27	.27	.53	1.75	2.01	1.34	2.03	2.06	2.62	2.28
.58	.39	.55	.54	.44	.30	.52	.61	.64	.51	.55	.71	.17	.17	.25	.17	.31	.26	.31
5.4	17	5.2	6.4	49	20	4.6	5.2	19	3.3	8.8	.49	2.6	8.2	14	18	5.5	2.9	2.2
1.19	1.06	1.16	.84	.91	.80	1.26	.71	.84	2.14	1.33	1.49	1.63	1.59	1.03	1.23	1.36	1.43	1.42
110	300	99	89	730	270	95	61	270	115	190	12	68	220	230	360	120	67	50
30	120	23	28	200	60	15	15	53	12	23	5.1	16	40	73	130	33	22	17
28	38	23	31	27	23	16	25	20	10	12	43	24	19	31	35	27	33	34
.065	.082	.23	.24	.006	.011	.009	.18	.11	.12	.075	1.7	.63	.56	.21	.10	1.8	2.5	.68
5.1	6.5	15	17	—	1.6	5.1	—	7.0	11	6.1	300	39	75	22	10	80	210	70
12	13	21	22	4.6	5.7	9.3	8.4	10	12	8.9	210	33	81	27	17	91	280	97
2.26	2.02	1.38	1.30	—	3.56	1.82	—	1.43	1.07	1.46	.70	.85	1.08	1.22	1.65	1.14	1.35	1.39
12	14	23	24	4.8	5.5	9.5	9.0	8.5	12	9.0	120	35	85	28	17	97	280	110
10	12	19	19	3.8	4.0	7.5	7.0	7.0	7.5	6.0	95	20	60	22	9.0	70	230	85
17	15	16	19	21	27	21	22	24	38	33	19	48	29	23	47	27	19	26
7.5	9.5	14	14	2.8	3.4	6.0	6.0	5.5	5.5	4.7	76	13	32	16	5.5	37	140	54
63	70	60	60	59	61	63	67	57	46	52	65	37	37	55	32	38	55	39
74	50	240	150	6.0	17	60	65	37	84	44	94	160	170	81	43	330	560	340
52	49	210	130	4.0	9.0	29	38	20	32	27	92	160	190	81	53	400	860	480
.70	.98	.91	.83	.67	.53	.48	.59	.54	.38	.61	.71	.97	1.10	1.00	1.21	1.21	1.53	.40
53	47	210	120	4.0	9.0	30	39	22	36	28	570	160	190	81	58	400	840	480
47	41	140	94	3.7	6.0	26	29	17	24	21	380	120	130	66	41	230	610	360
12	15	31	24	10	39	15	30	21	29	25	33	27	29	25	30	41	27	23
26	25	83	47	1.2	1.2	9.5	20	5.5	6.0	6.0	200	55	60	38	15	150	360	200
48	52	40	38	28	12	31	43	26	18	21	35	34	32	46	26	36	42	43
1	2	3	3	1	38	2	2	3	27	18	5	6	10	2	10	11	10	2
4.5	3.7	10.3	5.7	.9	1.6	3.1	4.5	2.0	2.7	3.0	2.7	4.7	2.3	3.0	3.2	4.4	3.0	4.9
63	230	108	142	218	121	46	49	192	33	76	110	84	668	371	294	501	805	210
4.4	5.6	3.2	3.9	450	48	18	19	53	4.5	10	3.9	.28	1.7	2.1	.71	1.2	1.2	.40
120	21	120	66	2300	350	1100	1500	440	230	190	440	2.5	2.0	3.1	0.53	3.8	3.8	3.8
21	5.0	11	10	1300	140	230	210	150	59	45	140	.62	1.0	1.1	.20	1.1	1.6	.82
37	13	19	19	3000	460	430	340	230	120	82	190	3.7	6.0	4.4	1.7	3.3	6.0	2.7
71	83	76	76	79	81	68	50	59	64	72	70	56	56	79	62	68	83	73

* Du Pont trademark.

TABLE I—Continued

	Spun rayon. Plain weave. Curtain fabric	Rayon/cotton/polyamide. Nonwoven fabric	Silk/wool. Plain weave. Dress fabric	Cotton/filament cell. acetate. Dress fabric	Cotton. Plain weave. Dress fabric	Spun rayon/flax. Plain weave. Dress fabric	Wool/filament rayon. Dress fabric	Flax/spun rayon, 50/50. Plain weave. Dress fabric	Cotton/flax. Broken 2/2 twill. Towelling fabric	Wool/spun rayon/cotton. Plain weave. Interlining fabric
Fabric number	57	58	59	60	61	62	63	64	65	66
Weight, W, g./m.^{2}	79	85	125	181	217	234	236	253	341	392
Thickness, t, mm.	.31	.42	.30	.54	.46	.62	.64	.47	.57	.92
Volume weight, $\frac{W}{t}\cdot 10^{-3}$, g./cm.^{3}	.25	.21	.42	.34	.47	.38	.37	.54	.60	.43
Shear angle, γ, degrees	36	.19	9.3	14	2.4	6.4	22	17	3.1	.35
Shape index of shear curve	.77	.87	1.19	1.29	1.53	1.16	1.24	.69	1.43	1.47
Shear energy, A_s, g. degrees	450	2.7	180	300	60	120	440	190	73	8.4
Recovered shear energy, C_s, g. degrees	150	2.7	41	53	15	51	76	100	45	4.0
Recovered shear energy, $\frac{C_s}{A_s}\cdot 100$	33	100	22	18	25	41	17	54	62	48
Bending stiffness, cantilever method, b, g. cm.^{2}/cm.	.17	1.6	.085	.51	.33	.20	.31	.13	—	.75
Plate buckling force, P_{p1}, g.	—	74	7.9	32	21	12	29	13	89	74
Plate buckling force, P_{p2}, g.	9.1	44	11	27	27	15	26	20	90	44
Shape index of plate buckling curve, $\frac{P_{p2}}{P_{p1}}$	—	.60	1.45	.85	1.26	1.25	.90	1.62	1.02	.60
Plate buckling energy, A_p, g. cm.	9.0	51	12	30	27	16	28	18	89	45
Plate buckling energy, B_p, g. cm.	7.5	32	10	22	21	13	21	15	62	32
Plate buckling noncyclical energy loss, $\frac{A_p - B_p}{A_p}\cdot 100$	17	37	17	27	22	19	25	17	31	29
Recovered plate buckling energy, C_p, g. cm.	6.0	25	7.5	14	14	9.0	14	13	39	17
Recovered plate buckling energy, $\frac{C_p}{A_p}\cdot 100$	67	48	63	46	52	56	48	72	44	25
Shell buckling force, P_{d1}, g.	14	520	64	86	220	130	110	62	850	720
Shell buckling force, P_{d2}, g.	13	160	39	84	140	79	78	62	580	490
Shape index of shell buckling curve	.93	.31	.61	.98	.64	.61	.70	1.00	.68	.67
Shell buckling energy, A_d, g. cm.	13	200	40	52	140	84	77	60	600	500
Shell buckling energy, B_d, g. cm.	9.5	83	34	36	97	62	63	45	250	280
Shell buckling, noncyclical energy loss, $\frac{A_d - B_d}{A_d}\cdot 100$	27	58	17	31	33	26	20	25	58	45
Recovered shell buckling energy, C_d, g. cm.	5.5	33	15	12	40	31	25	28	130	120
Recovered shell buckling energy, $\frac{C_d}{A_d}\cdot 100$	40	17	37	23	27	37	32	46	21	48
Permanent deformation, shell buckling	5	9	3	18	10	2	6	3	17	15
Shell buckling force/plate buckling force, $\frac{P_{d2}}{P_{p2}}$	1.4	3.6	3.4	3.1	5.2	5.3	3.0	3.0	6.4	10.9
Formability, $P_{p2}\cdot\gamma$	323	8.4	107	380	64	97	560	346	282	16
Anisotropy, $\frac{P_{p2}\cdot\gamma}{t^2}\cdot 10^{-2} = \text{const.}\cdot\frac{E_{a1}}{E_{a2}}$	34	.48	12	13	3.0	2.5	14	16	8.7	.19
Apparent shell buckling modulus, $\frac{P_{d2}}{t^{3.25}}\cdot 10^{-1} = \text{const.}\cdot E_{a1}\cdot\sqrt[4]{E_{a2}}$	58	270	200	62	170	37	33	69	360	64
Apparent bending modulus, $\frac{P_{p2}}{t^3}\cdot 10^{-1} = \text{const.}\cdot E_{a1}$	31	60	42	17	27	6.3	9.9	20	49	5.7
Stiffening index, $\frac{P_{p2}}{W\cdot t^2}\cdot 100 = u_1$	120	300	100	51	58	170	27	37	82	130
Crease recovery angle, %	56	91	69	73	48	68	66	62	41	48

In shell buckling quite a large permanent deformation is sometimes obtained. This is given in Table I. Permanent deformation will be further discussed under crease recovery.

Repeated Buckling Cycles

The second buckling cycle does not generally give the same buckling curve as the first. The third and subsequent curves, however, show very small additional deviations. The difference between the first and the second curve is called noncyclical energy loss. This loss can be appreciable even if the deformation is zero at zero load, or if the sample is stretched to attain zero deformation. This shows that the fibers will never return to their original position even if the fabric appears smooth. On the other hand, it also means that the first-time

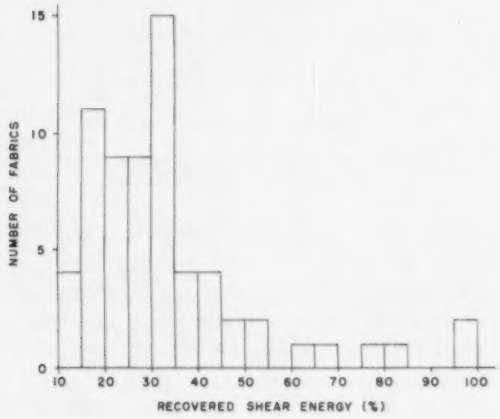

Fig. 17. Histogram of recovered energy at shearing.

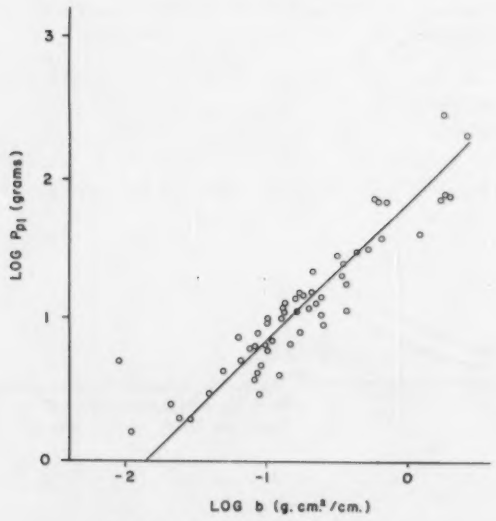

Fig. 18. Plate buckling force P_{p1} versus bending stiffness b.

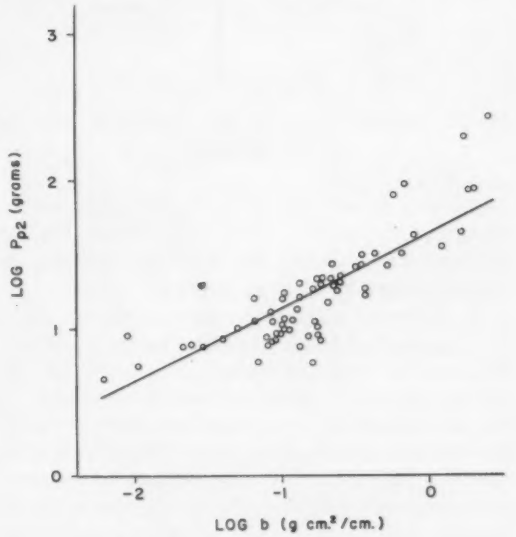

Fig. 19. Plate buckling force P_{p2} versus bending stiffness b.

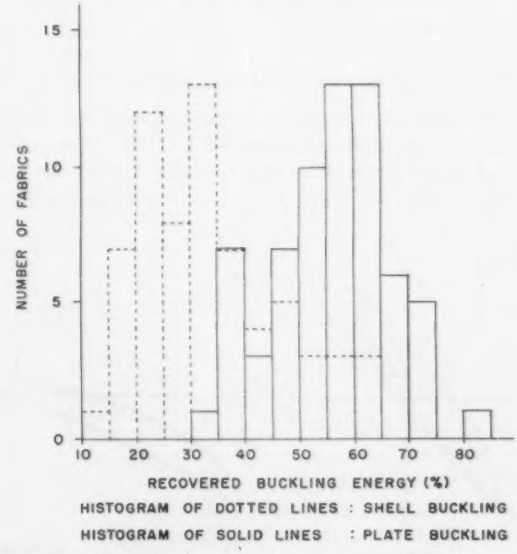
NUMBER OF FABRICS
RECOVERED BUCKLING ENERGY (%)
HISTOGRAM OF DOTTED LINES : SHELL BUCKLING
HISTOGRAM OF SOLID LINES : PLATE BUCKLING

Fig. 20. Histogram of recovered energy at buckling.

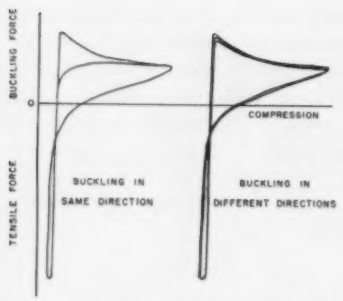

Fig. 21. Successive curves of plate buckling in same and in opposite directions.

curve may be subject to error, depending on the history of the sample. This phenomenon has not yet been studied, but from general experience the influence does not seem to be great.

If, however, a plate-buckling cycle is made, buckling to the left, and then another cycle is made, this time buckling to the right, it is found that the previous first-time buckling curve is repeated. A second cycle in the same direction, however, gives again a noncyclical energy loss. These curves are shown in Figure 21. This phenomenon is consistent with the hypothesis that the energy loss is due to friction. The values for the noncyclical energy loss for plate buckling are given in Table I and in Figure 22.

The recovery properties will be further discussed under crease recovery.

Influence of Setting on Fabric Properties

Setting has been shown to have sometimes a very large influence on fabric properties [3]. Figures 13 and 14 gives shearing and buckling curves for set and unset nylon fabrics. There is a remarkable

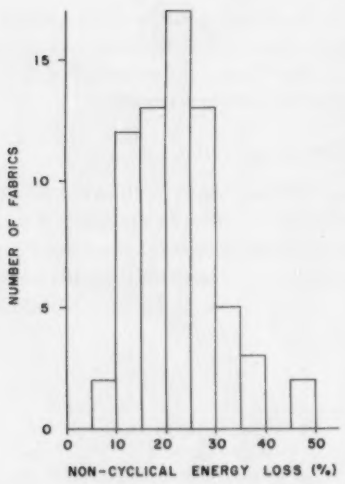

Fig. 22. Histogram of the noncyclical energy loss at plate buckling.

increase in the shear angle with setting and also a marked increase in recovered buckling energy.

Figures 23 and 24 give shearing curves for a dry and wet wool fabric, set and unset. Setting increases the shear angle, particularly that of the wet fabric.

Setting will be further discussed under crease recovery.

Relations Among Shell Buckling, Plate Buckling, and Shearing

As shown in Figure 5, Part II, the deformation pattern in shell buckling is more complex than in the case of plate buckling. It is very similar to the pattern obtained when a sleeve is buckled. The shell buckling load ought to be more closely

Fig. 23. Change in shearability for a dry worsted fabric (186 g./m.^{2}); (a) unset fabric, (b) set fabric.

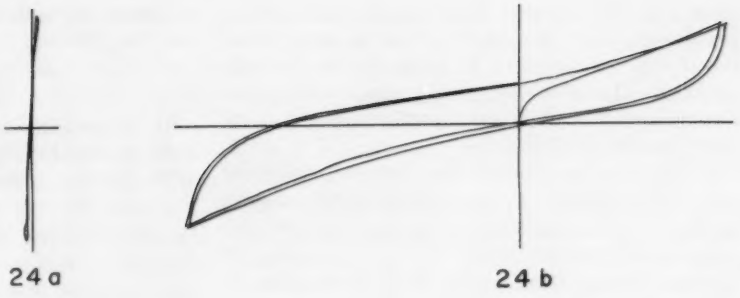

Fig. 24. Change in shearability for the worsted fabric in Figure 23, when wet. Chart and cross-head speed as well as full scale load of Instron are equal in all the four measurements; (a) unset fabric, (b) set fabric.

related to the handle of a fabric than is plate buckling load or bending stiffness. But what is the relation between shell buckling load and plate buckling load?

By taking the ratio of these values, i.e., P_{d2}/P_{p2}, values between 1 and 11 are obtained (see Table I). It was observed that low values are associated with high values of the shear angle, γ. If the ratio is plotted against log γ (Figure 25), a definite relation between P_{d2}/P_{p2} and γ is obtained. Three values are marked with a circle. These are for a nonwoven fabric and two fabrics showing large differences between the warp and weft values of P_{p2}.

By means of multiple regression analysis we can obtain the following empirical relation among P_{d2}, P_{p2}, and γ.

$$P_{d2} = \text{const.} \frac{P_{p2}}{\sqrt[4]{\gamma}} \qquad (1)$$

This relationship explains 85% of the total variation. In Figure 26 we have plotted $P_{d2(\text{calc.})}$ against $P_{d2(\text{meas.})}$.

It is evident that the shear properties of fabrics are important in determining handle.

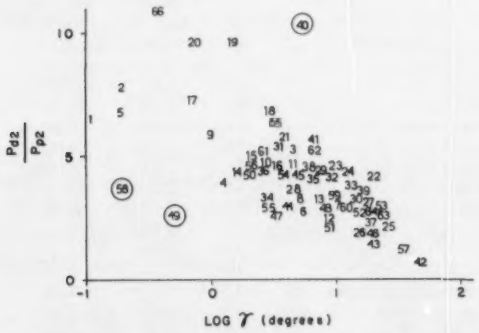

Fig. 25. Ratio of buckling force P_2 from shell and plate buckling versus shear angle.

Formability

Formability of a fabric is a term used by the tailor to express ease of making up. It is found that, under certain circumstances, formability is dependent on the total amount of compression a fabric can take up in the plane in a certain direction before it buckles [7]. The total compression is called buckling compression and is denoted by B. For the case of plate buckling we can write $B = \text{const.} \cdot b \cdot C$, where b is the bending stiffness and C the compressibility. A material constant, F, is now defined as $F = b \cdot C$ and is called the formability of a fabric. It is further shown that forming of spherical and saddle-shaped shells also leads to compression and ultimately to buckling at certain places in the fabric [7]. If the compression takes place in different directions at the

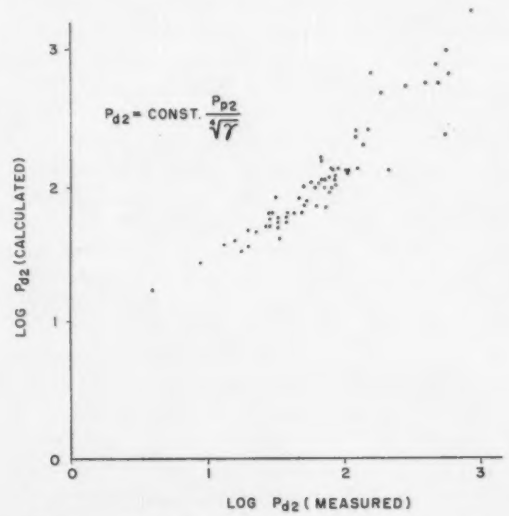

Fig. 26. Calculated value of $P_{d2} = c \cdot P_{p2}/\sqrt[4]{\gamma}$ versus measured value of P_{d2}.

same time, the direction which has the highest compressibility will dominate. The highest compressibility of a fabric is generally in the bias direction. There is also a relationship between the compressibility in the bias direction and the shear angle of a fabric [7].

For a complex deformation like shell buckling there will obviously be spherical and saddle-shaped surfaces and, consequently, compression in the plane in different directions. Since $P_{p2} \approx \text{const.} \cdot b$ and $C_{45°} \approx \text{const.} \cdot \gamma$ we can write the formability of a fabric as $F \approx P_{p2} \cdot \gamma$. This expression is used in the following discussions to characterize the fabric in certain respects. The values of $P_{p2} \cdot \gamma$ are given in Table I; they vary from 2 to 800 for the different fabrics.

Observations have shown that higher formabilities give rounder creases, which affect the appearance of a creased fabric, but no quantitative measurements have yet been made. Since we have shown previously that the forces necessary for complex deformations are dependent on both P_{p2} and γ and it is now seen that formabilities and crease patterns depend on the same factors, it is of interest to study how the values for these factors vary for different fabrics.

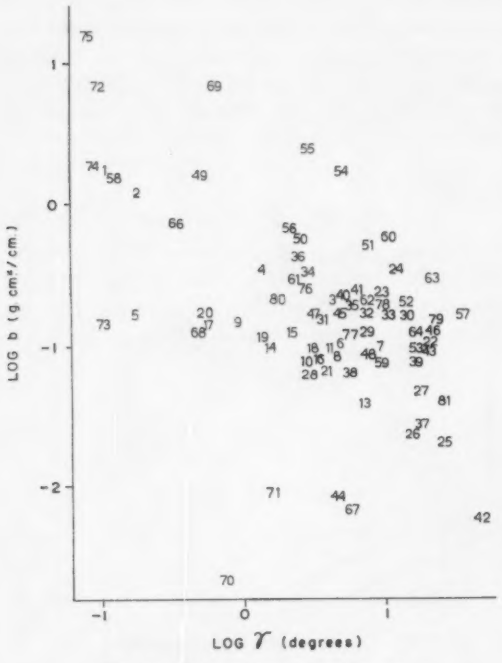

Fig. 27. Map of bending stiffness b versus shear angle γ.

Fabric Map

It is possible to draw a map giving bending stiffness (log b) and shear angle (log γ). Bending stiffness b was chosen instead of the related buckling load P_{p2}, so that some materials for which buckling curves were not measured could be included. On such a map we can study the relative positions of the different fabrics.

The map is shown in Figure 27. The data for materials not included in Table I are given in Table II. They include sheet rubber, plastic films, papers, and some fabrics treated in special ways.

It is seen immediately that there is no relationship between bending stiffness and shear angle; hence the use of the word map. It is also seen that the different materials are scattered over a wide area and that there is very little overlapping of textile (No. 1–66, 76–81) and nontextile materials (No. 67–75). The character of a material depends largely on its position on the map.

If $\gamma < 0.1$ the materials have the character of paper or cardboard. When γ increases the material becomes softer. The bending stiffness influences the character in the following way: if γ is small and b large we get a rigid plate (direction of upper left corner); if γ is small and b small we get films which crackle and break (direction of lower left corner); if γ is large and b large the material will show a full handle (direction of upper right corner); and if γ is large and b is small the material

TABLE II

Material	Number	Shear angle, γ, degrees	Bending stiffness, b, g.cm.²/cm.
Sheet rubber, 207 g./m.²	67	6.0	0.007
Sheet rubber, 407 g./m.²	68	0.50	0.15
Sheet rubber, 1715 g./m.²	69	0.64	7.2
Plastic film, 28 g./m.²	70	0.73	0.0023
Plastic film, 127 g./m.²	71	1.64	0.0092
Plastic film, 338 g./m.²	72	0.094	7
Paper, 30 g./m.²	73	0.102	0.15
Paper, 65 g./m.²	74	0.086	2.0
Paper, 128 g./m.²	75	0.065	15
Flameproofed fabric	76	2.7	0.26
Number 76, charred	77	6.0	0.16
Worsted fabric	78	10.2	0.19
Number 78, set	79	24.1	0.15
Number 78, wet	80	1.7	0.22
Number 79, wet	81	27.0	0.040

will show a soft and limp handle (direction of lower right corner).

If the position of the different materials on the map is studied it will be evident that each type of end-use occupies a certain distinct area. This means that end-uses can in part be characterized by bending and shearing properties, although only stiffness properties are being considered here. Recovery properties will be discussed later on. It is not necessary to underline the advantage of being able to show the relative positions of various fabrics on such a map as described above.

The formability $P_{p2} \cdot \gamma$ or $b \cdot \gamma$ increases in the direction of a line upwards to the right of an angle of 45°. It must be remembered that the formability as defined here has nothing to do with the force required to do the actual forming.

The force required for complex deformation, e.g., shell buckling, increases in the direction of a line upwards to the left at an angle of 104° to the shear axis.

All wool fabrics are found within an area representing high formability, which is in accordance with practical experience.

The same fiber type can be found over large areas in Figure 27. This supports the view that the mechanical properties of fibers have relatively little influence on the stiffness properties of fabrics. In the next paragraph, evidence is presented to show that it is fabric construction rather than any fiber property which determines the position in Figure 27. The fiber properties, however, may influence the stiffness properties indirectly by permitting only certain fabric constructions during spinning, weaving, and finishing. The relatively much greater influence of construction than of fiber properties on the character of a fabric was dramatically shown by taking a flameproofed cotton fabric (TPHC–APO) obtained from Southern Regional Research Laboratory, New Orleans, and heating it to red heat. The fibers were completely converted to carbon, but the sample maintained the character of a fabric. The resistance to higher loads was very low, but shearing and both plate and shell buckling could be measured without affecting the sample. The sample shrunk considerably during burning and its weight per unit area decreased to one half of its original value. This treatment moved the fabric from position 76 to 77 in Figure 27 (see Table II), which is rather insignificant in view of the drastic change which must have taken place in the fibers themselves. The change of position can probably be explained by the decrease in weight and density.

Another example of change in position in Figure 27 is obtained when wool fabrics are set. In Table II values are given for b and γ for set (2% $NaHSO_3$ at 100° C. for 10 min.) and unset wool fabrics, conditioned and wet. These values are taken from Cednäs [3]. In the conditioned state the fabric is moved from position 78 to 79 by setting, a change of the same magnitude as with the flameproofed fabric. A still larger difference is obtained in the wet state: a change from position 80 to 81. It should be remarked here that mechanical properties in the wet state might be of great importance for wash-and-wear fabrics.

It is generally assumed that setting of wool fibers has very little influence on the mechanical properties of the fibers. On the other hand, there is evidence of a change in the fabric construction by shrinkage and stress relaxation due to setting [3]. In the term fabric construction we include both the geometrical arrangement of the fibers and interaction between them by friction and adhesion.

Analysis of Formability and Shell Buckling Load

If a thin plate is subjected to a compressive load, the plate can theoretically buckle in two directions; perpendicular to the plane of the plate and in the plane of the plate. Naturally it will always buckle in the direction of least resistance which, for a free plate, is perpendicular to the plane (Figure 28a).

If, however, a fabric is placed between two glass plates to prevent buckling perpendicular to the fabric plane, it is possible to obtain buckling in the plane of the fabric (Figure 28b). According to Part I, the buckling load in that direction will be dependent on the shear properties. When buckling a shell, it is not self-evident that buckling perpendicular to the fabric plane gives the least resistance at all points. The fact that shell buckling is related to shear shows there may be buckling in both directions.

But P_{p2} can be written as $P_{p2} \approx \text{const.} \cdot b_1$, where b_1 is the bending stiffness perpendicular to the fabric plane. We can also write $1/\gamma \approx \text{const.} \cdot b_2$, where b_2 is the bending stiffness in the fabric plane. The formability $P_{p2} \cdot \gamma$ could then be written

$$P_{p2} \cdot \gamma \approx \text{const.} \cdot \frac{b_1}{b_2} \qquad (2)$$

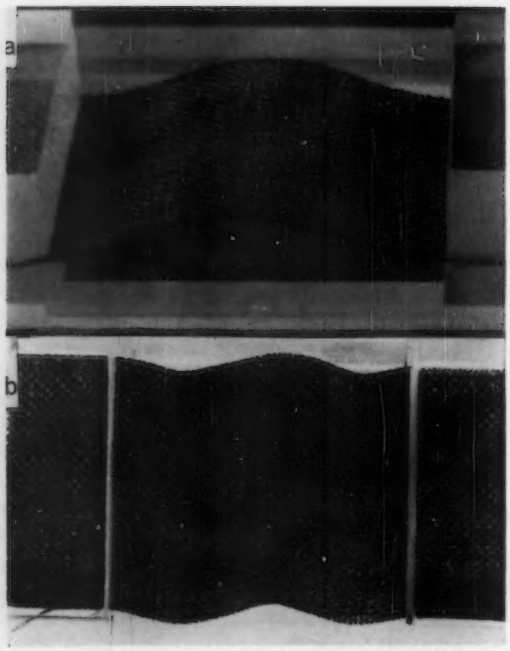

Fig. 28. Buckling of a fabric (a) perpendicular to the plane and (b) in the plane of the fabric.

This means that formability in this case can be expressed as the ratio between the bending stiffnesses in the two directions.

It is very important to know how formability can be influenced by changing the values of b_1 and b_2, and thus to be able to control important properties of a fabric.

According to the theory of elasticity, $b_1 = E \cdot I_1$ where E is the modulus of elasticity of the fibers and I_1 the resulting moment of inertia for the fibers. If the moment of inertia for the fiber i is I_{0i}, its cross-sectional area is A_i, and the distance between the neutral plane and the center of gravity of the fiber cross-section is a_i, we can write

$$I_1 = \sum_1^n I_{0i} + \sum_1^n A_i \cdot a_i^2 \qquad (3)$$

where n is the number of fibers in the fabric cross section. We then have

$$\frac{b_1 - E \cdot \sum_1^n I_{0i}}{E \cdot \sum_1^n A_i} = \sum_1^n a_i^2 \qquad (4)$$

if

$$\sum_1^n A_i \cdot a_i^2 \approx \sum_1^n A_i \cdot \sum_1^n a_i^2$$

The term $\sum_1^n a_i^2$ is a factor which gives the stiffening effect of construction and friction.

If E, I_0, A, n for the fibers and b_1 for the fabric are known, it should be possible to calculate this stiffening factor. We can now write

$$P_{p2} \cdot \gamma = \text{const.} \cdot \frac{b_1}{b_2} = \text{const.} \cdot \frac{(\sum_1^n I_{0i} + \sum_1^n A_i \cdot a_i^2)_1}{(\sum_1^n I_{0i} + \sum_1^n A_i \cdot a_i^2)_2}. \qquad (5)$$

If

$$\sum_1^n I_{0i} \ll \sum_1^n A_i \cdot a_i^2$$

and

$$(\sum_1^n A_i)_1 = (\sum_1^n A_i)_2$$

we have

$$P_{p2} \cdot \gamma = \text{const.} \cdot \frac{(\sum_1^n a_i^2)_1}{(\sum_1^n a_i^2)_2} \qquad (6)$$

Equation 6 means that such an important factor as formability is independent of the mechanical properties of the fiber. The same result is obtained by defining

$$I = r^2 \cdot \sum_1^n A_i$$

where r is the radius of inertia for the fabric. We then have

$$b = E \cdot I = E \cdot r^2 \cdot \sum_1^n A_i,$$

and

$$P_{p2} \cdot \gamma = \text{const.} \cdot (r^2)_1 / (r^2)_2$$

Unfortunately the values for the fiber parameters in our commercial fabrics are not known, so we cannot calculate either the stiffening factor, $\sum_1^n a_i^2$, or r^2 for these. However, we can choose

another line of attack on this problem, which may have certain practical advantages. If the fabric is regarded as a thin plate with thickness t and width h, and the structure is disregarded, we can write

$$b_1 = E_{a1} \cdot I_{g1} = E_{a1} \cdot \frac{t^3 \cdot h_1}{12} \quad (7)$$

and

$$b_2 = E_{a2} \cdot I_{g2} = E_{a2} \cdot \frac{t \cdot h_2^3}{12} \quad (8)$$

where E_a is an apparent modulus of elasticity of the fabric and I_g the moment of inertia based on the geometrical dimensions of the fabric. We can then write

$$P_{p2} \cdot \gamma = \text{const.} \cdot \frac{E_{a1}}{E_{a2}} \cdot t^2 \cdot \frac{h_1}{h_2^3} \quad (9)$$

but as h_1 and h_2 have constant values

$$P_{p2} \cdot \gamma = \text{const.} \cdot \frac{E_{a1}}{E_{a2}} \cdot t^2 \quad (10)$$

If E_{a1} and E_{a2} have different values, the material is anisotropic in nature. It is very interesting to see that the formability is directly related to the thickness of the fabric and also to the anisotropy of the fabric. Increased thickness increases the formability; at constant thickness, an increased ratio of E_{a1} (for bending perpendicular to the plane) to E_{a2} (for bending in the plane) also increases the formability. It is now possible to calculate an expression for E_{a1} by taking the ratio P_{p2}/t^3 and another for E_{a1}/E_{a2} by taking the ratio $(P_{p2} \cdot \gamma)/t^2$. These values are given for our commercial fabrics in Table I. If the bending stiffness and the shearability vary with the deformation, which generally is the case, E_{a1} and E_{a1}/E_{a2} will also give variable values.

It should also be noted that bending and extension–compression, which gives a formability of $F = b \cdot C$, can be treated in the same manner as above. Equation 10 then takes the form

$$b \cdot C = \text{const.} \cdot \frac{E_{a1}}{E_{a2}} \cdot t^2 \quad (11)$$

where E_{a2} now means the modulus of elasticity for extension–compression.

From Table I it is seen that very dense and very porous fabrics have low values of E_{a1}/E_{a2}. A low cover factor generally increases this value. All silk fabrics give very high values and natural silk an extremely high one. There is no notable difference between normal worsted fabrics and cotton fabrics; they all belong to a middle group. The high formability of wool fabrics evidently depends on a higher thickness.

But if high formability is to be combined with soft handle, the shell buckling load must have a fairly low value. According to Equation 1

$$P_{d2} = \text{const.} \cdot \frac{P_{p2}}{\sqrt[4]{\gamma}} = \text{const.} \cdot t^3 \cdot \sqrt[4]{t} \cdot E_{a1} \cdot \sqrt[4]{E_{a2}} \quad (12)$$

If the value of t is high to give good formability, the values of E_{a1} and E_{a2} must be low to give low values for shell buckling. From Table I it is seen that all wool fabrics and other porous fabrics have very low values for E_{a1}. Cotton and silk fabrics show much higher values.

If we calculate $(P_{d2})/(t^3 \cdot \sqrt[4]{t})$ we obtain an expression for $E_{a1}\sqrt[4]{E_{a2}}$, which could be regarded as a modulus of elasticity for shell buckling. Values for this are given in Table I. It is evident from these values and the values for E_{a1} and P_{d2}, that Peirce's assumption [8] that handle is directly related to bending stiffness is not correct. The fabric anisotropy will obviously influence the behavior of a fabric to a very large extent. Knowledge of the anisotropy of fabrics is therefore very important.

The volume weight or density W/t, where W is the weight per square meter and t the thickness, has a large influence on E_{a1}. This can be seen from Figure 29, where log E_{a1} is plotted against log W/t. The line represents an equation of the type $E_{a1} = \text{const.} \cdot (W/t)^5$, which shows that very small changes in the volume weight will lead to large changes in the modulus of elasticity.

As mentioned previously, the bending stiffness or the fabric modulus of elasticity will be determined by the stiffness of the fibers themselves and by the fabric construction, or rather the extent to which the fibers are prevented from taking up a position in the neutral plane. We describe this latter phenomenon as stiffening. Since the fiber stiffness is not known, we can relate the stiffening effect to the volume weight. We can write

$$\frac{E_{a1} \cdot t}{W} = u_1$$

or

$$\frac{E_{a2} \cdot t}{W} = u_2$$

where u_1 and u_2 are stiffening factors which give the increase in E_{a1} or E_{a2} for each unit of volume weight. The value of u_1 is given in Table I. As can be expected from previous results, u_1 is very low for wool fabrics and porous fabrics and much higher for normal cotton fabrics.

The reason for introducing the volume weight is that the weight of a fabric is a very important factor in determining the comfort of a garment. We are, in fact, faced with the problem of making light fabrics which have soft handle and high formability. From the analysis of the data given above, the following principal way can be suggested. Assume that W is small. In order to increase formability, the thickness t can be increased. This lowers the values for the volume weight and E_{a1}. In order to keep E_{a1} reasonably high, the stiffening factor u_1 must be increased. If it is impossible to obtain sufficiently high values of t and u_1, the ratio E_{a1}/E_{a2} must be increased. This means that u_1 can be increased but not u_2, which is related to shearing. Increasing u_1 must be done by spot-welding between the fibers, as friction will not be sufficient. The spot-welding process then has to be done without affecting u_2 (that is, shearing); in fact it may be necessary to take special care to reduce the value of u_2. This points to a spot-welding treatment of the yarn, retaining its low density and special treatment to give the fabric maximum shearability or maximum compressibility in warp and weft directions, if we are interested in high formabilities in these directions.

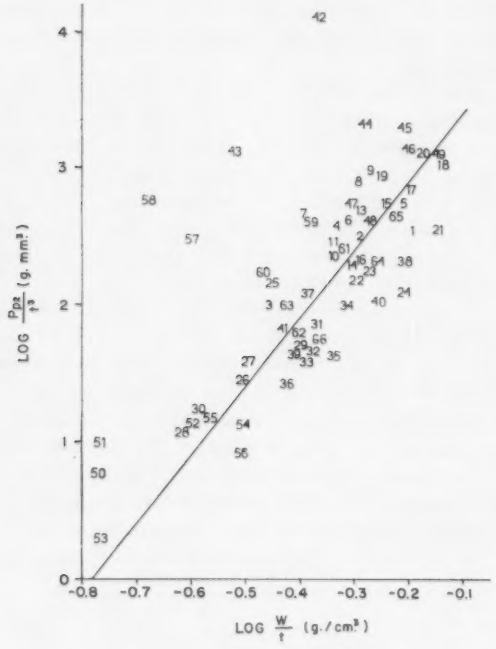

Fig. 29. Apparent bending modulus E_{a1} versus volume weight.

Crease Recovery

The recovery properties of various fabrics have already been discussed under buckling and shearing. The crease recovery of our fabrics has been measured by the Monsanto method and the results examined to see whether there is any correlation with some other mechanical properties of these fabrics as measured by our methods.

Quite surprisingly, it was found that there was some relationship between crease recovery angle and formability $P_{p2} \cdot \gamma$. This is shown in Figure 30. Even the shear angle itself gives a certain relationship (Figure 31). The only fabric falling completely outside the scatter is a nonwoven one. Generally it is assumed that there is a simple bending deformation when making the crease, and therefore it is rather surprising that shearability is involved. This is probably due to the fact that, at a certain bending degree of deformation, the deformation sideways requires less force and shearing occurs just in the bend. Figure 32, where the fabric is

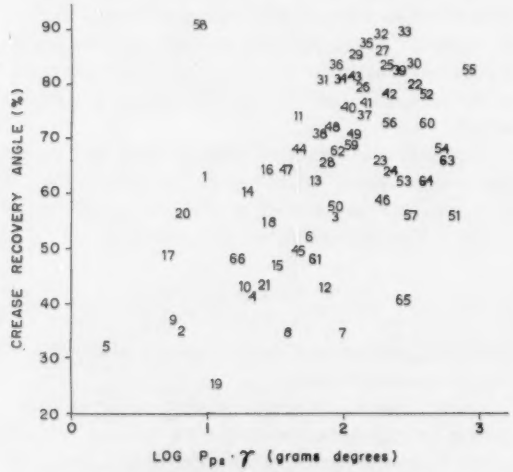

Fig. 30. Crease recovery versus formability.

pressed between two glass plates, illustrates just what may happen.

But the recovery from deformation evidently is not solely dependent on the degree of deformation given to the fabric. Previously the energy losses due to deformation were discussed and it was shown that they are different for different fabrics. This difference in energy loss may also have an influence on the crease recovery angle. A permanent deformation must always be associated with a loss of energy, but the reverse is not always true.

It is therefore fairly obvious to assume that the crease recovery angle is related to the noncyclical energy loss and, since we have reasons for believing that creasing is a complex deformation, to the noncyclical energy loss in shell buckling.

A value can be obtained for the permanent deformation in shell buckling, but this is difficult to use because of the geometrical relation between this value and the value for the actual radius of curvature in the buckled sample.

Unfortunately, we have two different series of values for the noncyclical energy loss in shell buckling. For half of the fabrics, the second cycle was started when the load was zero. This should give the correct values; in Figure 33 the crease recovery angle is plotted against this energy loss. For the other half, the second cycle was started when the sample was stretched to attain zero deformation. The relation between these values for the noncyclical energy loss and the crease recovery angle is given in Figure 34. There is also a good agreement between these values.

Theoretical Analysis and Discussion of the Recovery Process

It has been shown that crease recovery may depend on the mechanical properties of the fabric and especially on the formability and the noncyclical energy loss in shell buckling. We have previously put forward the hypothesis that the energy loss is mainly dependent on fiber-to-fiber friction. This means that, when there is a permanent deformation in creasing and other types of deformation, there may be either a permanent deformation of the fibers themselves or the friction between the fibers may prevent them from returning to their original positions in the fabric.

The question of whether crease recovery properties depend on permanent fiber deformation or on fiber friction has been discussed very extensively in the literature [1, 2, 4, 5, 6, 9, 10].

It is assumed here that the permanent deformation of a fabric depends only on fiber friction; we will try to show how fiber properties and fabric construction may interact to give a permanent deformation.

In every state of deformation, all fibers must be in a state of force equilibrium. At each point of contact, there are two equal reaction forces P. These forces can be split up into the components P_z perpendicular to the plane of contact and P_x parallel to the plane of contact. At force equilibrium we have $P_x < \mu \cdot P_z$ where μ is the coefficient of friction. The value of P differs from point to point and changes with the deformation. It

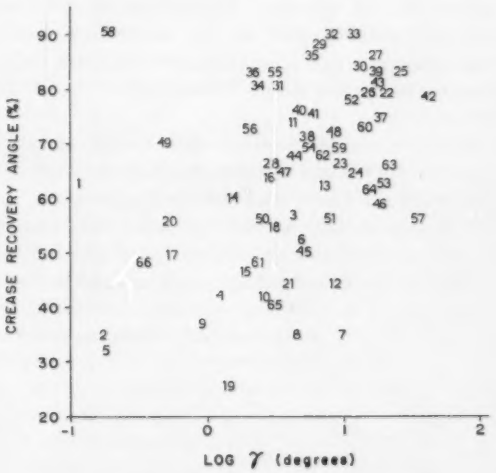

Fig. 31. Crease recovery versus shear angle.

Fig. 32. Folding a crease in a fabric, showing shear in the fold.

should be noted that setting of fibers, i.e., permanent stress relaxation, will diminish the value of P. The value of P will further depend on the fiber stiffness.

The distribution of the value and direction of P at different points of contact and the change in this distribution with deformation are extremely complicated to calculate. However, one point of contact can be selected and certain assumptions made about P, and thus a qualitative picture of what may happen at each point of contact can be obtained.

Assume that there is a permanent deformation due to the fact that the elastic forces in the deformed fibers cannot overcome the frictional forces at each point of contact. But the frictional forces can be written as $N \cdot \mu$, where N is the normal force in the point of contact. The permanent deformation will then depend on the interaction among fiber stiffness, coefficient of friction, and fabric construction when we go from a higher to a lower deformation.

However, the forces obtained in the fibers during recovery from deformation are dependent on the visco-elastic properties of the fiber.

It is now possible to illustrate what may happen by means of a simple rheological model (Figure 35).

The springs and the dash-pot illustrate the visco-elastic fiber; the friction element represents the point of contact. In actual fact, the fabric must be illustrated by a whole series of such models with varying values of N, spring constants k_1 and k_2, and dash-pot viscosity, but we will here study only the behavior of this simple model. For simplicity it is also assumed that N, k_1, and k_2 have constant values.

In Figure 36 we have given load–deformation curves for this model under certain defined conditions. The factor that will be varied is the speed of deformation.

First, assume that the deformation is so rapid that there is no movement of the dash-pot. The force immediately increases to $N \cdot \mu$. Sliding then occurs in the friction element and the force increases with a slope of k_1 to the deformation ϵ_1 and the force P_1, where $P_1 = k_1\epsilon_1 + N\mu$. The model is then immediately unloaded. The force decreases, first to P_2, where $P_2 = P_1 - 2N\mu$ and with the slope k_1, until $P = 0$ and $\epsilon = \epsilon_2$, where $\epsilon_2 = N\mu/k_1$. The deformation ϵ_2 is then the permanent deformation of the model. This explains why permanent deformations can occur in a glass fabric made of almost perfectly elastic fibers. If, instead of immediately unloading the model at P_1 and ϵ_1, the deformation is maintained for an infinitely long period, there will be flow in the dash-pot until there is equilibrium between the springs k_1 and k_2. The

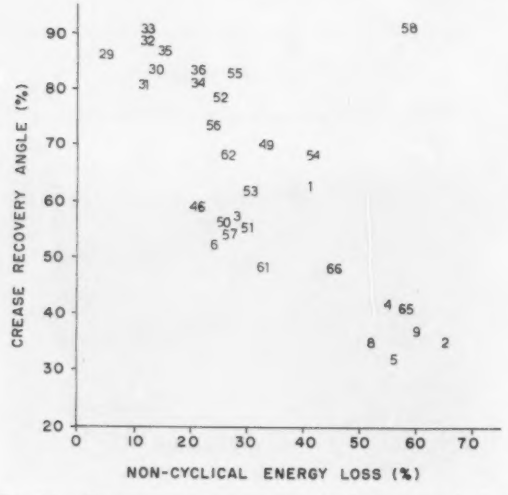

Fig. 33. Crease recovery versus noncyclical energy loss at shell buckling. Direction of cross-head changed at $P_d = 0$.

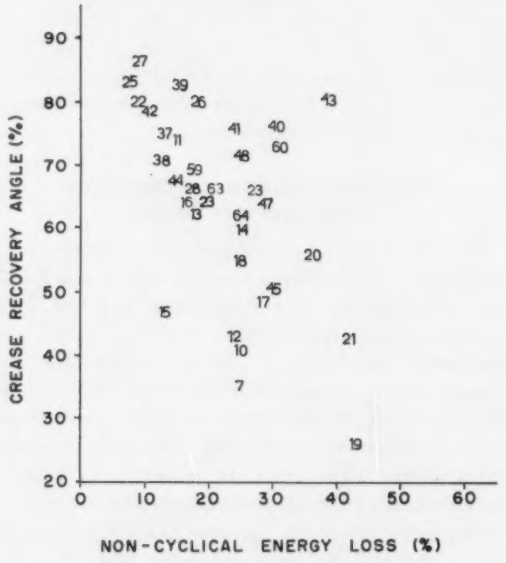

Fig. 34. Crease recovery versus noncyclical energy loss at shell buckling. Direction of cross-head changed at deformation = 0.

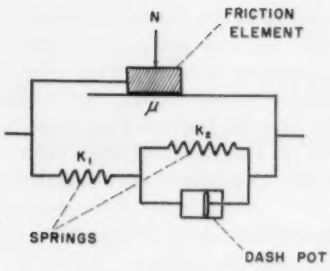

Fig. 35. Rheological model.

force then decreases to P_3, where $P_3 = k_3 \cdot \epsilon_1 + N\mu$ and $k_3 = (k_1 \cdot k_2)/(k_1 + k_2)$.

The same point would have been reached if the model had been deformed infinitely slowly. At this point the model is suddenly unloaded. The force will then decrease immediately to P_4, where $P_4 = P_3 - 2N\mu$ and then with the slope of k_1 until $P = 0$ and $\epsilon = \epsilon_3$, where $\epsilon_3 = \epsilon_1 - P_4/k_1$. At this point, however, the springs k_1 and k_2 are not in equilibrium, so that there is flow in the dash-pot until equilibrium is reached, and then the model has retracted to the deformation ϵ_4, i.e., the same deformation which would have been reached if the model had recovered infinitely slowly with the slope of k_3. We then have $\epsilon_4 = \epsilon_1 - P_4/k_3$.

The recovery of this model can be divided into three steps: immediate recovery ($\epsilon_1 - \epsilon_3$ or $\epsilon_1 - \epsilon_2$), delayed recovery ($\epsilon_3 - \epsilon_4$ or 0), and permanent deformation (ϵ_4 or ϵ_2), dependent on speed of deformation.

These values can be expressed in ϵ_1, k_1, k_3, N and μ.

a. immediate recovery

$$\epsilon_1 - \epsilon_2 = \epsilon_1 - \frac{N\mu}{k_1}$$

$$\epsilon_1 - \epsilon_3 = \frac{k_3\epsilon_1 - N\mu}{k_1}$$

b. delayed recovery

$$\epsilon_3 - \epsilon_4 = (k_3 \cdot \epsilon_1 - N\mu)\left(\frac{1}{k_3} - \frac{1}{k_1}\right)$$

c. permanent deformation

$$\epsilon_2 = \frac{N\mu}{k_1}$$

$$\epsilon_4 = \frac{N\mu}{k_3}$$

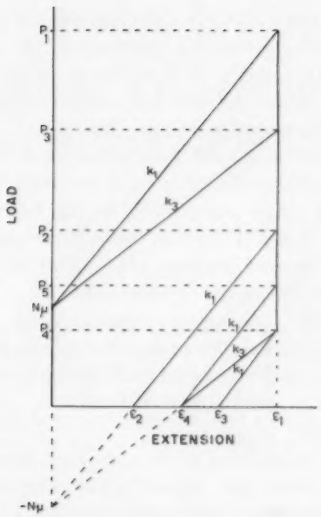

Fig. 36. Force–deformation diagram for the rheological model in Figure 35.

These equations hold only if $N\mu < k_1 \cdot \epsilon_1$; otherwise there will be no slippage in the friction element.

For this simple model it is found that the permanent deformation as suggested depends on the normal force, the coefficient of friction, and the fiber stiffness—but on what value for the fiber stiffness?

We now draw a line through ϵ_4 with the slope k_1. This line intersects the vertical line through ϵ_1 in P_5. If the force decreased from P_2 to P_5 instead of P_4, the delayed recovery will disappear but the permanent deformation will still be ϵ_4, which is determined by the stiffness k_3. If $(P_2 - P_5)/(P_2 - P_4)$ gives the relative relaxation in the model, we have

$$\frac{P_2 - P_5}{P_2 - P_4} = \frac{N\mu}{k_3 \cdot \epsilon_1}$$

If the relative relaxation is greater than that given by the equation, we get delayed recovery, and the permanent deformation will be $\epsilon_4 = N\mu/k_3$. If the relative relaxation is less, there will be no delayed recovery, but a permanent deformation between ϵ_2 and ϵ_4. This means that the fiber stiffness obtained when the fiber is loaded infinitely slowly will be one very important factor in determining the permanent deformation. Since we go from a higher to a lower deformation, it is seen that the original deformation need not be maintained until we obtain complete relaxation in the

fibers in order to obtain the maximum permanent deformation. Since the first part of the relaxation takes place rapidly, it is to be expected that the minimum fiber stiffness very soon will determine the permanent deformation.

It should again be mentioned that the model described above can only be a very rough approximation of what takes place in the fabric, and in order to obtain a precise description the problem must be treated statistically. This is, however, far beyond the scope of this paper.

From this qualitative treatment we can, however, obtain many ideas as to which factors should be isolated and measured and also under what conditions the permanent deformation should be determined.

It was mentioned previously that setting processes influence the recovery behavior of fabrics. Two phenomena may be responsible for this. Setting causes a relaxation of the normal forces between the fibers and thereby influences the recovery. Alternatively, fabric shrinkage may occur as in wool fabric setting, which may lead to a change in fabric construction and thus also in the normal force between fibers. Furthermore, after setting, the original positions of the fibers in the fabric are the positions of zero potential energy, so that the fibers are now unable to find any other position with lower potential energy which they would naturally do if such positions existed.

From Table I it is seen (Fabric Numbers 10, 11, 12, and 13) that resin treatments of cotton do not appreciably and constantly change any mechanical properties other than the crease recovery angle and other recovery properties. It may be assumed that in this case the effect of the treatment is to increase the minimum fiber stiffness.

From the discussion above it is evident that if $N \cdot \mu$ is very small we get a small permanent deformation, but if $N \cdot \mu$ is very large—for instance if the fibers are spot-welded together—there will be no slippage and no friction-dependent permanent deformation. This means that there are two minima for the permanent deformation at extreme values of $N \cdot \mu$; accordingly, there ought to be an intermediate value where the permanent deformation has a maximum value.

This may explain why a nonwoven fabric (No. 58) in which the fibers are spot-welded shows very good crease recovery according to Table I.

Acknowledgment

Our thanks are due to the Swedish Technical Research Council and the Swedish Consumer Research Council, who sponsored this work.

Literature Cited

1. Beste, L. F. and Hoffman, R. M., TEXTILE RESEARCH JOURNAL **20**, 441–453 (1950).
2. Buck, G. S. and McCord, F. A., TEXTILE RESEARCH JOURNAL **19**, 216–247 (1949).
3. Cednäs, M., to be published.
4. Gagliardi, D. D. and Gruntfest, I. J., TEXTILE RESEARCH JOURNAL **20**, 180–188 (1950).
5. Hamburger, W. J., TEXTILE RESEARCH JOURNAL **18**, 102–113 (1948).
6. Hamburger, W. J., Platt, M. M., and Morgan, H. M., TEXTILE RESEARCH JOURNAL **22**, 695–729 (1952).
7. Lindberg, J., Waesterberg, L., and Svenson, R., *J. Textile Inst.*, **51**, T1475–T1492 (1960).
8. Peirce, F. T., *J. Textile Inst.* **21**, T377–416 (1930).
9. Sommer, H., *Faserforsch. u. Textiltech.* **2**, 467–481 (1951).
10. Wilkinson, P. R. and Stanley, H. E., TEXTILE RESEARCH JOURNAL **28**, 669–673 (1958).

Manuscript received June 7, 1960.

Response of Cottons to Chemical Treatments

Part I: Fiber Mercerization and Urea Treatments[1]

L. Rebenfeld

Textile Research Institute, Princeton, New Jersey

Abstract

In order to determine whether different cottons respond differently to identical chemical treatments, single fibers from six carefully selected cottons were subjected to four treatments under a tensile force of 0.1 g. The treatments which were investigated were water, 10 *M* urea, mercerization, and a combination of 10 *M* urea and mercerization. The initial, nondestructive portion of the fiber stress–strain curve was evaluated for each fiber prior to the treatment and the entire stress–strain curve was evaluated after the chemical treatments. Thus it was possible to determine the changes in fiber properties on a fiber-to-fiber basis at least as far as the non-rupture fiber characteristics are concerned. Fiber length, elastic modulus, breaking extension, and breaking tenacity were considered in this research. Many changes in fiber properties due to the chemical treatments could be interpreted in terms of fibrillar orientation of the six cottons as estimated by the X-ray angle. Under mercerizing conditions, it was observed that cottons with high X-ray angles underwent greater increases in fiber length and elastic modulus and greater decreases in fiber breaking extension than did cottons with low X-ray angles. Changes in fiber breaking tenacity could not be related to known structural features of the cotton fiber.

Introduction

The increasing emphasis on the development of functional cotton types has introduced another variable into the textile industry. The word "cotton" must now be considered a generic term for a class of natural cellulosic fibers possessing a wide range in geometrical, mechanical, physical, and chemical characteristics.

Certain differences among cottons have been recognized for many years and have formed the basis for cotton classification, commerce, and ultimate utilization. Factors such as fiber length and fineness are well known to the textile industry and are today the basis on which cotton is commercially traded. During the past two decades a great deal of research has been conducted in measuring and evaluating the significance of fundamental mechanical properties of cotton fibers, and the fact that cottons differ in such properties is now generally accepted. Research has not been confined to measuring these mechanical properties nor to interpreting their commercial and technological significance. Many serious investigations have been conducted to establish the morphological and physicochemical structure of cotton fibers with a view toward understanding the differences in cotton fiber mechanical properties in terms of fiber structure [1, 6, 9, 10, 16, 17, 20].

Differences in cellulose crystallinity, fibrillar orientation, helical reversals, degree of polymerization, and nature and amount of noncellulosic component have been shown to exist among different cottons. It is difficult to isolate the origin of these structural differences, since the genetic differences among cotton varieties and strains are often masked or confounded by environmental growth conditions. It has been possible to relate many cotton fiber mechanical properties to structural characteristics. Properties of the entire fiber, such as extensibility and stiffness, are primarily correlated with structural characteristics of the entire fiber, such as fibrillar orientation. A fiber characteristic such as strength is more readily correlated with localized structural features such as helical reversals and other sources of structural imperfections. There remain many

[1] Presented at the Spring Meeting of the Fiber Society, Inc., Fontana Village, N. C., April 29, 1959.

properties of cotton fibers which are not yet understood in terms of fiber structure. It is only logical to assume, however, that fiber properties are reflections of morphological and physico-chemical structure and that eventually all fiber properties will be understood in terms of fiber structure.

The cotton textile industry is careful in selecting cottons to suit the requirements of manufacture and end-product quality. Commercial selections are currently made on the basis of fiber length, length distribution, fineness, maturity, and character. To a certain extent fundamental mechanical properties are also considered during the selection of cotton. These fiber properties are either considered by direct independent measurement or through indirect correlations of these properties with fiber length and fineness [18]. While cotton is then selected on the basis of macroscopic properties and characteristics, the selections are in fact based on morphological and physico-chemical structural features which are the underlying causes of differences in macroscopic properties. If, then, it is granted that cottons represent different morphological and physico-chemical structures, it would be reasonable to inquire whether these cotton structures react differently during chemical operations such as are encountered in normal and functional cotton finishing.

Chemical finishing treatments of cotton textiles to impart certain desirable characteristics have gained an ever-increasing degree of importance [4]. Some of the treatments are primarily designed to alter the chemical properties of the fiber, whereas others are more specifically designed to alter the fiber's mechanical properties. In view of the relationships between fiber structure and the mechanical properties of the fiber, it would seem reasonable that the response of a cotton to chemical treatments designed to alter fiber mechanical properties would be highly dependent upon fiber structure.

Mercerization, which involves the treatment of cotton under tension with an aqueous solution of sodium hydroxide, is undoubtedly one of the most widely practiced chemical treatments of cotton. While the process is often carried out primarily to increase fabric luster and dye receptivity, it also causes marked changes in the mechanical properties. Although dependent upon several variables in the mercerization treatment, the effect is normally an increase in strength and stiffness and a decrease in extensibility [13].

This paper considers in detail the manner in which different cottons respond to laboratory mercerization and related treatments and has two main objectives: to determine whether different cottons exhibit different responses and, if possible, to establish the structural characteristic of a cotton fiber which governs the response pattern. For the purposes of this research, the response is defined and evaluated in terms of changes in fiber mechanical properties resulting from the treatments.

In reviewing the literature it can be noted that several studies indicate differences in response to chemical treatments. Clegg [3] observed varying increases in fiber strength for a wide variety of cottons after mercerization.

In a series of papers from the Southern Regional Research Laboratory it was noted that, when six different cottons in yarn state were subjected to identical chemical treatments, such as acetylation [7], mercerization [8], and carboxymethylation [5], the cottons were found to differ in their response to the chemical treatment. No quantitative attempt was made to relate the differences in response to fiber structure. In a study of the comparative mercerization of yarns from various cottons, Murphy and Goldthwait [11] observed that a higher gain in strength was typical of Karnak relative to Pima S-1. Rebenfeld [15] reported on single-fiber mercerization experiments involving twelve different cottons; it was again observed that the cottons responded differently to the treatment. In this work it was further observed that many changes in the fiber mechanical properties could be related to the original fiber elastic modulus, which was taken to be an indirect index of the degree of fibrillar orientation.

Orr, Burgis, Andrews, and Grant [12] observed greater fiber strength increases as a result of yarn mercerization for samples with lower strength–length uniformity. Radhakrishan, Iyer, Viswanathan, and Wakeham [14] subjected several cottons to bundle mercerization under controlled strains and observed varying changes in fiber strength and extensibility.

Experimental

The six cottons which were used in these experiments were chosen on the basis of their divergent fiber characteristics, as shown in Table I. Particular emphasis was placed on the X-ray angle in choosing these cottons in view of the known relationship be-

tween fibrillar orientation and fiber mechanical properties [16]. The cottons were made available through the courtesy of the Agricultural Research Service, U. S. Department of Agriculture. A single fiber treatment sequence which was described in a previous publication was used exclusively in this work [15]. Several treatments which do not represent normal mercerization but which should exert similar swelling effects were included. These treatments were not intended to duplicate commercial cotton finishing procedures but rather to provide controlled chemical treatments by which it might be possible to discern differences in response of the experimental cottons. In these experiments, then, the variable to be considered is the cotton fiber with all other possible variables being held constant.

For the single-fiber treatment, fifty fibers from each of the six cottons were randomly selected and mounted singly on brass tabs at ½-in. gauge length. The mounting and testing methods have been described previously [19]. Before the chemical treatments were carried out the following non-rupture fiber properties were determined on an Instron tensile tester equipped with an automatic vibroscope: specimen test length, linear density, and Hookean slope. This is accomplished by stressing the fiber to a 1-g. force level at a constant rate of extension (10%/min.). When the 1-g. force level is attained the cross-head of the Instron is reversed and the fiber unloaded to a zero force level. After the evaluation of these initial mechanical properties, the fibers were removed from the Instron tensile tester but allowed to remain on the fiber jig. The lower tab, which hung freely from the suspended fiber, provided a tensile force of 0.1 g. on each fiber. It was found from previous experiments that this tension provided a suitable restraining force to prevent excessive shrinkage, but did not cause excessive extension [15]. The following treatments were then performed on sets of fifty single fibers from each cotton type.

Water Treatment

Fibers were suspended under 0.1-g. tension in distilled water at room temperature (approximately 27° C.) for 5 min. The fibers were dried for 5 min. at 105° C. and subsequently conditioned in an atmosphere of 65% RH and 70° F. prior to mechanical testing.

TABLE I. General Properties of Experimental Cottons

No.	Cotton designation	Linear density, tex	Single fiber elastic modulus, Mg./cm.²	Micronaire fineness, μg./in.	X-ray angle, deg.
5	Hopi Acala	0.177	68.7	4.0	26.3
36	Paymaster	0.206	30.9	4.0	39.6
37	Pima S-1	0.149	63.1	3.3	31.8
38	Amsak	0.151	60.0	3.1	30.8
41	Acala 4–42(S)	0.200	44.6	4.0	33.7
49	Smooth Leaf	0.240	27.6	4.8	41.8

Urea Treatment

Fibers were suspended under 0.1-g. tension in a 10 *M* urea solution at room temperature for 30 min., washed in distilled water at room temperature for 5 min., dried in an oven at 105° C. for 5 min., and conditioned at 65% RH and 70° F.

Mercerization

Fibers were suspended under 0.1-g. tension in a 25% (by weight) sodium hydroxide solution at room temperature for 5 min., washed in distilled water, soured in a 1.0% acetic acid solution at room temperature for 5 min., washed, dried, and conditioned as described above.

Urea and Mercerization

This combined treatment consisted of a treatment with 10 *M* urea, followed by mercerization. The fibers were not dried between the urea treatment and mercerization, although the washing step was carried out after the urea treatment. The final steps of washing, drying, and conditioning were carried out as described above.

After suitable conditioning the fibers were returned to the Instron tensile tester and the following properties evaluated: specimen test length, Hookean slope, breaking load, and breaking extension. Fiber linear density, which was determined on each fiber prior to the chemical treatment, was used to normalize Hookean slope and breaking load values to obtain the corresponding elastic modulus and breaking tenacity.

Information is available on the changes resulting from the treatments in the following fiber properties: specimen test length, elastic modulus, breaking tenacity, and breaking extension. The changes in specimen test length and elastic modulus are to be considered particularly significant since these non-rupture characteristics were evaluated on each fiber

before and after the treatments, thus allowing fiber-by-fiber comparison without recourse to the comparison of mean values from two sets of fibers (treated and untreated). Obviously, this is not possible in the case of rupture properties, where it is necessary to determine the values for the untreated condition on a separate set of single fibers for each cotton.

There is no doubt that the initial cycling to a 1-g. force level prior to the chemical treatment has an effect on fiber properties. One may therefore consider the water treatment to be a blank for the three remaining chemical treatments (urea, mercerization, and combination urea and mercerization).

Results

In Table II are listed the changes in fiber length for the six cottons resulting from the four chemical treatments. These changes are expressed in percentages of the original length before each treatment. Positive values indicate extensions, whereas negative values indicate contractions due to the chemical treatments. These results are more clearly indicated in bar graph form in Figures 1 and 2. It will be noted from Figure 1 that the water treatment causes an extension of approximately 1% for all six of the cottons. The somewhat higher extensions for three of the cottons may be explained in terms of their fineness. Cottons 5, 37, and 38 are considerably finer (Table I) and the effective stress on these fibers during the treatments is greater than for the other three cottons, since a constant 0.1-g. tensile force was used for all six cottons. In contrast to the water treatment, the 10 *M* urea causes about 1% contraction for all six of the experimental cottons.

The mercerization treatment causes, as shown in Figure 2, a contraction for all six cottons similar in magnitude to the contraction caused by the 10 *M* urea treatment. Of particular interest are the changes in length induced by the fourth treatment, which is a combination of the 10 *M* urea and mercerization treatments. In this case the six cottons do not show the same behavior, as can be seen in Figure 2. Three of the cottons contract and the other three cottons extend. Further, the magnitudes of these changes in length cover an extremely wide range. In Figure 3 is shown the relationship between the change in length due to the combination

TABLE II. Changes in Fiber Test Length, %

No.	Cotton designation	Water treated	10 *M* Urea treated	Mercerized	10 *M* Urea and mercerized
5	Hopi Acala	+1.21	−0.85	−0.61	−1.84
36	Paymaster	+0.76	−0.55	−0.23	+2.76
37	Pima S-1	+1.53	−0.86	−1.32	−0.68
38	Amsak	+1.58	−1.41	−0.94	+0.62
41	Acala 4-42(S)	+0.84	−1.01	−0.93	−0.30
49	Smooth Leaf	+0.83	−0.78	−0.31	+3.78

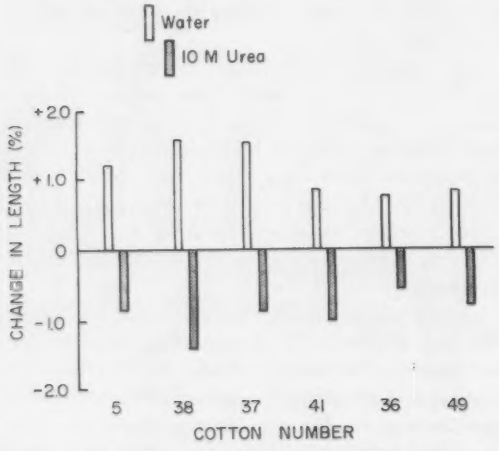

Fig. 1. Changes in fiber length due to a water and a 10 *M* urea treatment.

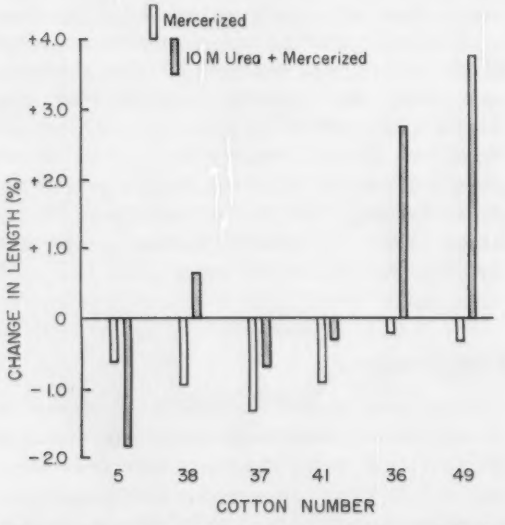

Fig. 2. Changes in fiber length due to a mercerization and a combination urea and mercerization treatment.

urea and mercerization treatment and the X-ray angle of the six experimental cottons. The 0.95 correlation coefficient, which is statistically significant at the 1% level, indicates a clear relationship between the change in fiber length and the degree of fibrillar orientation. Thus, in the case of this fiber characteristic, there is observed a difference in response among the six cottons to an identical chemical treatment. More significantly, however, it has been possible to relate this difference in response to a structural feature of the cotton cellulose.

In Table III are listed the changes in the elastic modulus for the six cottons as a result of the four chemical treatments. This fiber property expresses the resistance of a fiber to an initial extension and is, therefore, a measure of stiffness. The changes are listed as percentages of the original elastic modulus and are all positive, indicating an increase in fiber stiffness. The results are more clearly shown in bar graph form in Figures 4 and 5. The water treatment and the 10 *M* urea treatment appear to increase the elastic modulus by approximately 80%; there is no significant difference among the six cottons. Further, there appears to be no consistent or significant difference between the water and the 10 *M* urea treatment.

TABLE III. Increases in Fiber Elastic Modulus, %

No.	Cotton designation	Water treated	10 *M* Urea treated	Mercerized	10 *M* Urea and mercerized
5	Hopi Acala	57.0	49.0	243	230
36	Paymaster	83.5	128.0	390	344
37	Pima S-1	77.1	74.0	222	179
38	Amsak	77.8	60.9	260	252
41	Acala 4-42(S)	66.0	90.2	326	284
49	Smooth Leaf	76.5	71.1	340	412

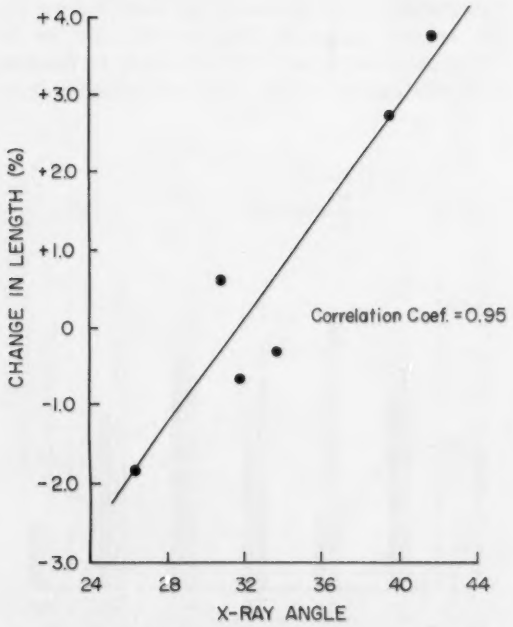

Fig. 3. Relationship between changes in fiber length due to a combination urea and mercerization treatment and the X-ray angle of the experimental cottons.

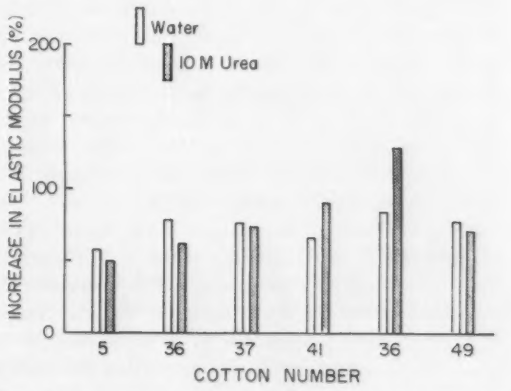

Fig. 4. Increases in elastic modulus due to a water and a 10 *M* urea treatment.

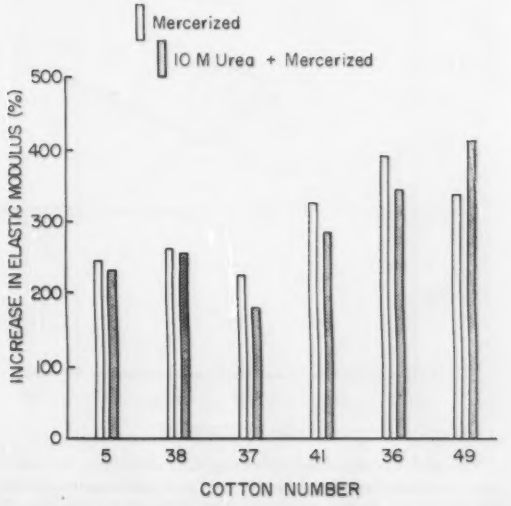

Fig. 5. Increases in elastic modulus due to a mercerization and a combination urea and mercerization treatment.

TABLE IV. Fiber Extension at Break, % *

Cotton	Untreated	Water treated	10 *M* Urea treated	Mercerized	10 *M* Urea and mercerized
5	6.26 ± 0.52	5.26 ± 0.52	5.72 ± 0.52	5.16 ± 0.38	5.50 ± 0.38
36	10.87 ± 0.99	8.58 ± 0.99	9.59 ± 0.99	5.98 ± 0.41	5.82 ± 0.41
37	9.82 ± 0.89	8.15 ± 0.59	8.81 ± 0.74	6.14 ± 0.38	6.06 ± 0.38
38	9.35 ± 0.75	7.59 ± 0.75	8.85 ± 0.75	6.06 ± 0.26	5.64 ± 0.26
41	8.01 ± 0.81	6.83 ± 0.81	6.73 ± 0.81	5.47 ± 0.45	5.15 ± 0.45
49	11.60 ± 1.02	9.52 ± 1.02	10.90 ± 1.02	6.36 ± 0.45	5.69 ± 0.45

* Confidence limits are at the 95% significance level.

The increases in the elastic modulus due to the mercerization treatment and to the combination urea and mercerization treatment are much larger, being in the order of 300%. There is no consistent difference between the effects induced by mercerization on the one hand and by mercerization preceded by the 10 *M* urea treatment on the other. In the case of the mercerization treatments, either alone or in combination with the urea treatment, there is a significant difference among the six cottons. The relationship between the changes in the elastic modulus and the X-ray angle is indicated in Figure 6. The 0.89 correlation coefficient, which is statistically significant at the 1% level, indicates that the change in fiber elastic modulus due to mercerization treatments is related to the degree of fibrillar orientation of the cotton cellulose.

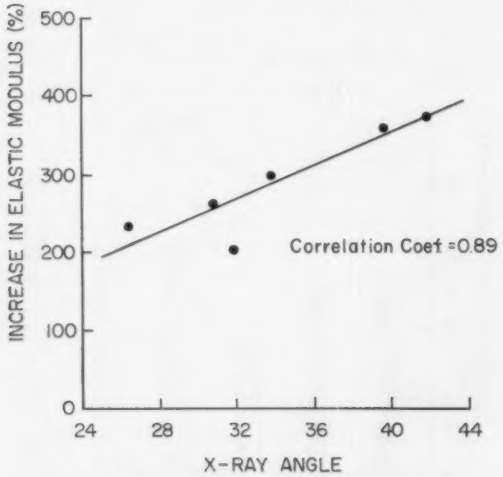

Fig. 6. Relationship between the increases in elastic modulus and the X-ray angle of the experimental cottons. Increases in elastic modulus are average values for the mercerization and the combination urea and mercerization treatments.

In Table IV are listed the breaking extensions of the six cottons in each of the four treated conditions as well as in the untreated condition. An analysis of variance indicates highly significant differences among the cottons as well as among the chemical treatments. A strong cotton-by-treatment interaction indicates that the cottons do not respond in an identical manner to the chemical treatments. These results are shown in bar graph form in Figures 7 and 8, where the changes in breaking extension are expressed as percentages of the original untreated fiber breaking extension. Regardless of the treatment or of the cotton type, there is observed in all cases a decrease in the fiber breaking extension. Considerably larger decreases are noted for the two mercerization treatments than for the water or the 10 *M* urea treatment. The decreases in breaking extension caused by the two mercerization treat-

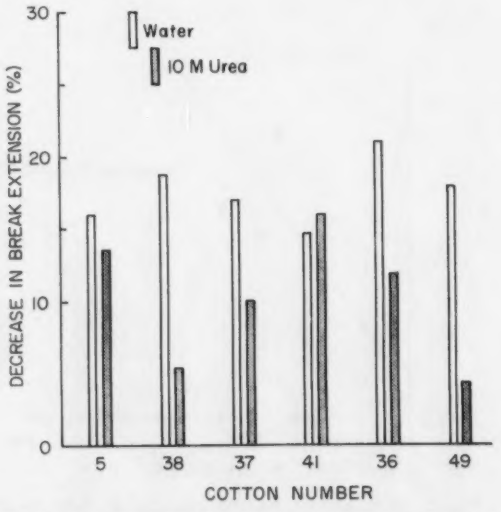

Fig. 7. Decreases in the breaking extension due to a water and a 10 *M* urea treatment.

TABLE V. Fiber Tenacity at Break, g./tex *

Cotton	Untreated	Water treated	10 *M* Urea treated	Mercerized	10 *M* Urea and mercerized
5	36.7 ± 3.6	33.0 ± 3.6	32.6 ± 3.6	40.6 ± 3.6	44.4 ± 3.6
36	22.4 ± 2.5	22.2 ± 2.5	22.7 ± 2.5	29.6 ± 2.5	29.6 ± 2.5
37	41.8 ± 3.8	40.1 ± 3.8	37.0 ± 3.8	48.0 ± 3.8	49.0 ± 3.8
38	42.0 ± 3.8	40.0 ± 3.8	38.7 ± 3.8	44.7 ± 3.8	42.1 ± 3.8
41	31.9 ± 4.9	30.6 ± 4.9	25.2 ± 2.9	30.4 ± 2.9	32.2 + 2.9
49	25.0 ± 4.1	18.0 ± 2.5	20.6 ± 2.5	24.8 ± 2.5	26.8 ± 2.5

* Confidence limits are at 95% significance level.

ments are indicated in Figure 9, where the average decrease is plotted against the X-ray angle. Generally, the changes in breaking extension reflect the changes in the fiber elastic modulus. Thus, treatments which greatly increase the elastic modulus will correspondingly decrease the breaking extension. Similarly, cottons which show greater changes in elastic modulus upon any given treatment will show greater changes in the breaking extension. This, of course, is a direct result of the well-known inverse relationship between elastic modulus and breaking extension [18].

In Table V are listed breaking tenacity values for the six cottons in each of the four treated conditions as well as in the untreated condition. An analysis of variance indicates highly significant differences among the cottons, but insignificant treatment effects. A strong cotton-by-treatment interaction, however, indicates that some of the cottons responded differently to the treatments, although it was not possible to relate changes in fiber strength to fibrillar orientation or to other known features of the six cottons.

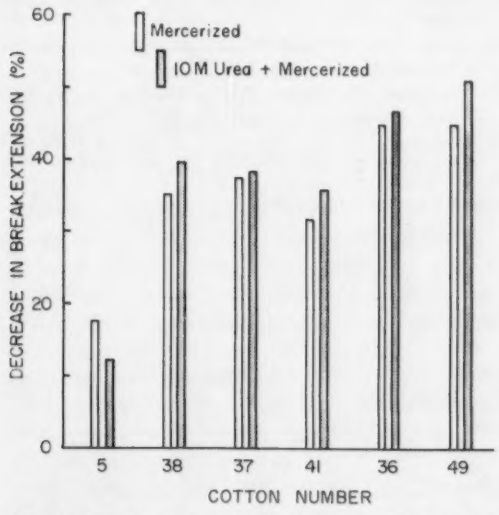

Fig. 8. Decreases in the breaking extension due to mercerization and a combination urea and mercerization treatment.

Discussion

While some of the effects of these chemical treatments appear to be anomolous, it has been demonstrated that different cottons respond differently to certain treatments. Thus, under conditions where all variables in a treatment sequence are maintained constant and the only variant is the cotton fiber, the magnitude of the changes in fiber mechanical properties resulting from the treatment is in many cases related to fibrillar orientation. Such a dependence on fibrillar orientation is particularly evi-

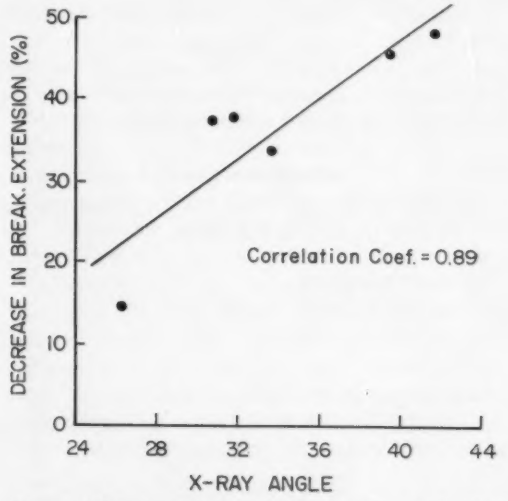

Fig. 9. Relationship between the decreases in breaking extension and the X-ray angle of the experimental cottons. Decreases in breaking extension are average values for the mercerization and the combination urea and mercerization treatments.

dent in those fiber properties which are themselves highly dependent upon fibrillar orientation. For example, changes in fiber elastic modulus and breaking extension resulting from the mercerization treatments are strongly dependent upon orientation, as are the absolute values of these two properties. Since mercerization is known to have an effect on fibrillar orientation, it is quite reasonable that changes in mechanical properties which are dependent upon orientation would also be a function of the fiber's fibrillar orientation.

The changes in fiber breaking tenacity resulting from the treatments are not dependent upon orientation. However, absolute values of breaking tenacity ($\frac{1}{2}$-in. gauge length) are only weakly dependent upon orientation in view of the well-known concept of weak spots. Thus, a treatment which is designed to alter fibrillar orientation cannot be expected to have a marked effect on a fiber property which reflects a localized portion of the fiber, namely, a weak spot.

The conclusions which may be drawn from this work are that cottons respond differently to certain chemical treatments and that it is important to consider different cottons as unique fiber types, each possessing different mechanical and chemical properties.

Acknowledgment

The author is pleased to acknowledge the assistance of Mrs. Virginia Milloway, Mrs. Polly Way, and Mrs. Anna Gombar, who performed the fiber tests reported. This work is part of the Textile Research Institute Cotton Research Project.

Literature Cited

1. Berkley, E. E. and Conrad, C. M., TEXTILE RESEARCH JOURNAL **8**, 341 (1938).
2. Berkley, E. E., Woodyard, O. C., Barker, H. D., Kerr, T., and King, C. J., U. S. Dept. of Agriculture, Tech. Bull. No. 949 (1948).
3. Clegg, G. G., *J. Textile Inst.* **15**, T1 (1924).
4. Fisher, C. H. and Perkerson, F. S., TEXTILE RESEARCH JOURNAL **28**, 769 (1958).
5. Grant, J. N., McDonald, A. W., and Humpreys, G. C., TEXTILE RESEARCH JOURNAL **28**, 60 (1958).
6. Hertel, K. L. and Craven, C. J., TEXTILE RESEARCH JOURNAL **26**, 479 (1956).
7. McDonald, A. W., Humpreys, G. C., Orr, R. S., and Grant, J. N., TEXTILE RESEARCH JOURNAL **26**, 646 (1956).
8. McDonald, A. W., Orr, R. S., Humpreys, G. C., and Grant, J. N., TEXTILE RESEARCH JOURNAL **27**, 641 (1957).
9. Meredith, R. J., *J. Textile Inst.* **37**, T205 (1946).
10. Meredith, R. J., *J. Textile Inst.* **42**, T291 (1952).
11. Murphy, A. L. and Goldthwait, C. F., TEXTILE RESEARCH JOURNAL **28**, 267 (1958).
12. Orr, R. S., Burgis, A. W., Andrews, F. R., and Grant, J. N., TEXTILE RESEARCH JOURNAL **29**, 349 (1959).
13. Ott, E., Spurlin, H. M., and Grafflin, M. W., Editors, "Cellulose and Cellulose Derivatives," Vol. V, High Polymers, 2nd ed., New York-London, Interscience Publishing Co. (1954–55).
14. Radhakrishnan, T., Iyer, B. V., Viswanathan, G. S., and Wakeham, H., TEXTILE RESEARCH JOURNAL **29**, 322 (1959).
15. Rebenfeld, L., TEXTILE RESEARCH JOURNAL **28**, 462 (1958).
16. Rebenfeld, L. and Virgin, W. P., TEXTILE RESEARCH JOURNAL **27**, 286 (1957).
17. Sisson, W. A., TEXTILE RESEARCH JOURNAL **7**, 425 (1937).
18. Virgin, W. P. and Wakeham, H., TEXTILE RESEARCH JOURNAL **26**, 177 (1956).
19. Wakeham, H., Virgin, W. P., and Spicer, N., TEXTILE RESEARCH JOURNAL **24**, 802 (1954).
20. Wakeham, H. and Spicer, N., TEXTILE RESEARCH JOURNAL **21**, 187 (1951); **25**, 585 (1955).

Manuscript received June 29, 1960.

Physical Properties of Wool Fibers at Various Regains

A. R. Haly and M. Feughelman

C.S.I.R.O. Wool Research Laboratories, Division of Textile Physics, Ryde, N.S.W., Australia

Part I: Stresses Developed at Constant Strain Due to Regain Change by Absorption or Desorption

Abstract

The paper reports determinations of stress changes which take place in wool fibers held at constant extension of 1.5 or 20% and subjected to various relative humidity changes. Stresses may be very different according as equilibrium at a given relative humidity is approached by absorption or desorption of water by the fiber. At 1.5% strain, when approach was by absorption, for all relative humidities used the stress fell to a level lower than when the fiber was in water and then increased. A qualitative explanation is given in terms of changes analogous to sol–gel transformations.

Introduction

When a wool fiber at room temperature is extended at high relative humidity and held extended while the humidity is reduced, it tends, on subsequent release, to retain part of the extension. The increase of length is referred to as "cohesive set." There is a rapid restoration of natural fiber length if the humidity is raised to saturation. The phenomena associated with cohesive set are of interest in the fields of wrinkling of fabrics, wrinkle recovery, and relaxation shrinkage.

A change of humidity results in a change of stress in a fiber held at constant strain. Values of stress developed in this way have been reported by Feughelman [2], who showed that the stress was a function of strain. Strain dependence was further studied by Haly and Feughelman [6], and a minimum in the hygrostress [1]-against-strain curve was found at approximately 1.5% strain.

At this time only the relative humidity step 0–100% had been employed. It is clear that, in practical cases of wrinkling and relaxation shrinkage, many different changes in humidity are encountered. The purpose of this report is to give results of a study of stress changes following changes from dryness to various relative humidities as well as from saturation to various relative humidities. Strains of 1.5 and 20% were used, the first to indicate behavior to be expected in the region of the minimum in the hygrostress-against-strain curve [6] and the second to be representative of behavior in the higher strain region up to about 30% strain.

It is shown that stresses in a wool fiber at constant strain are very dependent on direction of approach to the final relative humidity and depend also on other aspects of the previous history of the fiber.

[1] The word "hygrostress" is used to mean the *change* of stress produced, at constant fiber length, by changing the water content of the fiber.

Experimental

The extensometer plus strain gauge apparatus previously described [2] was used for measurements of stress. Quoted strains are based on the water-saturated length of the fiber; this was established by extending a fiber until the force rose to 0.5 g. Experience showed that with a fiber in water this procedure removed practically all crimp.

When the final RH was approached from saturation the fiber was merely extended in water and left for 1 hr., after which it was enclosed in a system through which air of the required RH was circulating. In all cases the humidity was controlled by passing the air over a sulfuric acid solution. To achieve dryness, analytical reagent sulfuric acid was used.

When the final RH was approached from the low RH side, the fiber was extended in water and left for 1 hr. as before; it was then enclosed in the circulation system and dried until at least 90% of

the maximum hygrostress was developed. This was followed by exposure to air at the required relative humidity.

Fibers were relaxed, unconstrained, in water at 52° ± 1° C. for 1 hr. between each set of tests at a particular relative humidity. The wool used was from a Corriedale sheep (designated S W 13) hand-fed for uniformity of wool growth.

Results

1.5% Strain: Relative Humidity Approached by Absorption

When a nearly dry fiber at 1.5% strain was placed in an environment at any of the selected relative humidities in the range 17.6–88% RH, its stress fell to a value lower than that obtained in water prior to drying. Furthermore, in every case, the stress fell to a minimum and then increased. As may be seen in Figure 1, the rate of decay of stress increased with increase in the value of the final relative humidity.

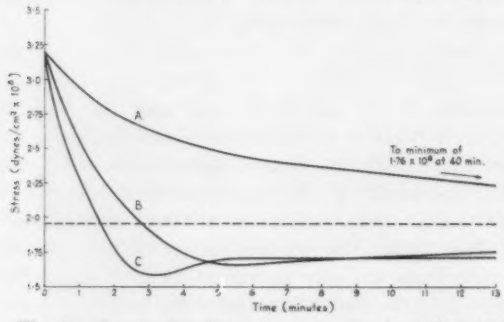

Fig. 1. Curves showing values of stress in a fiber held at 1.5% strain and 20° C. when the relative humidity is changed at zero time from 0 to (A) 17.6%, (B) 58%, (C) 79%. The stress which existed in the fiber after it had been held extended 1.5% in water at 20° C. for 1 hr., prior to beginning the tests, is given by the dashed line.

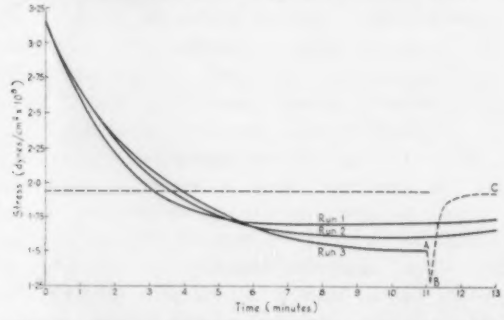

Fig. 2. Curves showing values of stress in a fiber held at 1.5% strain and 20° C. when, three times in succession, the relative humidity is changed from 0 to 49%. After 11 min. of Run 3, the fiber was placed in water and the stress changed as indicated by dashed curve A B C. The stress which existed in the fiber after it had been held extended 1.5% in water at 20° C. for 1 hr., prior to beginning the tests, is given by the horizontal dashed line.

The minimum value of stress depends on the previous history of the fiber. In most cases fibers were dried and brought to the required relative humidity two or three times in succession. Figure 2 shows that, when the relative humidity step was 0–49%, the minimum stress was lower in each succeeding test but that, when the fiber was placed in water, the stress recovered to that holding before initial drying. This is typical behavior.

In Figure 3 (experimental points) differences of *minimum stress* from the stress in water are plotted for all the relative humidities used. It will be seen that at all relative humidities except two the second and third tests led to lower minimum stresses. The two exceptions are 69% and 88% RH, and at one of these (69%) the fiber was left overnight between the first and second tests. The slow increase of stress after the minimum is reached occupies a very long time at low relative humidity, but the accumulated evidence points to a leveling-out at a stress value always well below the value in water.

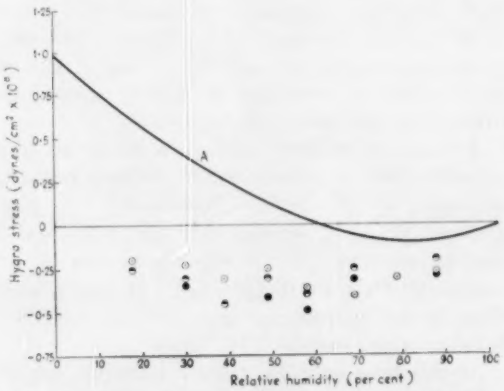

Fig. 3. Curve A: a fiber was held extended 1.5% in water at 20° C. for 1 hr. (Stress X); the relative humidity was then changed to a new value and maintained for 1 hr. (Stress Y). The curve gives the values of (Y-X) at various relative humidities. Experimental points: a fiber was held, as above, in water for 1 hr. (Stress X); it was then dried and brought to a new relative humidity. Stress fell to a minimum (Y). The points show values of (Y-X). ⊙ First run; ◒ Second test at same relative humidity. After the first test the fiber was merely dried, then brought to the required relative humidity. There was no intermediate relaxation. ● Third test at same relative humidity. Test was done in the same way as the second.

This is illustrated by the curve for 79% RH in Figure 1.

Figure 2 shows that, with a relative humidity change from 49% to saturation, there is first a sharp drop in stress (A to B) followed by an increase to the initial value in water. Thus the phenomenon of a minimum stress is not dependent on having the fiber initially dry; in other experiments minima were observed when the relative humidity changes were from 49% to 69, 80, 88, or 96%.

1.5% Strain: Relative Humidity Approached by Desorption

Curves showing how stress changed with time when the relative humidity was changed from saturation to some other value were presented by Haly and Feughelman [6]. In all cases stress rose to a maximum and then began to decay. The rate of decay after 1 hr. was slow, and a plot of stress at this time against relative humidity was presented. For convenience this curve is reproduced as Curve A, Figure 3. Clearly the stress in a fiber at a certain relative humidity is very dependent on the direction of approach to the relative humidity, on the value of the relative humidity, and on the elapsed time since the change to that relative humidity.

20% Strain

At 20% strain, when the required relative humidity is approached from dryness, the stress does not fall below the stress in the water-saturated fiber. Neither is there a minimum in any of the stress-against-time curves. These points are illustrated in Figure 4. Stresses do, however, differ with direction of approach to the final relative humidity and, as Figure 5 shows, the differences may be substantial.

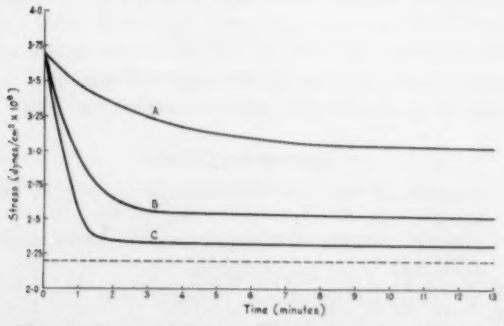

Fig. 4. Curves showing value of stress in a fiber held at 20% strain and 20° C. when the relative humidity is changed at zero time from 0 to (A) 20%, (B) 59%, (C) 88%. The stress which existed in a fiber after it had been extended 20% in water at 20° C. for 1 hr., prior to beginning the tests, is given by the dashed line.

Discussion

Perhaps the most striking aspect of the present results is that the stress in a fiber at constant strain, and at any of a wide variety of relative humidities, is very dependent on the direction of approach to the chosen relative humidity. As is well known, the wool regain-against-relative humidity curve shows hysteresis, but the maximum hysteresis is only 2% of regain, and this is obviously inadequate to explain the stress results. It is probable that the greater release of stress when the final relative humidity is approached by absorption is due to two causes.

During absorption a steep concentration gradient traverses the fiber [4] and, as Feughelman [3] has pointed out, this requires substantial shape changes. The resulting movement, together with the weakening of hydrogen bonds due to water absorption, leads to a solution-like state; i.e., the stress falls to a low value. In desorption there is no moving concentration boundary [5], a steep gradient being established near the fiber surface and remaining in that position; as water is lost the concentration level falls throughout the whole fiber. Shape changes during desorption are therefore minimized, and stress reaches a higher value than when the final relative humidity is approached by absorption.

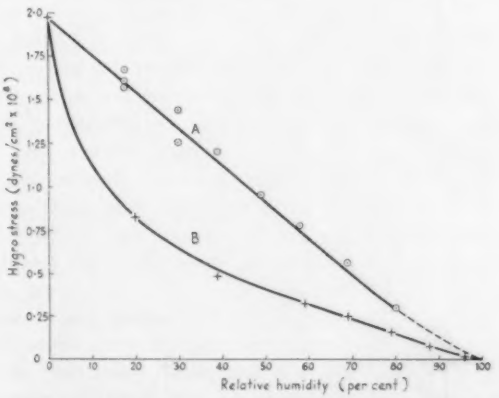

Fig. 5. Curve A: a fiber was held extended 20% in water at 20° C. for 1 hr. (Stress X); the RH was then changed to a new value at which the maximum stress reached was Y. The curve gives values of (Y-X) Curve B: a fiber was held as above in water for 1 hr. (Stress X); it was then dried before being brought to a new relative humidity which was maintained for 1 hr. (Stress Y). The curve shows values of (Y-X).

While an extended fiber is absorbing water, H-bonds under stress are being weakened by the increase of activity of water. A natural consequence is increased displacement between the groups participating in a bond; the state is unstable and the bond is ruptured. The process continues until the stress in the fiber is low. During desorption, H-bonds under stress are strengthened due to decreased activity of water, more bonds remain intact, and the stress rises to a higher value than is reached when the final relative humidity is approached by absorption.

At 1.5% strain, release of stress is particularly effective for the reason, given by Haly and Feughelman [6], that in a dry fiber at this strain many groups participating in hydrogen bonds are separated to such an extent that the force between them is low or even absent. The fiber is therefore initially less stabilized by hydrogen bonds and, as we have seen, even an absorption step from 0 to 17.6% RH suffices for release of stress to a value below that with the fiber in water. When the fiber is placed in water, water molecules can mediate the bonds and produce finally an increase of stress [6]. The special situation with respect to extended hydrogen bonds does not exist at 20% strain, hence the stress does not fall below the stress in water. Neither was there observed at 20% strain, under the conditions discussed in this paper, a minimum in any stress-against-time curve.

The first concept outlined above is of use in explaining why minima should be observed. When a fiber is brought to a lower relative humidity, the mechanical effects of the desorption are slight, and loss of water is concurrent with re-formation of hydrogen bonds. On the other hand, when a fiber is brought to a higher relative humidity, the mechanical effects are greater and re-formation must await completion of the absorption process; i.e., during absorption, rupture of bonds takes place, but relative motion within the fiber allows less concurrent rebuilding. The stress in the fiber falls to a minimum and then rises. The rise may be very slight: at 17.6% RH it was only 0.02×10^8 dynes/cm.^{2} after 130 min. Feughelman [3] has noted the resemblance between events of this nature and sol–gel transformations.

The fact that at 1.5% strain successive desorption–absorption cycles give, in general, lower minimum stresses (Figure 2) follows from the same concept. Before the gel process is complete the fiber is dried and subjected to another absorption step. In this way increased bond rupture and lower stresses are obtained. When now the fiber is placed in water (Figure 2), there is an even closer approach to a solution-like state, and the stress falls from A to B. Re-formation follows with stress rise to C, which is almost the same as the level early in the experiment after the fiber had been in water for 1 hr. The stress at point B is more than 30% lower than at point C. In a water-saturated fiber the stress is mainly carried by the microfibrils [1], the fraction supported by the swollen matrix being only about 0.08 of the total. Thus, on the basis of the two-phase model for a wool fiber, the low value of stress at B would be interpreted to mean that for a short time there is a decrease in the stress supported by the microfibrils. This decrease may indicate a transient opening up of the microfibrillar structure. At 1.5% strain a fiber is very near the commencement of the yield region of the stress–strain curve; hence a relatively small physical disturbance may well initiate some temporary change in the microfibrils. Such a disturbance is provided by the relative humidity change from 49% to saturation. Even with fibers under no external force, experiments using a deuterium–hydrogen exchange technique have shown that changes of relative humidity from dryness to saturation must cause a transient increase of accessibility of the microfibrils in wool [5].

Under the conditions applying in this work no sol–gel transformations were observed when the strain was 20%; i.e., as would be expected, such changes are much less probable when the strain is above the region where large numbers of hydrogen bonds are uniformly extended. However, Haly and Feughelman [6] showed minima in stress-against-time curves for relative humidity changes from 78 and 88% to saturation when the strain was 20%.

Literature Cited

1. Feughelman, M., TEXTILE RESEARCH JOURNAL **29**, 223 (1959).
2. Feughelman, M., TEXTILE RESEARCH JOURNAL **29**, 967 (1959).
3. Feughelman, M., *J. Appl. Polymer Sci.* **2**, 189 (1959).
4. Haly, A. R., *Proc. 1st Int. Wool Text. Res. Conf. (Australia) (1955)* **D**, 195 (1956).
5. Haly, A. R., *Aust. J. Appl. Sci.* **9**, 410 (1958).
6. Haly, A. R. and Feughelman, M., paper presented at 2nd Int. Wool Text. Res. Conf., Harrogate, England (1960).

Part II: Recovery from Extension

Abstract

Under all conditions of extension and relative humidity which were used, length recovery took place in two stages: an early, rapid recovery was followed by a slow recovery which was, in most circumstances, linear with log (time). The amount of rapid recovery depends on the stress in the fiber at the instant of release. Recovery from 20% strain is greatly accelerated as relative humidity increases above 60%; this is probably due to a sharp increase in the amount of "free" water in the wool fiber. Recovery from 1.5% strain is different in character, and the reason may be that the recovery from low strain contains a large elastic component.

Introduction

It was shown previously [2] that recovery of nearly dry wool fibers from a cohesive set took place in two stages. For all setting strains used there was an early rapid recovery, and this was followed by a slow recovery which continued indefinitely and was approximately proportional to the logarithm of the time measured from the moment of release of the fiber.

In this paper results are presented which demonstrate that behavior was similar when strained fibers recovered at various relative humidities. Two strains, 1.5 and 20%, were used.[1] At either of these strains, as was shown in Part I of this series [3], the value of stress in an extended fiber is dependent on the direction of approach to the final relative humidity. We would expect, therefore, the amount of the early rapid recovery to be dependent on direction of approach to the final relative humidity. The results given here establish that such a dependence exists.

Experimental

The apparatus for measuring stress and recovery was the same as that used for the work described in Part I.

As in Part I, extensions were based on the length of the straightened, water-saturated fiber, and this was established by extending until the force rose to 0.5 g. It might be thought that at lower relative humidities a greater straightening force should be used. At these relative humidities, however, we were dealing with fibers already cohesively set in a straightened form; consequently a force rise to 0.5 g. was used in all cases as a criterion of straightness.

When the final relative humidity was approached by absorption, the first step was to extend the fiber in water and leave it for 1 hr.; it was then enclosed in the circulation system and dried over analytical reagent sulfuric acid until at least 90% of maximum hygrostress was developed; the relative humidity in the circulation system was changed to the required value and the fiber left for 1 hr.; finally the fiber was released and the amount of recovery measured at suitable time intervals.

When experiments were done specifically to compare recoveries following approach to the final relative humidity by absorption or desorption, the drying which preceded absorption was continued for 1 hr. In this time maximum hygrostress was developed.

In the case when the final relative humidity was approached by desorption from saturation, the fiber was stretched and left in water for 1 hr. as before. It was then enclosed in the circulation system through which air at the required relative humidity was passing. After 1 hr. the fiber was released and recovery measured. The manner in which fiber stresses change when these procedures are followed may be seen in Part I.

The wool used was from Corriedale sheep SW 13; between each test, fibers were relaxed in water for 1 hr. at $52 \pm 1°$ C.

Results

With the present technique it is not possible to determine accurately the recovery curve during the first minute after release of a fiber. In general the amount of recovery in the first minute will be given on graphs showing recovery against log (time) curves for the subsequent period.

[1] Astbury and Woods [*Phil. Trans. Roy. Soc.* **A232**, 383 (1933)] reported some data on recovery from a strain of 50%. This strain, unlike strains below 30%, produce irreversible changes in wool fibers.

1.5% Strain

Some results of recovery from 1.5% strain when various humidities are approached by absorption are given in Figure 1. Results for two different fibers which were each dried for 2 hr. in a circulation system containing analytical reagent sulfuric acid are shown in the figure. These are typical fiber-to-fiber differences, and may follow at least partially from failure to obtain comparable straightening due to different crimp forms. For times greater than 2 min. all graphs are, at least to a good approximation, linear with log (time) at the various relative humidities. The slopes of the lines do not change to a great extent over the range 0–87% RH (see Table I). In the case of recovery in the first minute after release, there is a minimum between 0 and 30% RH. This is shown clearly in Curve A of Figure 2.

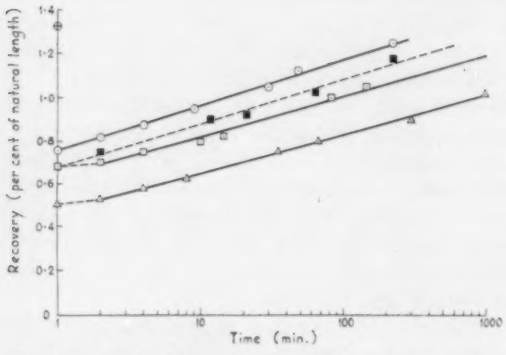

Fig. 1. Graph showing low wool fibers recover from 1.5% strain when the final relative humidity is approached by absorption. The time axis has a logarithmic scale. △, 19.6% RH; ⊡, 0% RH; ■, 0% RH (a different fiber); ⊙, 87% RH.

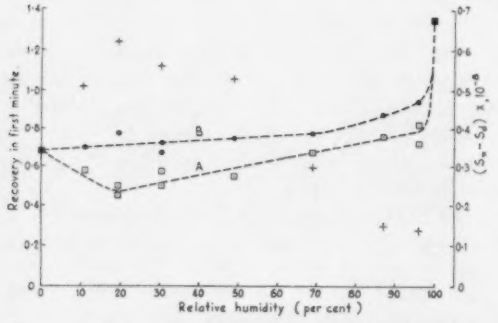

Fig. 2. Recovery in first minute after release plotted against relative humidity for fibers initially at 1.5% strain. ⊡, relative humidity approached by absorption; ●, relative humidity approached by desorption. The crosses (+) show (scale on right) the stress difference $(S_w - S_d)$ where S_w = stress at instant of release when relative humidity was approached by desorption and S_d = corresponding quantity when relative humidity was approached by absorption.

Corresponding data for the same fibers, but when the final relative humidity was approached by desorption, are given as Curve B of Figure 2. There is no minimum, and at every relative humidity at which experiments were done the value of the first-minute recovery was greater than when the final relative humidity was reached by absorption.

As was shown in Part I, the stress in a fiber at constant strain depends on the direction of approach to the required relative humidity. Stresses at the instant of release of these same fibers were measured, and in Figure 2 are given values of the difference $(S_w - S_d)$, where S_w = stress when relative humidity was approached by desorption and S_d = stress when relative humidity was approached by absorption. The differences are similar to values which can be obtained from Figure 3 of Part I; a small deviation would be expected due to the fact that here S_d is the value of stress 1 hr. after change to the final relative humidity, whereas in Figure 3 of the previous paper minimum values of stress are plotted.

It is convenient to note at this stage that regain is not a primary parameter. There is only a small difference between first minute recoveries at 0 and 70% RH, whereas the corresponding regain difference is about half of saturation regain. All the evidence is in agreement with this conclusion. Thus,

TABLE I. Comparison of the Slopes of Recovery against Log (Time) Lines for Fibers Recovering from 1.5% Extension. Slope is Expressed as Percent of Natural Length per Decade of Time in Minutes

$(\text{Slope})_w$ = Slope when relative humidity was approached by desorption.
$(\text{Slope})_d$ = Slope when relative humidity was approached by absorption.

Relative humidity	$(\text{Slope})_w$	$(\text{Slope})_d$
10.8	0.18	0.18
19.6	0.18	0.18
30.4	0.18, 0.17	0.18
49	0.16	0.17
69	0.16	0.18
87	0.21	0.21
96	0.27	0.30, 0.32

although for two reasons we would expect a higher regain in desorption than in absorption, the difference between Curves A and B of Figure 2 is not to be ascribed simply to regain difference. The reasons are that in desorption the hysteretic behavior of wool leads to a higher regain and that equilibrium will usually be reached more rapidly by absorption than by desorption; hence, under our conditions, a slightly higher regain would be expected in the desorption case.

A comparison of the slopes of the recovery against log (time) lines when the final relative humidity was approached by absorption or by desorption is given in Table I. There is no real difference between the slopes at any one relative humidity.

20% Strain

When the setting strain was 20% the second stage of recovery again gave a graph which was, to a good approximation, linear with log (time). Figures 3 and 4 show results for the type of experiment in which the final relative humidity was approached by absorption. In a number of cases experimental points are reproduced. In considering these, it is necessary to remember that within an experiment the points gave a straight line; the distribution of points results from failure to reproduce conditions from experiment to experiment. One important cause follows from the fact that the room temperature could vary by about 2° C., and this variation leads to substantial changes of relative humidity in the chamber containing the wool fiber. These

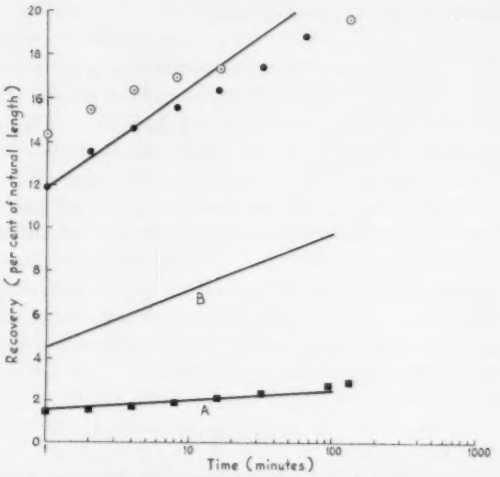

Fig. 4. Graph showing recovery from 20% strain when the final relative humidity was approached by absorption. Time axis has logarithmic scale. A, 0% RH: 3 experiments; ■, 30.4% RH; B, 88% RH: 6 experiments; ⊙, 96% RH; ●, 96% RH. The true slope of the recovery-against-log (time) line for 96% RH is unlikely to be less than that of the line shown.

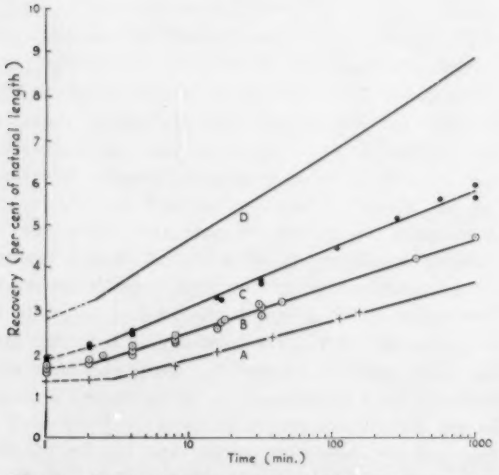

Fig. 3. Graph showing how wool fibers recover from 20% strain when the final relative humidity is reached by absorption. Time axis has logarithmic scale. A, 49% RH: 1 experiment; B, 59% RH: 3 experiments; C, 69% RH: 2 experiments; D, 79% RH: 5 experiments.

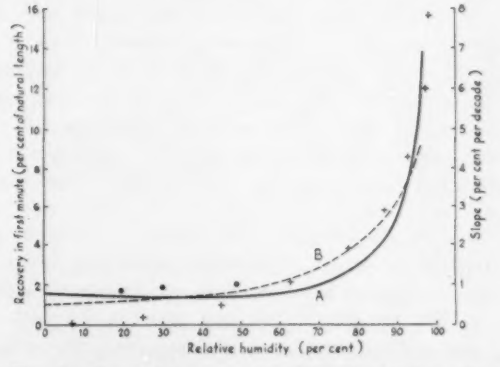

Fig. 5. Curve A: recovery in first minute after release plotted against relative humidity for fibers initially at 20% strain; relative humidity reached by absorption. ●: Same, but relative humidity reached by desorption. Curve B: slope of the second-stage recovery-against-log (time) lines plotted against relative humidity (scale on right). The crosses (+) show the shape of the curve when quantity of "free" water [1] is plotted against relative humidity. The values were normalized to agree with dashed curve at 78% RH.

changes are of greatest consequence above 80% RH, in which region both first-minute recovery and the slope of the log (time) curves increase rapidly with increase of regain. As an example, the results from two experiments at a nominal 96% RH are given in Figure 4. In addition, genuine fiber-to-fiber differences are to be expected.

Figure 5, Curve A, shows how recovery in the first minute from 20% extension depends upon relative humidity. There is some slight evidence of a minimum in the curve between 0 and 30% RH, but important changes do not begin until about 60% RH is reached. In a few cases the final relative humidity was approached by desorption, and, as at 1.5% strain, this technique gave a larger first-minute recovery (see Figure 5). The second-stage slope-against-relative humidity curve is also presented in Figure 5. As at 1.5% strain, no difference was found in slope whether the relative humidity was reached by absorption or desorption.

Discussion

The experimental data show that recovery from cohesive set takes place in two stages: an early rapid recovery and a slow second-stage recovery which, under most circumstances, is linear with log (time). Linearity is lost when recovery approaches completion, as is shown by the data for 96% RH in Figure 4.

With only a few exceptions the results indicate that at the end of the first-stage recovery there is a period (recovery time less than 2 min.) when the recovery-against-log (time) slope is less than the subsequent slope. The same indication appears in previously published results for "dry" fibers recovering from various setting strains [2]. This phenomenon could be consistent with a simple view of the process of recovery [2]. When a wool fiber is held for a period at a fixed strain and relative humidity, bonds are formed in equilibrium with the extended length. When the fiber is released it achieves a very rapid, partial recovery; the stress falls to zero. At this stage a force balance exists between strained bonds which will become less strained (Group A) and bonds which will be strained further or break (Group B). Subsequent recovery depends on the rate at which displacement in the Group B bonds is permitted under the retractive force developed by Group A bonds. It is reasonable to suppose that during a short period after release the retractive force changes sharply, but that then a "steady" state is reached during which the force falls very slowly to zero and recovery is linear with log (time) until the state of complete recovery is approached.

1.5% Strain

The results of Figure 2 show that recovery in the first minute from 1.5% strain is dependent on the value of stress in the fiber at the instant of release. The difference between Curves A and B in the figure, which gives the difference in first-minute recovery at fixed relative humidity, is small at low relative humidity, where the stress difference $(S_w - S_d)$ is small, rises to a maximum, and then decreases as the stress difference decreases.

The fact that no results are available for times less than 1 min. means that we are unable to see the extent of true first-stage recovery. The shapes of the recovery-against-log (time) curves both from 1.5 and 20% strain suggest, however, that first-minute recovery and first-stage recovery are the same up to at least 60% RH. At higher relative humidity some of the increase in first-minute recovery is probably due to the inclusion of part of the second-stage in the first minute. Indeed, the period of slow recovery usually seen between 1 and 2 min. becomes less evident at high humidity, and was not seen at either 87 or 96% RH.

The results of Figures 1 and 2 do not take into account the fact that a dry fiber recovering from 1.5% strain (based on the wet length) is contracting towards the dry length; i.e., the initial strain is greater than 1.5%. Similarly, fibers at other relative humidities recover towards lengths less than the wet length. The minimum in Curve A, Figure 2, is partly due to this circumstance. Correction is possible by plotting recovery at each relative humidity as a percentage of the total possible recovery. The curve showing length swelling of wool fibers as a function of relative humidity is required, and has been obtained (Figure 6) using the same criterion of fiber straightness as in the recovery work. In the same figure, length swelling results of Speakman [6] are shown for comparison, but the present data were used to calculate the curves of Figure 7. It will be seen from Curve B of Figure 7 that for a setting strain of 1.5%, when the final relative humidity is approached by absorption, the minimum in the

curve still exists, but is shallow. The minimum is still less evident but is not removed if Speakman's length swelling data [6] are used for correction.

It will be realized that if the slope data given in Table I were corrected to show the slope as a fraction of the total possible recovery, an increase of slope as relative humidity increased would be obtained. In such a calculation one ought to exclude first-stage recovery from the total possible recovery, and it is not yet possible to do this satisfactorily at all relative humidities.

20% Strain

As in the case of 1.5% strain, the recovery in the first minute after release depends on the direction of approach to the final relative humidity, i.e., on the stress at the instant of release. The effect is less than for 1.5% strain, and this would be expected because the stress difference $(S_w - S_d)$ is a smaller fraction of the total stress at the instant of release.

The correction for the differences in total possible recovery due to length swelling is much less important for a setting strain of 20%; however, the corrected curve is reproduced in Figure 7. It will be noted that, for all relative humidities up to more than 90%, the first-minute recovery is a smaller fraction of the total possible recovery when the initial strain is 20% than when it is 1.5%. This could follow from the notion that at low strain the material is a better approach to a truly elastic substance than at high strain. Such a view is in accord with the picture developed from mechanical investigations and is reflected by the stresses in the fibers at the instant of release; e.g., at approximately 0% RH the stresses *per unit strain* at 1.5% and 20% strain were respectively 2.1×10^{10} dynes/cm.^{2} and 0.25×10^{10} dynes/cm.^{2}

Figures 5 and 7 show that, in the case of recovery from 20% extension, both first-minute recovery and the slope of the second-stage log (time) curve change only slightly in the range 0–60% RH. At higher relative humidities, both quantities increase rapidly. It appears probable that recovery is very dependent on the amount of loosely bound water in the fibers. One might deduce that at relative humidities greater than 60% the fraction of loosely bound water in wool begins to increase rapidly. These water molecules have more freedom to move from site to site, and in this way any one molecule may play a part in breaking several hydrogen bonds, each cleavage permitting more recovery. Cassie's analysis [1] of the wool–water isotherm indicates that the amount of "free" water in wool increases sharply with increase of relative humidity; his theory is consistent with results in diffusion of water into horn and wool [4, 5]. In Figures 5 and 7 the crosses show how, according to the data given by Cassie, the amount of free water increases as relative humidity increases; values were normalized to agree with the dashed curves at 78% RH. The amount of free water is small (less than 10% of the maximum amount of free water) up to 50% RH. Above this the shape of the curve representing increase in free

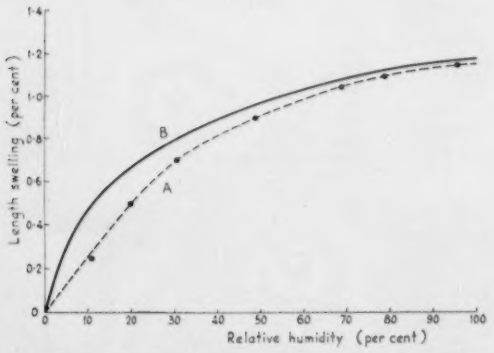

Fig. 6. Length swelling of wool fibers as a function of relative humidity. A: Present results for Corriedale wool; B: Speakman's results [6] for Cotswold wool.

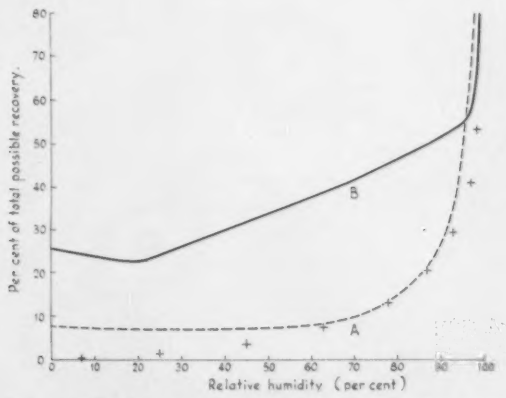

Fig. 7. Percentage (first minute) of total possible recovery plotted against relative humidity. A: Recovery from 20% extension; B: recovery from 1.5% extension. The crosses show the shape of the curve when quantity of "free" water [1] is plotted against relative humidity. The values were normalized to agree with Curve A at 78% RH.

water is in fair agreement with the shapes of the curves representing both first-minute recovery and slope of the recovery-against-log (time) graphs. All this is in accord with the idea that the second stage of recovery is much assisted by the presence of free water. The same is probably true for the first stage; however this is less certain for, as we have seen, at least some of the increase of first-minute recovery with increasing relative humidity can be ascribed to inclusion of second-stage in the first minute. The freedom of a water molecule may arise from its being condensed onto another water molecule and not directly onto a group in the protein.

Water will assist recovery for another reason. In a manner similar to the plasticizing effect in polymers, the dilution due to added water molecules will make molecular motion easier, and recovery will follow because of a concomitant increase in entropy.

The data on recovery from 1.5% strain do not show a similar dependence on relative humidity. Once again this could be ascribed to the fact that at low strain there is a larger fraction of elastic recovery, and contraction is therefore less dependent on release of H-bonds by water molecules. There is no suggestion in any of the data that either first-minute recovery or second-stage slope would fall to zero if strict dryness were achieved; i.e., a recovery component analogous to elastic recovery always exists.

Literature Cited

1. Cassie, A. B. D., *Trans. Faraday Soc.* **41**, 458 (1945).
2. Haly, A. R. and Feughelman, M., paper presented at 2nd Int. Wool Text. Res. Conf., Harrogate, England (1960).
3. Haly, A. R. and Feughelman, M., TEXTILE RESEARCH JOURNAL **31**, 131 (1961).
4. Haly, A. R. and Roberts, N. F., *Proc. 1st Int. Wool Text. Res. Conf. Australia (1955)* **D**, 182 (1956).
5. King, G., *Trans. Faraday Soc.* **41**, 479 (1945).
6. Speakman, J. B., *Trans. Faraday Soc.* **25**, 92 (1929).

Manuscript received May 20, 1960.

Correction

Some of the copies of the January 1961 Journal were printed and mailed with uncorrected errors in the article, "Some Dyes Solubilized by Thiolsulfate Groups," by Brian Milligan and J. M. Swan. The following changes should be made in those copies:

Page 18, column 2, line 8: Change *moylethyl* to *moylmethyl*
Page 19, column 2, lines 16 and 40: Change *4-Carboxybenzeneazo-2-naphthol* to *4'-Carboxybenzeneazo-2-naphthol*
Page 19, column 2, line 35: Add (*dec.*) after *m.p. 194° C.*
Page 19, column 2, line 43: Change *4'-Hydroxy-4'-nitroazobenzene to 4-Hydroxy-4'-nitroazobenzene*
Page 20, Table I: In title add *Fabric* after *Wool*
Page 20, Table II: Data are duplicate values; replace periods by commas, e.g., *7.5* to *7, 5*
Page 20, Table III: In line 2 of title change *Thiosulfate* to *Thiolsulfate*
Page 21, Table IV: Change *curies/min.* to *counts/min.*
Page 21, column 1, 3rd line from bottom: Change citations *7*, 8 to 3, 4
Page 21, column 2, line 2: Change *cunes/min.* to *counts/min.*

Studies in Adsorption

Part XIV: The Mechanism of Adsorption of Disperse Dyes by Cellulose Acetates and other Hydrophobic Fibers[1]

Charles H. Giles

Colour Chemistry Research Laboratory, Department of Chemical Technology, The Royal College of Science and Technology, Glasgow, C.1, Scotland

Abstract

Recent quantitative data for adsorption of disperse dyes on cellulose acetates and the relations between adsorption and dye structure are considered.

The dye probably enters the fiber partly in monodisperse and partly in associated form, and penetrates between the fiber chains in regions inaccessible to water. This type of adsorption produces the characteristic linear adsorption isotherms.

Several properties of the dye molecule determine the maximum adsorption of dye.

Size. The smaller the molecule the easier it can penetrate into the fiber structure, hence the higher the maximum adsorption.

Number of hydrogen donor atoms. The more donor atoms there are the higher is the adsorption, in certain cases; the dye forms —OH... and —NH... bonds with the fiber.

Number of hydrogen acceptor atoms. The dye forms —CH...O, —CH...N, and —CH...Cl bonds with the CH_3 groups of the acetyl residues in the fiber. Thus, the —CH...Cl bond between ethyl acetate and chlorobenzene in aqueous ethanol solution has an energy of about −3 kcal./mole and chlorobenzene itself is strongly adsorbed by cellulose triacetate from this solvent.

In some cases adsorption rises with the number of acceptor atoms; in some cases it *falls* because of opposing electronic effects of other substituent groups.

Steric effects. Functionality. There is a tendency for wide spacing (e.g. 1:4 disubstitution) of bonding atoms to reduce adsorption, probably by promoting dye–dye association rather than dye–substrate association.

Nylon and polyethylene terephthalate fibers appear to adsorb by a similar mechanism, polyethylene terephthalate showing additional (aromatic nucleus) dye–fiber association.

THE CHEMISTRY of dyeing of the hydrophobic fibers with nonionic dyes has long been a subject of investigation [7, 19, 20, 21, 33, 44, 47]. The following mechanisms of adsorption of organic solutes by cellulose acetate have been proposed.

Solid solution [7, 47]. The responsible forces are not defined.

Polar forces (mainly hydrogen bonds). Marsden and Urquhart [40] suggested the formation of a hydrogen bond to an acetyl oxygen atom to explain adsorption of simple hydrogen-donor model solutes (phenol, aniline, etc.), and Vickerstaff [47] extended the suggestion to include disperse dyes. To account for adsorption of hydrogen-acceptor solutes, the author and collaborators [1, 2, 12] suggested hydrogen donation by the acetyl group. Dipole–dipole (non-hydrogen bond) forces have been suggested by Majury [37].

Nonpolar forces. Derbyshire and Peters [17] proposed, in general terms, the operation of dye–fiber van der Waals forces supplemented by polar forces. The author suggested [24] a membrane effect, in which small dye particles diffuse into the fiber and there associate by nonpolar forces.

It will be seen from the present paper that these hypotheses are not contradictory; each may be true in certain circumstances.

Experimental

Many detailed quantitative data of adsorption by cellulose acetates and polyethylene terephthalate have been published in recent years [3–8, 15, 37, 40, 41,

[1] Part XIII *J. Chem. Soc.*, in press.

49]. The author and collaborators have used model compounds in adsorption experiments and in refractometry and monolayer processes [1, 2, 10, 11, 12, 28, 29, 35].

Marsden and Urquhart [40], Daruwalla and Limaye [15], and Majury [37] used secondary cellulose acetate film (acetyl values 53–54%), and Majury also used triacetate film (acetyl value 60.5%) with very similar results; Bird and Harris [4] used secondary acetate fiber; Jain [35] used triacetate powder (acetyl value 62.2%); Wahl et al. [49] used Rhodiaceta fiber (cellulose acetate). Daruwalla and Limaye's adsorption values at 100° C. are with one or two exceptions close to those given by Bird and Harris for the same dyes at 80° C.; values for the two series have been plotted together in some cases in this paper.

Molecular areas (approximate values for smallest enclosing rectangle) were estimated from Catalin (Stuart-type) models.

Discussion

General Nature of the Adsorption

Two features distinguish disperse dye adsorption from water on cellulose acetate: a linear isotherm [3–8, 15, 28, 37, 41, 47] and an increase in saturation adsorption ("solubility" in the substrate) of the dye with increase in its water solubility (Figure 1).

The isotherms. Linear isotherms are obtained [22, 27, 28] for adsorption of a high-affinity nonionic solute from a nonpenetrating or low-affinity solvent (e.g., n-butanol or n-heptane as solvent with wool [28]; water [28] or carbon tetrachloride [33] as solvent with hydrophobic fibers. The solute is then apparently adsorbed in regions of the substrate which the solvent does not penetrate as well as in those which it does penetrate.

The solubility effect. The log saturation adsorption of disperse dyes adsorbed from water by cellulose acetate rises with log dye solubility (Figure 1), suggesting that there is only weak competition for dye [2] between substrate and water and that the dye–fiber attraction is of the same nature as the dye–water attraction, and is therefore mainly polar. The relation appears to be linear for several dye series; the lines have slopes lower than unity, which implies that increase in adsorption is more difficult to achieve than increase in solubility, i.e., that a dye molecule must have more energy to penetrate between fiber molecules than to penetrate between water molecules. Cf. also nylon and cellulose acetate, Figure 6; nylon is the more crystalline and therefore more difficult to penetrate.

The accessibility of the adsorbing surface here clearly varies greatly with the solubility and reactivity of the solute. Unfortunately there is very little quantitative information available upon the variation of saturation adsorption with solute solubility in other systems of nonionic adsorption, for comparison. Qualitatively, adsorption on cellulose seems to follow an opposite rule to adsorption on

[2] If such competition were evident at all, it would be expected to be revealed in an increased adsorption on cellulose triacetate, compared with diacetate, of weakly hydrogen-bonding dyes. This condition appears to be seen in some data given by Fortress and Salvin ([20], Table VII).

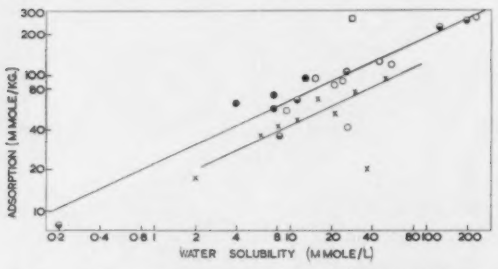

Fig. 1. Relation between water solubility of disperse dyes and their saturation adsorption in cellulose acetate (Bird and Harris data, see Tables II, III). × = anthraquinone dyes, ● = benzeneazo-N-ethyl-N-β-hydroxyethylaniline dyes, ○ = benzeneazo-NN-bis-β-hydroxyethylaniline dyes, ◒ = other benzeneazobenzene and diphenylamine dyes, □ = benzeneazonaphthelene dye.

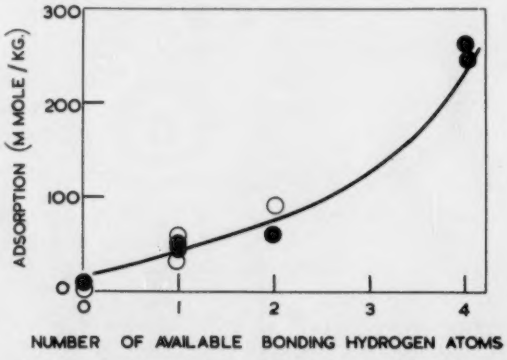

Fig. 2. Relation between number of available hydrogen atoms in multifunctional azobenzene dyes (no 2- or 2'-substituents) and their maximum adsorption by secondary cellulose acetate.

cellulose acetate; i.e., on cellulose it rises with fall in solubility. Thus sodium benzene sulfonate is unadsorbed by cellulose from water, but the much less soluble direct cotton dyes are considerably adsorbed, and acid wool dyes are intermediate in both solubility and degree of adsorption [26]. On the present theory, in cellulose the internal surface available to solutes in water is limited to that in the water-swollen parts, because interchain hydrogen bonds in the crystalline regions are very strong; no nonionic compounds, and only a very few large cations (e.g., cuprammonium ions), can penetrate these regions. In cellulose acetate the internal surface available to the solutes under discussion here is apparently not limited to that in the water-swollen parts; the interchain bonds in cellulose acetate are weaker than in cellulose, and many nonionic compounds may have sufficient energy to break them. If they can do this more readily than water can, the internal surface available to such solutes is not limited to that in the water-swollen regions.

In a case where the surface is rigid and completely accessible to the solvent and to solute molecules of any size (*viz.* metal surfaces adsorbing long paraffin chain derivations from benzene), the saturation adsorption remains constant for solutes of different reactivity and solubility [14].

Evidence for polar attraction. The evidence that polar forces are more important than nonpolar in this type of dyeing includes the parallelism (see above) between water-solubility of disperse dyes and their ability to penetrate the fiber, and the much greater swelling power for cellulose acetate of polar liquids compared with nonpolar. Thus Heit et al. [33] give the following figures for the percentage swelling of cellulose acetate fibers in pure liquids

Carbon tetrachloride	3.5
Benzene	7
Water	20?
Butyl acetate	≥26
Methanol	45

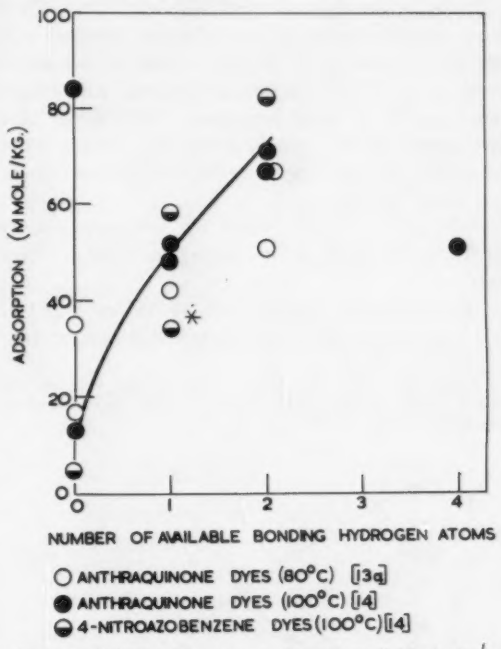

Fig. 3. Relation between number of available hydrogen atoms in all nonhydroxylic anthraquinone dyes and in some azo dyes, and their maximum adsorption by secondary cellulose acetate.

* The two $-C_2H_4OH$ groups are here assumed to be intramolecularly bonded.

TABLE I. Maximum Adsorption Data for Miscellaneous Solutes on Cellulose Triacetate (CTA) and Secondary Cellulose Acetate (CA) [35, 37]

Solute, etc.		Temp., ° C.	Mol area, A²*	Max. adsorption, mmole/kg.
Aniline, phenol, *m*- or *p*-chloro-, methyl- or nitro-substituted phenols	(from water)	25	40–50	>6500 (CA)
Methanol	(from benzene)	59	(12)	*ca.* 1300 (CTA)
Methanol	(from benzene)	23.5	(12)	*ca.* 6000 (CTA)
Quinol	(from water)	60	50	>1500 (CTA)
p-Nitroaniline	(from water)	80	50	945 (CTA)
p-Aminoazobenzene	(from water)	80	90	675 (CTA)
Azobenzene	(from water)	80	80	269 (CTA)
NN-Dimethyl-*p*-nitroaniline	(from water)	80	60	117 (CTA)
NN-Dimethyl-*p*-aminoazobenzene	(from water)	80	110	108 (CTA)

* Molecular area (flat); approximate value for smallest enclosing rectangle.

Tests here (see below) show also that phenol and chlorobenzene, as solutes, are strongly adsorbed by cellulose triacetate, but benzene is very little adsorbed, if at all, from the same solvent.

Effect of Structural Features in the Dye Molecule

Tables I through III and Figures 2 through 4 show that adsorption of any solute by cellulose acetate is increased by a decrease in size of the solute molecule (*cf.* Table I), the presence of a hydrogen atom capable of bond formation, the presence of a hydrogen-accepting group, interaction effects when substituent groups are in certain relative positions, and steric effects.

Molecular size. Obviously the substrate is more accessible to small solute molecules than to large ones.

Free hydrogen atoms. Data in Tables I and II and Figures 2 and 3 show that free hydrogen atoms have a very marked effect on adsorption, especially if they form very strong hydrogen bonds, e.g., phenols (Table I). This confirms that hydrogen bonding (to the keto- or ether oxygen of the acetyl group) is one of the principal adsorption forces.

Hydrogen-accepting groups. It is also clear from Tables II and III and Figure 4 that hydrogen-acceptor groups can, when suitably oriented, increase adsorption. The cause is the hydrogen-donating power of the $—CH_3$ group in esters, activated by the C=O group. The bonding of a typical disperse dye to cellulose acetate may be shown thus [3]:

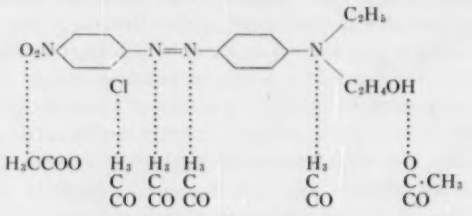

Other quantitative evidence of this type of bond is now available [29]. Thus, the heat of bonding in

[3] Apparently [18, 36] there is a chelate ring in the $R_2N \cdot C_2H_4OH$ group. This would reduce the adsorption-promoting power of this type of group.

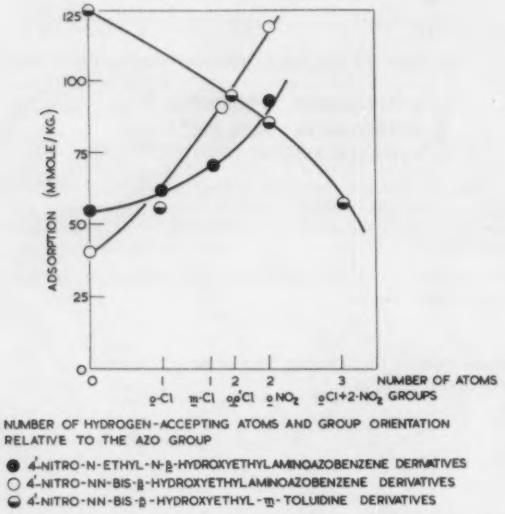

Fig. 4. Relation between number of hydrogen-acceptor atoms (additional to the 4'-nitro-group) in 4'-nitro-β-hydroxyethylaminoazobenzene dyes and their maximum adsorption by secondary cellulose acetate. The chloro and nitro groups accept one and two hydrogen bonds, respectively [2, 10, 11]. The position of the nitro group on the *x*-axis is moved arbitrarily half a unit to the right to improve the fit of the points to the lines. The position of the *m*-chloro group on the horizontal axis has been arbitrarily chosen for the same reason.

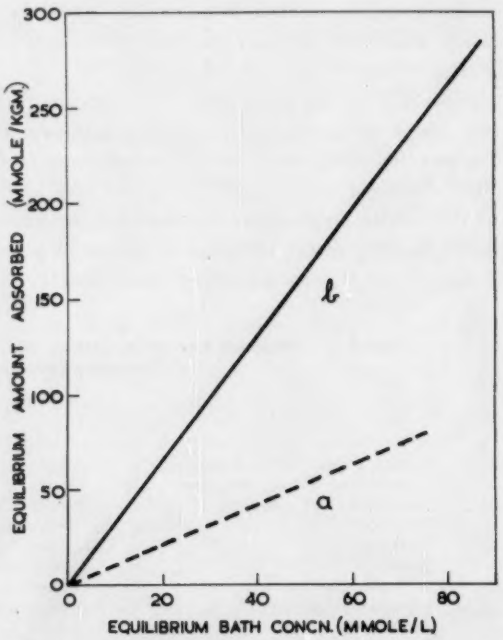

Fig. 5. Adsorption isotherms of (a) phenol and (b) chlorobenzene on cellulose triacetate from 50% (vol./vol.) aqueous ethanol at 53° C. [29].

0.05 *M* solution in 50% aqueous ethanol of ethyl acetate with chlorobenzene is *ca.* − 3.4, compared with values of *ca.* − 3.4 for phenolchlorobenzene and *ca.* − 6 kcal./mole for phenol-N-methylacetamide. This shows that the ester-chloro-group bond in presence of excess water is of moderate strength. Further, it is found [29] (see Figure 5) that chlorobenzene is quite strongly adsorbed by cellulose triacetate from 50% aqueous ethanol—more strongly, in fact, than is phenol—probably because of the much lower water solubility of chlorobenzene (0.0488 g./100 cc. at 30°) compared with phenol (6.7 g./100 cc. at 16°). Both substances are completely miscible with ethanol.

TABLE II. Relation between Constitution of Azo (etc.) Disperse Dyes and their Adsorption by Secondary Cellulose Acetate

Azo dyes Substituents								Mol. area (approx.), A²	Aq. sol., 80° C.*	Maximum adsorption, mmole/kg.
2′	3′	4′	6′	2	3	4	5			
Benzeneazobenzene compounds										
Data of Daruwalla and Limaye [15] (100° C.)										
		NO_2				NMe_2		100		4.8
		NO_2				$N(C_2H_4OH)_2$		150		34
		NO_2				$NEt{\cdot}C_2H_4OH$		130		58
		NO_2				NH_2		100		82
Data recalculated from Wahl et al. [49] (80° C.)										
		NO_2				NEt_2				13.4
		NO_2				$NEt(C_2H_4OH)$				47.9
		NO_2				$N(C_2H_4OH)_2$				27.2
		NO_2				$NEt(C_2H_4O{\cdot}C_2H_4OH)$				157.0
		NO_2				$NEt(C_2H_4O{\cdot}C_2H_4O{\cdot}C_2H_4OH)$				114.2
Data recalculated from Bird and Harris [4] (80° C.)										
		NO_2				$NEt{\cdot}C_2H_4OH$		130	7.7	56
Cl		NO_2				$NEt{\cdot}C_2H_4OH$		130	4.0	61.5
Cl		NO_2	Cl			$NEt{\cdot}C_2H_4OH$		130	7.6	71
NO_2		NO_2				$NEt{\cdot}C_2H_4OH$		160	13.0	95
		NO_2				$N(C_2H_4OH)_2$		150	26.4	41
		NO_2			Cl	$N(C_2H_4OH)_2$		150	24.8	93
NO_2		NO_2				$N(C_2H_4OH)_2$		150	56	119
		NO_2	OMe			$N(C_2H_4OH)_2$		150	230	268
		NO_2		Me		$N(C_2H_4OH)_2$		150	45	124
		NO_2	Cl	Me		$N(C_2H_4OH)_2$		150	7.9	57
Cl		NO_2	Cl	Me		$N(C_2H_4OH)_2$		150	15.7	94
NO_2		NO_2		Me		$N(C_2H_4OH)_2$		150	21.6	85
NO_2		NO_2	Cl	Me		$N(C_2H_4OH)_2$		150	9.4	55
		NO_2				NEt_2		130	*ca.* 0.2	*ca.* 8
	NO_2					NH_2		130	8.4	36
		NO_2				NH_2		100	11.4	66
		NHAc		OH			CH_3	130	26.1	104
		NH_2				NH_2		100	200	250
Benzeneazonaphthalene compound										
		NH_2				NH_2			*ca.* 28	*ca.* 267
		2:4-Dinitro-4′-hydroxydiphenylamine							125	224

* Aq. sol. = aqueous solubility (mg./l.).

TABLE III. Relation between Constitution of Anthraquinone (etc.) Disperse Dyes and their Adsorption by Secondary Cellulose Acetate

Anthraquinone dyes

Substituents					H-bonding property		Mol. area (approx.), A²	Maximum adsorption, mmole/kg.	
1	2	4	5	8	acc.	dnr		Aq. sol., 80° C.*	
Data of Daruwalla and Limaye [15] (100° C.)									
NHMe		NHMe			2	0	130		13
NH_2					3	1	90		48
NH_2		NH_2	NH_2	NH_2	0	4	90		51
NH_2	Me				3	1	100		52
NH_2	OMe	NH_2			3	2	130		67
NH_2		OH			2	1	90		71
NH_2		NH_2			2	2	90		71
NHMe					3	0	110		84
Data recalculated from Bird and Harris [4] (80° C.)									
NHMe		NHMe			2	0	130	*ca.* 2	*ca.* 17.3
NHC_2H_4OH		$NH{\cdot}C_2H_4OH$			4	2	175	36.6	20.2
NHMe					4	0	110	6.1	35.9
NH_2	Me				3	1	100	8.3	42.2
NH_2		OH			2	1	90	11.7	46.1
NH_2		NH_2			2	2	90	21.7	50.8
NH_2	OMe	NH_2			2	2	130	16.0	67.5
NHMe		$NH{\cdot}C_2H_4OH$			3	1	140	30.3	74.5
NHC_2H_4OH					4	1	130	50.5	93.7

Acc. = probable number of atoms accepting a —CH··· bond per dye molecule (assuming each quinone oxygen atom can accept two bonds, as in 1:8-dihydroxyanthraquinone) [12]; Dnr. = probable number of —OH··· or —NH··· bonds donated per dye molecule.

* Aq. sol. = aqueous solubility (mg./l.).

Interaction effects. Adsorption normally rises with increase in number of hydrogen-acceptor groups, but if there is a methyl group ortho to the azo group, adsorption, which is at first very high, *falls* with increase in number of hydrogen-acceptor groups (Figure 4). The *o*-methyl group increases the electron density at the azo group and thus enhances its ability to accept a bonding hydrogen atom. Addition of electron-attracting groups (Cl, NO_2) then progressively neutralizes this effect, and adsorption falls,[4] in spite of the hydrogen-accepting power of these groups [5] themselves. The influence of an ortho-methoxy group on adsorption is even more marked than that of the ortho-methyl group (Table II), in accordance with its greater power of electron-release (Table IV).

Other interaction effects (Tables I–III), which may be compared with appropriate Hammett σ-values [32] (Table IV) are that the nitro group promotes adsorption (by facilitating —NH_2 . . . bonding) better in the 4′- than in the 3′-position in an aminoazobenzene derivative and that the *p*-nitro group promotes adsorption more effectively than the *p*-phenylazo group in aniline derivatives, but less effectively in *p*-dimethylaniline derivatives. (The amino group in aniline *donates* hydrogen and is therefore activated by an electron-attracting group, but the dimethylamino group *accepts* hydrogen.)

Steric effects. When either hydrogen donating or accepting groups are widely spaced in the solute molecule (especially in the para-position) their ability to promote both adsorption and solubility is usually reduced (Tables I, III, V, VI). Normally, an increase in number of (unchelated) polar groups in a molecule increases its solubility (Table VI).

[4] There is an unexplained anomaly in the low value for the 2′-chloro dye.

[5] Flett [18] has suggested that the "bonding" of chloro-groups with hydrogen may be a simple electrostatic interaction, not due to overlap of the hydrogen orbital by lone pair electrons; but some infrared absorption bands in *o*-halogeno-phenols are usually attributed to a normal type of bond (see, e.g. [36]).

TABLE IV. Hammett [32] σ-values *

Substituent	"σ"-value
Electron-releasing groups	
p-OCH_3	−0.268
p-$N(CH_3)_2$	−0.205
p-CH_3	−0.170
.....	
H	0
.....	
Electron-attracting groups	
p-Cl	+0.227
m-Cl	+0.373
p-C_6H_5—N=N—	+0.640
m-NO_2	+0.710
p-NO_2	+0.778 (+1.27 for aniline derivatives)

* The σ-value of a group is a measure of its electron-repelling or attracting power; one with a low value (e.g., OCH_3) will release electrons to an adjacent azo group and so facilitate its intermolecular bonding with hydrogen.

There are at least two reasons for such effects.

Intermolecular association, with face-to-face packing, is easier for 1 : 4-substituted aromatic molecules than for the 1 : 2- or 1 : 3-isomers. This makes the crystal lattice energy of the 1 : 4-compounds higher and their molecules are thus less readily broken away to pass into solution.

In adsorption, cross-linking of adjacent substrate molecules could occur most readily with 1 : 4-disubstituted solute molecules; thus access to the internal structure of the substrate would be more restricted.

A parallel has recently been found in the reactions of some dyes with certain biological tissues. Holt and Sadler [34] find that indigoid dyes with substituent groups suitably placed for intermolecular bonding have reduced affinity for the substrates.

Adsorption Forces other than Hydrogen Bonds

Nonpolar (van der Waals) forces and dipole–dipole forces almost certainly contribute to the ad-

TABLE V. Effect of Spacing of Bonding Groups in Disperse Dye Molecules upon their Water Solubility and Saturation Adsorption in Secondary Cellulose Acetate [4, 15, 37]

	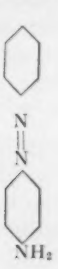	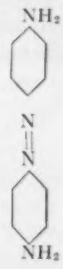	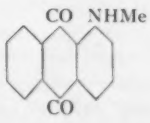	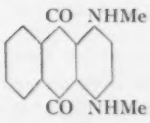
Aq. sol.*	370	200	6.1	*ca.* 2
Sat. ads.*	708	250	35.9	17.3

	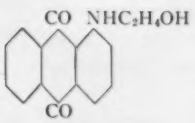	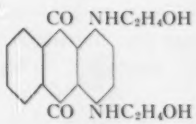
Aq. sol.	50.5	36.6
Sat. ads.	93.7	20.2

	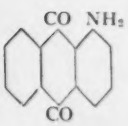	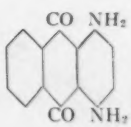
Aq. sol. (95° C.)	35.8	26.3
Sat. ads. (100° C.)	48	71

* Aq. sol. = water solubility (mg./l.); sat. ads. = saturation adsorption in cellulose acetate (mmole/kg.); all at 80° C., except where shown.

TABLE VI. Water Solubility (g./l.) of some Mono- and Bifunctional Polar Compounds

Monofunctional			Bifunctional		
Aniline	34	(20° C.)	*p*-Phenylenediamine	38	(24° C.)
			m-Phenylenediamine	351	(25° C.)
4-Aminoazobenzene	0.370	(80° C.)	4:4′-Aminoazobenzene	0.20	(80° C.)
Azobenzene	0.076	(80° C.)	NN-Dimethyl-*p*-aminoazobenzene	0.0167	(80° C.)
Benzoic acid	2.7	(18° C.)	Terephthalic acid	0.016	(20° C.)
			Isophthalic acid	0.013	(25° C.)
			4-Nitrobenzoic acid	2.4	(25° C.)
Phenol	67	(16° C.)	Quinol	59	(15° C.)
			Resorcinol	2290	(30° C.)

sorption energy. The evidence for van der Waals forces is the tendency for the partition coefficient between cellulose acetate and water to rise with molecular weight (*cf.* data in [4]). There is no direct evidence of dipole–dipole forces, but in any case they would be much weaker than the hydrogen-bond forces. In a series of intermolecular reactions between small organic molecules studied by Sutton and collaborators [16], the association constants of those involving a hydrogen bond were found to lie between 3.5 and 230 (moles/l.) but those for dipole–dipole (non-hydrogen bond) reactions were much lower, *ca.* 0.2–0.4.

Phototropism

The reversible *trans* → *cis* change that some disperse azo dyes on cellulose acetate undergo in the presence of light (phototropism) [47] is evidence that change in the shape of the dye molecule can occur in the adsorbed state. This change in shape can occur readily in many azo disperse dye molecules because few of them have an amino- or a hydroxy-substituent ortho to the azo link. These two substituents, having, as they do, a free hydrogen atom, can promote the tautomeric change to the quinone-hydrazone structure. This structure cannot so readily undergo a *trans* → *cis* change because of the double bond between a nitrogen of the azo group and the attached benzene nucleus, which prevents free rotation. Even if the azo structure does persist, there is chelation between the hydrogen on the substituent and the azo group, and this also will prevent free rotation. Therefore phototropism is unlikely to occur with normal orthoaminoazo and orthohydroxyazo dyes (e.g., most anionic azo dyes for cellulose and wool), but it might occur in azo dyes with other ortho substituents not containing a free hydrogen and therefore incapable either of promoting the tautomerization to a quinone-hydrazone structure or of chelating with the azo group.

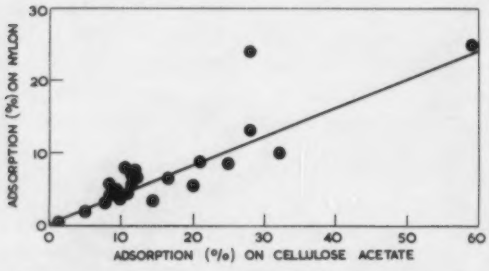

Fig. 6. Relation between saturation adsorption of disperse dyes on cellulose acetate and on nylon at 85° C. [47].

State of the Dye in Solution and Substrate

There is cumulative evidence that disperse dyes are aggregated in the adsorbed state.

Morey and Martin [39] found that a basic dye and a sulfate ester dye on cellulose acetate fiber showed considerably less dichroism when applied from water than from ethanol–water mixture. They explained this by assuming that the dye in the fiber is less dispersed when applied from water. It cannot therefore be entirely monodisperse.

The optical density of a typical disperse dye (1, 4,5,8-tetraminoanthraquinone; C.I.64500) adsorbed in cellulose triacetate film is increased by a disaggregating agent (phenol). This change is attributed to the presence of dye aggregates in the substrate dyed without phenol [13].

Examination of the relative extinctions of the *x* and *y* bands in absorption spectra of cellulose triacetate films dyed with the above dye (C.I.64500) gives evidence of dye aggregation [30].

The lightfastness of disperse dyes usually rises with concentration in the substrate, and is usually higher on secondary acetate than on triacetate fiber.

These facts are attributable to the presence of dye aggregates [25].

The absolute heat of association of a disperse dye with cellulose acetate is very similar to the heat of association in the dye crystal in the two recorded cases [38]. The most reasonable interpretation is that the quantity measured is the dye–dye association energy; hence that the dye is associated in the substrate.

Adsorption by Nylon and by Polyethylene Terephthalate

Similar mechanisms must operate in adsorption of disperse dyes on these substrates as on cellulose acetate. See, for example, Figure 6 (*cf.* [47], pp. 442–3). Glenz at al. [31, cf. 42] found that hydrogen bonding is effective in dyeing polyethylene terephthalate. They postulated hydrogen donation by the dye, but several of their dyes (e.g., 1, 2, 9, and perhaps 3, 4, 6) appear to have all their potential bonding hydrogen atoms chelated and so cannot donate hydrogen. These dyes may thus form bonds by accepting hydrogen from the ester groups in the substrate. Nonpolar forces between aromatic nuclei in dye and substrate must also play a significant part [23]; this would explain why unsubstituted aromatic hydrocarbons (used as "carriers") are readily adsorbed [43, 48], though some form of hydrogen bond to the aromatic nuclei is here a possibility.

The carriers appear to be adsorbed by two mechanisms: penetration into parts of the substrate inaccessible to water (probably the crystalline regions, since the amounts are greatly in excess of the normal moisture regain), which gives linear isotherms [43, 45, 48]; and condensation in internal pores thus opened up [43] (or on the outer surface [48]).

Additivity of Saturation Values

Saturation values in hydrophobic substrates of binary mixtures of some disperse dyes are additive [15, 45]. This effect is difficult to explain, but the following hypothesis may be suggested: the adsorbed dye is attached to only a small proportion of the substrate structure. For example, if one dye molecule were attached to *every* pair of acetylglucose residues in cellulose acetate, the adsorption would be *ca.* 2500 mmole/kg. This is far higher than any value actually obtained. Now suppose that the external pores of the substrate differ widely, but are capable of classification into groups according to size and shape. Each group of pores may be considered the entrances to particular regions of the internal structure, *independent of the regions entered from other groups of pores.* A given dye may then preferentially enter only one group of pores, the particular group being determined by some characteristic of the dye molecule, e.g., its geometry, its energy of binding with the substrate, or the nature of its solvation by the solvent. Dyes with markedly different structures would then be adsorbed in different regions of the substrate; i.e., they would be noncompetitive and in a binary mixture their adsorption values would be additive. Values for dyes of very similar structure would clearly not be additive; such dyes would tend to enter the same region of the substrate, so they would be competitive. The available facts do fit this hypothesis. Thus, the two dyes found to be additive on cellulose acetate [15] are quite different in structure.

C. I. Disperse Red 1 (11110) (*p*-nitroaniline → 2-(ethylanilino) ethanol) and C.I. Disperse Violet 1 (61100) (1:4-diaminoanthraquinone) and the two found to be additive on polyethylene terephthalate (Schuler and Remington) also differ: 1:4-NN-diphenyl-3-nitrosulfanilamide and 1-amino-4-hydroxyanthraquinone (Table VII). The opposite is the

TABLE VII. Distribution of Disperse Dyes (mg./g.) in Binary Mixtures at Different Concentration Levels in Polyethylene Terephthalate (89.3° C.) [45]

Dye			
I	II	II	III
4.9	32.4*	27.1	30.5*
23.0	28.3*	31.0*	16.1
25.7*	25.8*	30.9*	15.1
26.0*	24.5	31.4*	5.0
28.7*	16.1	14.2	14.6
29.7*	14.2		
29.8*	5.3		
26.6	6.0		
23.4	15.3		
9.5	8.1		
6.8	8.4		
5.1	4.8		

* Saturated.

Dyes: I, 1:4-dihydroxyanthraquinone; II, 1-amino-4-hydroxyanthraquinone; III, 1:4-NN-diphenyl-3-nitrosulfanilamide.

With the two similar dyes (I + II), as the adsorption of one dye increases, that of the other tends to decrease, but with the two different dyes (II + III), the saturation of one dye is only slightly affected by the other.

case with two dyes which are very similar, *viz.*, 1-amino-4-hydroxyanthraquinone and 1 : 4-dihydroxyanthraquinone are *not* additive on polyethylene terephthalate (Table VII).

Adsorption of Ionic Dyes by Cellulose Acetate

The reduction in affinity of dyes following anionic ionization has been attributed to the solvated water around the ionic groups, which prevents the close approach of dye molecule to substrate molecule necessary for "multipoint" hydrogen-bond adsorption [10, 11]. In agreement with this suggestion is the fact that Morey and Martin [39] found that an ionized anionic dye (Congo Red, C.I. 22120) adsorbed in cellulose acetate "is not following the internal structure of the yarn," i.e., is not oriented alongside the fiber molecule, as are adsorbed nonionic dyes.

Many basic dyes are hydrolyzed in water and may be adsorbed by cellulose acetate as the free bases (e.g., Chrysoidine, C.I. 11270) [9], which would penetrate regions inaccessible to water. This would account for the superior lightfastness of several basic dyes on this substrate compared with hydrophilic fibers (cotton, wool, silk, viscose rayon), as observed by Schwen and Schmidt [46].

Acknowledgment

The author thanks Professor P. D. Ritchie for his interest and encouragement.

Note Added in Proof

In the course of an interesting investigation of the relation between the nature of substituent groups in anthraquinone disperse dyes, and their gasfastness, Salvin and Walker [51] find that aniline derivatives with electronegative substituents (—SO_2-NH_2, —$COCH_3$, —$CONH_2$, —CF_3), when condensed with 1,5 (1,8)-dihydroxy-4-arylamino-8(5)-nitroanthraquinone give dyes of improved gasfastness, attributed to reduced electron availability at the arylamino nitrogen atoms. Qualitatively, these dyes were found to have "greatly reduced" affinity for cellulose acetate.

The reduced electron availability at the arylamino groups will increase their hydrogen-donating strength (thus strengthening their chelate bonds with the quinone oxygen atoms) and decrease their hydrogen-accepting strength. On the arguments of the present paper these effects would account for the reduced affinity of the dyes.

Literature Cited

1. Allingham, M. M., Giles, C. H., and Neustädter, E. L., *Disc. Faraday Soc.* **16**, 92 (1954).
2. Arshid, F. M., Giles, C. H., and Jain, S. K., *J. Chem. Soc.* 1272 (1956).
3. Bird, C. L., *J. Soc. Dyers Colourists* **70**, 68 (1954).
4. Bird, C. L. and Harris, P., *J. Soc. Dyers Colourists* **73**, 199 (1957).
5. Bird, C. L., Harris, P., and Manchester, F., *J. Soc. Dyers Colourists* **71**, 139 (1955).
6. Bird, C. L. and Manchester, F., *J. Soc. Dyers Colourists* **71**, 604 (1955).
7. Bird, C. L., Manchester, F., and Harris, P., *Disc. Faraday Soc.* **16**, 85 (1954).
8. Bird, C. L., Manchester, F., and Scott, D. F., *J. Soc. Dyers Colourists* **72**, 49 (1956).
9. Burr, A. H. and Burr, M. S., *J. Soc. Dyers Colourists* **50**, 42 (1934).
10. Cameron, A., Giles, C. H., and MacEwan, T. H., *J. Chem. Soc.* 4304 (1957).
11. Cameron, A., Giles, C. H., and MacEwan, T. H., *J. Soc. Dyers Colourists* **73**, 511.
12. Campbell, D. S. E., Cathcart, D., and Giles, C. H., *J. Soc. Dyers Colourists* **73**, 546 (1957).
13. Campbell, D. S. E., Cathcart, D., Giles, C. H., and Rahman, S. M. K., *Trans. Faraday Soc.* **55**, 1631 (1959).
14. Daniel, S. G., *Trans. Faraday Soc.* **47**, 1345 (1951).
15. Daruwalla, E. H. and Limaye, V. R., *J. Soc. Dyers Colourists* **74**, 464 (1958).
16. Denyer, R. L., Gilchrist, A., Pegg, J. A., Smith, T. E., and Sutton, L. E., *J. Chem. Soc.* 3889 (1955).
17. Derbyshire, A. N. and Peters, R. H., *J. Soc. Dyers Colourists* **71**, 530 (1955).
18. Flett, M. St. C., *Spectrochim. Acta* **10**, 21 (1957).
19. Fortress, F., TEXTILE RESEARCH JOURNAL **19**, 23 (1949).
20. Fortress, F. and Salvin, V. S., TEXTILE RESEARCH JOURNAL **28**, 1009 (1958).
21. Fourness, R. K., *J. Soc. Dyers Colourists* **72**, 513 (1956).
22. Giles, C. H., *Disc. Faraday Soc.* **16**, 112 (1954).
23. Giles, C. H., *Disc. Faraday Soc.* **16**, 248 (1954).
24. Giles, C. H., *Compt. rend. XXVII^e Congr. Internat. Chim. Ind.* 610 (Brussels, 1954).
25. Giles, C. H., *J. Soc. Dyers Colourists* **73**, 127 (1957).
26. Giles, C. H. and Hassan, A. S. A., *J. Soc. Dyers Colourists* **74**, 846 (1958) (Table III).
27. Giles, C. H. and MacEwan, T. H., *Proc. Int. International Congress Surface Activity* **3**, 457 (1957).
28. Giles, C. H., MacEwan, T. H., Nakhwa, S. N., and Smith, D., *J. Chem. Soc.* 3973 (1960).

29. Giles, C. H. and Nakhwa, S. N., unpublished. (Preliminary results.)
30. Giles, C. H. and Rahman, S. M. K., *J. Chem. Soc.*, in press.
31. Glenz, O., Beckmann, W., and Wunder, W., *J. Soc. Dyers Colourists* **75**, 141 (1959).
32. Hammett, L. P., "Physical Organic Chemistry," New York, McGraw-Hill, 188 (1940).
33. Heit, C., Moncrieff-Yeates, M., Palm, A., Stevens, M., and White, H. J., TEXTILE RESEARCH JOURNAL **29**, 6 (1959).
34. Holt, S. J. and Sadler, P. W., *Proc. Roy. Soc.* **B148**, 495 (1958).
35. Jain, S. K., Ph.D. Thesis, Glasgow (1956).
36. Jones, D. A. K. and Watkinson, J. G., *Chem. and Ind.* 661 (June 4, 1960).
37. Majury, T. G., *J. Soc. Dyers Colourists* **70**, 442 (1954).
38. Majury, T. G., *J. Soc. Dyers Colourists* **72**, 41 (1956).
39. Morey, D. R. and Martin, E. V., TEXTILE RESEARCH JOURNAL **21**, 607 (1951).
40. Marsden, R. J. B. and Urquhart, A. R., *J. Textile Inst.* **33**, T105 (1942).
41. Olpin, H. C. and Wood, J., *J. Soc. Dyers Colourists* **73**, 247 (1957).
42. Patterson, D. and Sheldon, R. P., *Trans. Faraday Soc.* **55**, 1254 (1959).
43. Rochas, P. and Courmont, M., IFATCC, Preprint, London conference 1959 (Soc. Dyers and Colourists).
44. Schaeffer, A., *Melliand Textilber.* **40**, 75 (1959).
45. Schuler, M. J. and Remington, W. R., *Disc. Faraday Soc.* **16**, 201 (1954).
46. Schwen, G. and Schmidt, G., *J. Soc. Dyers Colourists* **75**, 101 (1959).
47. Vickerstaff, T., "The Physical Chemistry of Dyeing," 2nd ed., London and Edinburgh, Oliver and Boyd (1954).
48. Vickerstaff, T., *Hexagon Digest* (I.C.I. Ltd.) **20**, 7 (1954).
49. Wahl, H., Arnould, Y., and Simon, M., *Teintex* **17**, 298 (1952).
50. Waters, E., *J. Soc. Dyers Colourists* **66**, 609 (1950).
51. Salvin, V. S. and Walker, R. A., TEXTILE RESEARCH JOURNAL **30**, 381 (1960).

Manuscript received June 14, 1960.

The Geometry and Properties of Two-Bar Tricot Fabrics of Acetate, Viscose, and Cotton

Hazel M. Fletcher and S. Helen Roberts

Clothing and Housing Research Division, Agricultural Research Service, U. S. Department of Agriculture, Washington 25, D. C.

Abstract

Previous investigations of tricot fabrics in relation to physical properties and dimensional change due to laundering were extended to include another fiber, cotton, and the determination of effect of different amounts of yarn twist on fabrics of the fibers previously studied. Twenty two-bar tricot fabrics of 70/1 cotton yarn with different runner ratios, and 20 each of acetate and viscose yarns of 75 denier with 2½, 10, 20, or 30 turns per inch were included in the research. The effect of twist upon other relationships was established from observed data of stitch length, stitch density, diameter of yarn, runner ratios, wales and courses per inch, strength, and elongation. Immediate elastic recovery, permanent set, and delayed recovery were evaluated for a wide range of stress–strain levels.

THE research reported here supplements an earlier study of 97 two-bar tricot fabrics [1]. The fabrics were knit from several deniers of acetate and viscose filament yarns with little or no twist; they varied in runner ratios and courses per inch. The data obtained showed that, unless a relaxation treatment was used to remove distortion, the dimensional changes in laundering were high. Fabrics with high runner ratios (7/5, 3/2, 8/5) were found to be lower in bursting strength than those with low ratios (11/10, 6/5, 5/4).

The supplementary study included 20 each of acetate and viscose fabrics knit from yarns of higher twist than those used in the previous research and

also 20 fabrics of cotton. Elastic properties, as well as the properties investigated in the earlier study, were evaluated for the 60 fabrics.

The acetate and viscose fabrics were made from commercial filament yarns (75/20 acetate and 75/30 viscose) which had 2½, 10, 20, and 30 turns per inch. The runner ratio 6/5, which had given optimum bursting strength in the previous study, was used for these fabrics, and the number of courses per inch was varied. The cotton fabrics were knit with various runner ratios and courses per inch from yarn of standard knitting twist.

As in the former study, the fabrics were knit on a 28-gauge two-bar tricot machine under controlled conditions in the Textile Research Department of the American Viscose Corporation.

Method

The procedures for the analyses of the fabric construction, measurement of diameter of yarns, shrinkage determinations, relaxation treatment, and bursting strength measurements were identical to those used in the former study [1].

Stress–strain and recovery measurements of yarns and fabrics were made with a table model Instron tensile tester. For the yarns, a 10-in. gauge was used with a jaw speed of 2 in./min. Fabric breaking strength and elastic recovery determinations were made on 12×4-in. specimens; a gauge length of 3 in. was used with a jaw speed of 5 in./min.

In order to measure the elastic behavior of these yarns and fabrics at various stress–strain levels, hysteresis curves were obtained at constant loads, varying from a low load to 80 or 90% of the breaking load. Five cyclic curves were recorded; the total elongation and immediate elastic recovery on the fifth cycle were measured as described by Hansen and Fletcher [3]. Thirty minutes after the specimens were removed from the machine, permanent set was measured. One measurement was made on each yarn specimen, but the average of three measurements was used for each fabric specimen. Delayed recovery was calculated as the difference between the total elongation at the fifth cycle and the sum of the immediate elastic recovery and the permanent set, as described by Susich and Backer for fibers [5].

Immediate elastic recovery, delayed recovery, and permanent set were plotted versus elongation. For each yarn and for each fabric a stress–strain curve was plotted showing the elongation on the fifth cycle at various loads and at break.

Results and Discussion

The properties of the yarns are shown in Table I. The twist and denier of the yarns, as determined in

TABLE I. Properties of Yarns

Yarn	Twist* (turns/inch) Number	Number, conditioned	Twist multiplier	Diameter, 0.001 in.	Breaking strength, g.	Tenacity, g./den.	Elongation, %	Yield stress, g./den.	Point strain, %	Stiffness,† g./den.	Toughness,‡ g. cm./den. cm.	Resilience,** g. cm./den. cm.	Resilience†† ratio, %
Cotton 70/1		Cotton:											
1.	38.5	67.0	4.71	4.584	159.9	2.02	6.90	1.01	3.9	24.7	0.063	0.0198	31.5
Acetate 75/20		Denier:											
2.	2.2	75.8	.34	5.364	87.5	1.15	22.65	.80	3.3	34.5	.206	.0160	7.7
3.	11.6	78.2	1.84	4.515	97.0	1.24	24.00	.86	4.6	32.9	.224	.0186	8.3
4.	18.8	78.6	2.98	3.924	95.9	1.22	25.95	.79	3.6	30.0	.240	.0166	6.9
5.	31.0	76.6	4.81	3.758	90.8	1.18	27.55	.77	4.5	26.2	.236	.0235	10.0
Viscose 75/30													
6.	2.4	74.8	.37	5.242	151.3	2.02	18.10	.81	1.4	80.0	.240	.0066	2.7
7.	10.4	78.5	1.65	4.303	152.6	1.94	15.65	.79	1.4	85.7	.210	.0078	3.7
8.	20.8	80.4	3.36	4.167	166.1	2.07	18.68	.73	2.3	62.8	.254	.0114	4.5
9.	29.0	82.1	4.77	3.667	163.4	1.99	19.90	.80	2.1	48.9	.253	.0101	4.0

* All yarns had Z direction of twist.
† Modulus of elasticity or initial Young's modulus.
‡ Work of rupture.
** Work (recoverable) at yield point.
†† Work at yield point/work of rupture.

the laboratory, agree closely with the manufacturer's data.

Tables II and III give the physical analyses of the 20 acetate and 20 viscose fabrics and of the 20 cotton fabrics.

Length of Stitch

The measured stitch length was compared with the calculated values of both the Allison and the Grosberg equations [2]. The Allison equation states that

$$l = \sqrt{c^2 + n^2w^2} + 2c + \left(6.3 + 4\,\frac{d}{c}\right) d$$

in which l is the stitch length, c the course spacing, w the wale spacing, n the number of wales crossed by the underlap, and d the diameter of the yarn. When this equation was applied to the finished fabrics, the calculated values agreed closely with the measured values, as shown in Tables II and III.

The Grosberg equation was applied to the relaxed fabrics. In this case, l_1 is the stitch length in the front runner, l_2 the stitch length in the back runner, and

$$l_1 = 1.29\,\sqrt{c^2 + n_f^2w^2} + 2.55\,c + 7.2\,d$$

$$l_2 = 1.29\,\sqrt{c^2 + n_b^2w^2} + 2.55\,c + 2.6\,d$$

The stitch length calculated from these equations likewise showed good agreement with the measured values.

Munden's equation [4] for stitch density of plain knit fabrics was also applied to the tricot fabrics. The relationship is

$$N = K/l^2$$

in which N is the stitch density (courses per inch × wales per inch), l is the stitch length, and K is a constant which depends upon the actual configuration of the knitted loops.

The stitch density was inversely proportional to the square of the stitch length for the front and back runners of the fabrics before and after laundering (Figure 1).

For both the unlaundered and laundered cotton fabrics, K was constant for the various runner ratios in the front runner but varied considerably in the back runner. K varied from 26.2 to 16.3 for the unlaundered and from 33.3 to 17.4 for the laundered fabrics as the runner ratio increased from 6/5 to 7/5.

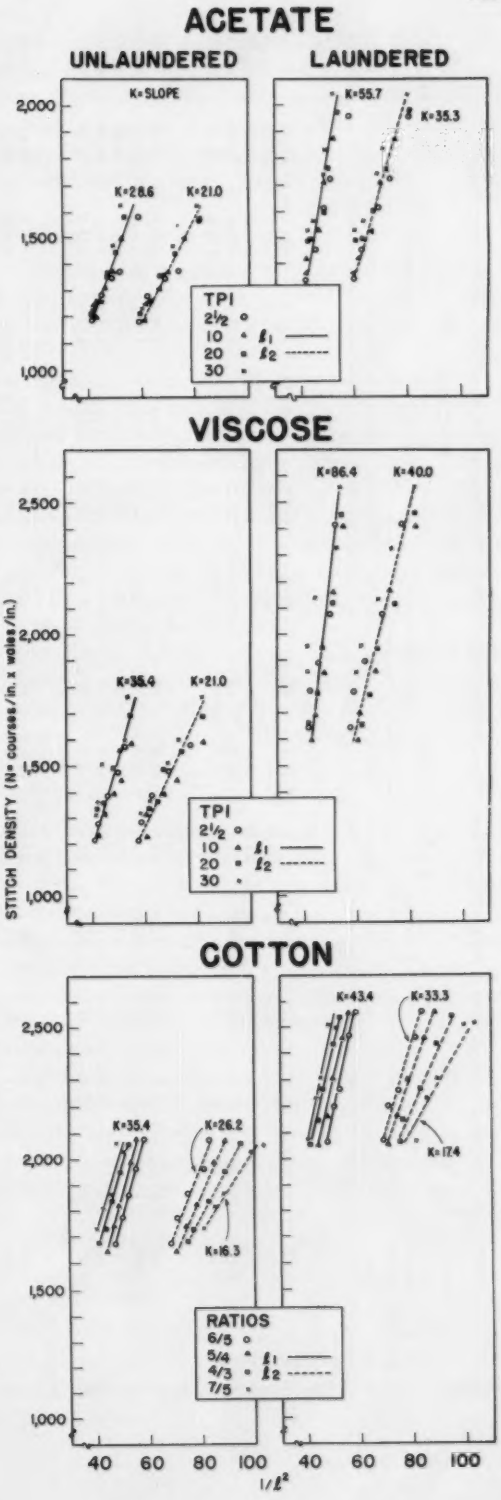

Fig. 1. Relation between stitch density (N) and $1/l^2$ for front (l_1) and back (l_2) runners of tricot fabrics.

TABLE II. Physical Analysis of 20 Acetate and 20 Viscose Tricot Fabrics Knit of Yarns With Different Twist and With a 6/5 Runner Ratio

Fabric and yarn	Weight per square yard, oz.	Thickness, 0.001 in.	Wales/ in.	Courses/ in.	Bursting strength, lb.	Breaking strength,† lb.		Elongation,† %		Stitch length, 0.001 in.				Runner length,‡ in.	
										Front runner‡		Back runner‡			
						Length	Width	Length	Width	Measured	Calculated	Measured	Calculated	Front	Back
Acetate															
2½ turns/in.*															
1	3.82	14.96	37.0	42.7	55.7	24.7	20.0	45.4	96.2	131.4	144.5	111.6	121.3	63.09	53.58
2	3.58	14.86	36.8	37.4	51.2	23.1	16.1	34.8	103.0	139.9	152.1	117.1	129.7	67.18	56.20
2	3.52	14.82	37.4	36.0	49.8	24.3	15.5	34.5	121.8	144.4	155.7	121.1	132.2	69.33	58.15
4	3.58	15.26	37.0	34.6	49.1	22.1	11.9	33.8	106.4	149.8	156.8	127.5	135.0	71.93	61.19
5	3.46	14.78	37.0	32.0	48.7	24.0	11.8	31.0	123.8	155.8	162.5	129.7	141.4	74.81	62.27
10 turns/in.															
6	3.86	16.02	36.7	40.9	52.8	23.8	16.9	42.0	94.6	139.2	140.4	115.4	117.3	66.84	55.38
7	3.68	15.82	36.6	37.5	49.0	21.8	12.3	35.9	86.0	143.6	145.6	119.8	123.0	68.91	57.52
8	3.56	15.28	37.0	35.4	49.4	22.9	12.7	34.6	99.0	147.4	148.8	122.7	126.9	70.80	58.88
9	3.64	15.52	37.2	33.4	47.9	21.6	12.0	31.7	107.2	155.2	152.6	128.5	131.3	74.50	61.69
10	3.62	15.88	37.0	32.1	47.7	22.6	8.9	29.8	96.4	155.0	155.7	129.6	134.6	74.39	62.21
20 turns/in.															
11	3.88	17.46	37.3	42.4	54.2	23.3	14.7	44.0	83.2	137.5	133.1	111.6	110.2	66.02	53.58
12	3.88	17.20	36.7	39.5	52.0	25.4	12.9	46.4	87.0	141.8	137.9	118.2	115.0	68.08	56.73
13	3.76	17.50	37.1	36.7	49.0	24.4	10.4	41.9	91.2	145.8	141.8	122.7	119.7	69.99	58.90
14	3.62	17.38	37.1	34.1	48.3	25.1	12.8	37.4	114.4	152.2	146.8	126.6	125.3	73.05	60.77
15	3.54	17.24	37.0	32.9	48.3	24.0	12.5	36.4	123.2	155.3	149.6	130.0	128.2	74.54	62.41
30 turns/in.															
16	4.38	18.64	36.5	44.6	51.1	27.8	17.4	58.1	84.3	140.0	130.2	112.2	106.5	67.22	53.87
17	4.02	18.40	36.8	39.8	50.7	26.0	15.6	42.2	91.2	143.9	136.0	118.9	113.2	69.06	57.08
18	3.90	18.42	36.4	37.5	47.7	24.7	14.6	38.9	96.0	145.5	140.2	121.2	117.4	69.84	58.16
19	3.78	18.40	36.4	34.8	46.5	26.8	13.4	44.8	112.4	151.6	145.1	126.6	122.9	72.78	60.75
20	3.80	18.36	36.6	33.4	47.1	25.8	11.7	37.6	101.6	155.9	147.7	129.6	126.0	74.82	62.22
Viscose															
2½ turns/in.															
21	3.90	14.88	40.6	38.8	78.3	35.4	25.6	36.9	122.0	138.2	144.4	114.1	124.5	66.31	54.76
22	3.80	14.58	40.8	36.2	77.7	32.9	20.4	33.8	131.0	141.6	148.5	119.9	129.2	67.96	57.55
23	3.86	14.02	40.1	34.6	76.5	32.6	17.9	30.9	115.0	147.6	152.3	125.5	132.8	70.87	60.25
24	3.76	13.92	39.9	32.2	70.5	32.9	16.0	28.1	137.4	153.2	157.6	130.3	138.6	73.53	62.56
25	3.54	13.28	39.3	30.9	72.3	33.0	18.0	26.3	140.0	154.9	161.4	131.7	142.3	74.35	63.23
10 turns/in.															
26	4.42	15.14	39.8	39.8	82.0	35.0	20.2	40.6	107.2	134.8	136.5	110.1	115.8	64.69	52.86
27	4.00	14.54	40.6	35.6	81.6	36.3	20.9	33.2	133.4	139.4	142.7	117.4	123.3	66.89	56.38
28	3.86	14.22	39.1	35.6	74.9	33.4	20.0	31.2	135.2	144.1	144.3	121.6	123.9	69.15	57.04
29	3.84	14.66	39.2	33.6	76.0	32.8	19.0	36.5	138.0	149.4	148.2	128.1	128.3	71.70	61.48
30	3.68	13.98	38.9	31.6	72.3	33.6	15.6	27.5	136.6	152.5	153.1	128.2	133.6	73.22	61.52

* Turns/in. in the yarn.
† Measurements made on 4 × 6-in. grab specimens with a 1-in. gauge length and a jaw speed of 1 in./min.
‡ Runner is inches of yarn in 480 stitches.

Table II—Continued

Fabric and yarn	Weight per square yard, oz.	Thickness, 0.001 in.	Wales/ in.	Courses/ in.	Bursting strength, lb.	Breaking strength,† lb.		Elongation,† %		Stitch length, 0.001 in.				Runner length,‡ in.	
										Front runner‡		Back runner‡			
						Length	Width	Length	Width	Measured	Calculated	Measured	Calculated	Front	Back
20 turns/in.															
31	4.56	16.48	40.5	41.7	82.6	35.0	17.9	48.8	95.8	135.6	132.0	110.3	111.5	65.08	52.95
32	4.26	16.16	40.2	38.6	78.8	38.9	21.2	46.0	129.0	139.7	136.8	115.7	116.7	67.07	55.54
33	4.14	16.46	39.4	37.8	76.2	38.2	23.0	49.3	132.6	144.5	139.0	121.1	118.5	69.34	58.11
34	3.72	16.02	39.3	34.6	74.4	36.9	21.6	44.2	149.0	149.5	145.0	123.9	125.0	71.81	59.47
35	3.86	15.58	39.6	33.7	73.9	34.6	19.7	42.6	167.0	155.0	146.5	127.0	126.9	74.41	60.97
30 turns/in.															
36	4.96	17.90	40.2	43.8	78.0	35.5	28.8	61.2	121.8	136.5	125.9	110.3	104.9	65.55	52.94
37	4.64	17.22	40.0	39.8	77.6	38.4	26.1	52.5	145.2	138.2	131.4	116.7	110.9	66.36	56.01
38	4.52	17.70	39.1	38.5	72.1	30.3	22.1	50.7	133.0	150.0	134.5	120.9	113.6	71.97	58.04
39	4.42	17.24	38.6	35.3	66.4	31.6	19.5	42.9	147.4	153.5	140.7	126.8	120.0	73.70	60.85
40	4.04	16.26	39.7	33.2	69.4	29.7	16.0	39.5	129.2	154.8	143.8	129.1	124.4	74.33	61.97

For the acetate and viscose fabrics, K did not change with the number of turns per inch in the yarn. Since the stitch density increased in laundering, the slopes (K) of the straight lines for the unlaundered fabrics were different from those for the laundered fabrics.

Shrinkage in Laundering

The wale–course spacing ratio of the unlaundered fabrics ranged from 0.86 to 1.22 for the acetate, from 0.79 to 1.09 for the viscose, and from 0.82 to 1.21 for the cotton. After five launderings, this ratio was approximately 1.1 for all the fabrics.

In fabrics that had not had the relaxation treatment of soaking out in warm water and drying on a screen [1], length shrinkage ranged from 10.0 to 14.4% for acetate, from 20.8 to 30.5% for viscose, and from 11.1 to 16.8% for cotton. The corresponding dimensional changes in width ranged from 0.1 to 11.7% shrinkage for acetate, from 4.6% stretch to 11.6% shrinkage for viscose, and from 3.2 to 11.6% shrinkage for cotton.

The fabrics which had received the relaxation treatment to remove distortion had a wale–course spacing ratio of approximately 1.1 and usually changed less than 5% in their dimensions.

Bursting Strength

The bursting strength of all the fabrics decreased as the course spacings increased, as was reported for the tricot fabrics in the former study [1]. These results are shown in Figure 2.

Figure 2 shows the effect of twist on the bursting strength of the acetate and viscose tricot fabrics. In both cases, fabrics made with yarns of high twist (turns/in. = 30) were considerably weaker than fabrics made with yarns of low twist.

Figure 2 shows the effect of runner ratio on the bursting strength of the cotton tricot fabrics. Those with the higher ratios (4/3 and 7/5) were considerably weaker than those with the lower ratios (6/5 and 5/4). These results are similar to those for the tricot fabrics of acetate and viscose of different ratios reported in the former study.

Elastic Behavior

Figure 3 shows the stress–strain curves of the nine yarns used in knitting the tricot fabrics. The acetate and viscose yarns with 30 turns/in. had less

TABLE III. Physical Analysis of 20 Cotton Tricot Fabrics Knit With Different Runner Ratios

Fabric	Weight per square yard, oz.	Thickness, 0.001 in.	Wales/in.	Courses/in.	Bursting strength, lb.	Breaking strength,* lb.		Elongation,* %		Stitch length, 0.001 in.				Runner length,† in.		Runner‡ ratio
										Front runner†		Back runner†				
						Length	Width	Length	Width	Measured	Calculated	Measured	Calculated	Front	Back	
1	2.47	22.2	41.5	50.1	119.6	51.3	40.4	88.0	91.0	130.4	120.7	109.6	100.0	62.60	52.59	6/5
2	2.44	22.2	42.5	48.9	121.4	49.2	42.1	82.2	94.5	131.6	120.9	106.0	100.8	63.19	50.87	5/4
3	2.41	22.2	42.1	48.8	117.4	42.9	45.3	75.2	103.0	137.8	121.4	102.5	101.1	66.12	49.20	4/3
4	2.42	21.8	41.8	48.6	104.7	39.7	49.1	67.8	108.7	140.0	122.0	100.2	101.5	67.18	48.12	7/5
5	2.41	23.1	41.8	46.9	114.3	53.2	40.5	80.9	106.1	133.8	123.7	111.0	102.3	64.24	53.28	6/5
6	2.39	22.3	42.3	46.9	116.6	48.5	42.1	71.6	109.9	136.4	123.1	108.5	103.1	65.48	52.07	5/4
7	2.41	22.7	41.7	46.6	106.8	39.7	41.2	65.0	112.1	141.3	124.0	105.8	103.6	67.82	50.77	4/3
8	2.52	22.9	41.8	49.2	93.0	38.3	48.7	63.3	117.3	143.2	121.4	98.3	100.8	68.72	47.17	7/5
9	2.41	23.2	42.2	44.1	113.8	52.7	30.7	73.0	107.3	137.9	126.2	115.5	106.5	66.17	55.45	6/5
10	2.38	22.5	42.2	43.0	115.1	48.0	39.0	71.9	119.0	142.1	127.6	113.4	108.0	68.21	54.46	5/4
11	2.36	23.2	42.5	43.1	105.0	43.4	41.7	64.1	129.6	146.4	127.3	109.8	107.5	70.27	52.68	4/3
12	2.40	22.9	42.7	43.6	94.7	39.8	41.3	62.6	130.0	148.4	126.4	106.0	107.0	71.21	50.86	7/5
13	2.32	23.2	41.6	42.5	112.8	51.7	35.5	72.2	119.2	141.1	128.9	118.6	109.0	67.75	56.91	6/5
14	2.29	22.8	41.6	41.6	112.4	46.8	35.0	65.4	128.6	144.8	130.2	115.7	110.4	69.50	55.53	5/4
15	2.28	22.8	41.7	41.4	101.2	41.1	36.4	55.7	139.7	149.8	130.2	114.7	110.6	71.90	55.05	4/3
16	2.41	23.9	42.1	43.1	96.4	37.6	40.9	65.0	139.8	152.3	127.6	108.3	107.9	73.10	51.96	7/5
17	2.25	23.0	41.8	39.9	107.4	49.5	31.7	65.6	118.2	145.1	132.3	120.4	112.9	69.63	57.81	6/5
18	2.26	22.3	41.6	39.4	107.1	44.5	32.8	55.2	139.8	149.1	133.3	119.2	113.9	71.57	57.20	5/4
19	2.30	22.6	42.1	39.8	98.4	38.8	36.0	57.7	126.4	156.0	132.1	115.3	113.0	74.89	55.34	4/3
20	2.31	23.2	42.1	41.0	86.6	39.7	38.2	59.1	142.7	156.3	130.3	111.2	111.0	75.04	53.37	7/5

* Measurements made on 4 × 6-in. grab specimens with a 1-in. gauge length and a jaw speed of 1 in./min.

† Runner is inches of yarn in 480 stitches.

‡ Runner ratio is ratio of length of front runner to length of back runner.

strength and greater elongation than those of lower twist.

The percent of elongation of the yarns versus recovery behavior obtained from hysteresis curves at various strain levels is shown in Figure 4. Also included are the stress–strain curves for each yarn showing the elongation at the various cycling loads and at break on the fifth cycle.

For acetate and viscose yarns after cycling, the stress–strain curves at different twists varied little. The influence of twist of the yarns upon the recovery behavior was also small. When elongation was less

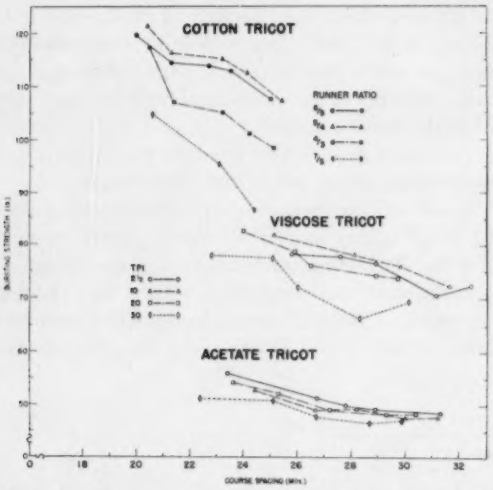

Fig. 2. The effect of twist and course spacing upon the bursting strength of cotton, acetate, and viscose tricot fabrics.

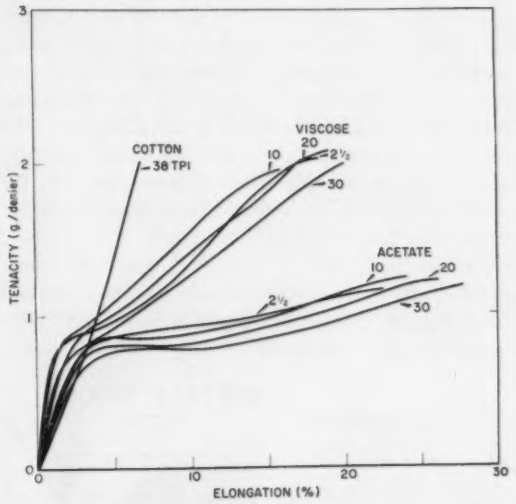

Fig. 3. Stress–strain curves of cotton, acetate, and viscose yarns broken within 20 sec.

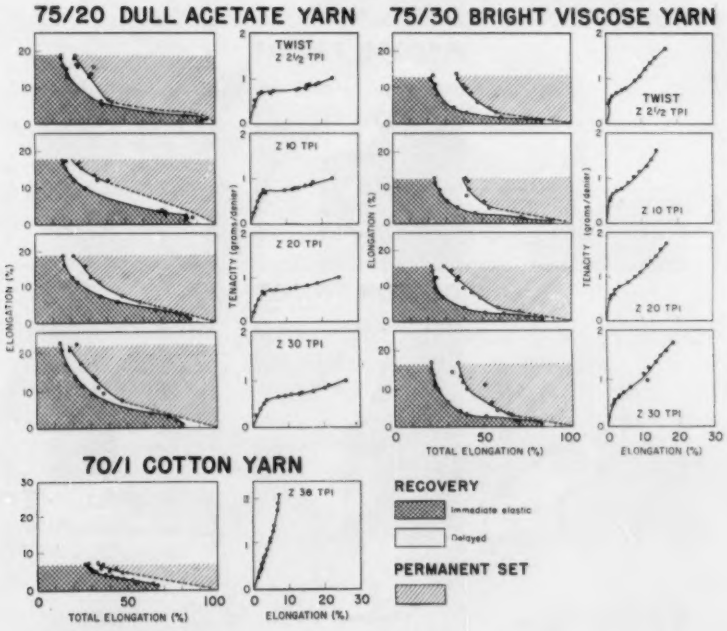

Fig. 4. Recovery behavior of yarns.

than 10%, the immediate elastic recovery was greater for the acetate than for the viscose yarns. The cotton yarn had less elongation and less immediate elastic recovery than either of the other two kinds of yarns.

Figure 5 shows the elastic properties of a fabric of each fiber—acetate (No. 16), viscose (No. 36), and cotton (No. 9). All were knit of yarn of maximum twist with a runner ratio of 6/5 and a course count of 44. The percentage of elongation is plotted against both the recovery and the various cycling loads from 2½ lb. to break at the fifth cycle. Like the yarns, the acetate fabrics had the most immediate elastic recovery and the smallest permanent set; the cotton fabrics had the smallest immediate elastic recovery and the largest permanent set.

Figures 6, 7, and 8 show the effect of course spacings upon the immediate elastic recovery and the elongation of the tricot fabrics before and after laundering, as determined by the hysteresis curves on the fifth cycle. With increase in course spacing, elongation in width increased for all fabrics, but elongation in length did not change. The immediate elastic recovery changed little with course spacing in either length or width.

Summary

In this study of the geometry of 60 two-bar tricot fabrics, relationships were derived from observed data on stitch length, stitch density, diameter of yarn, runner ratio, wales and courses per inch, strength, and elongation.

The stitch density was found to be inversely proportional to the square of the stitch length.

The wale-course spacing ratio was approximately 1.1 for all fabrics from which distortion was removed by either relaxation treatment or by laundering.

Bursting strength decreased as the course spacings increased. Fabrics of acetate and viscose made with yarns of high twist (30 turns/in.) were considerably

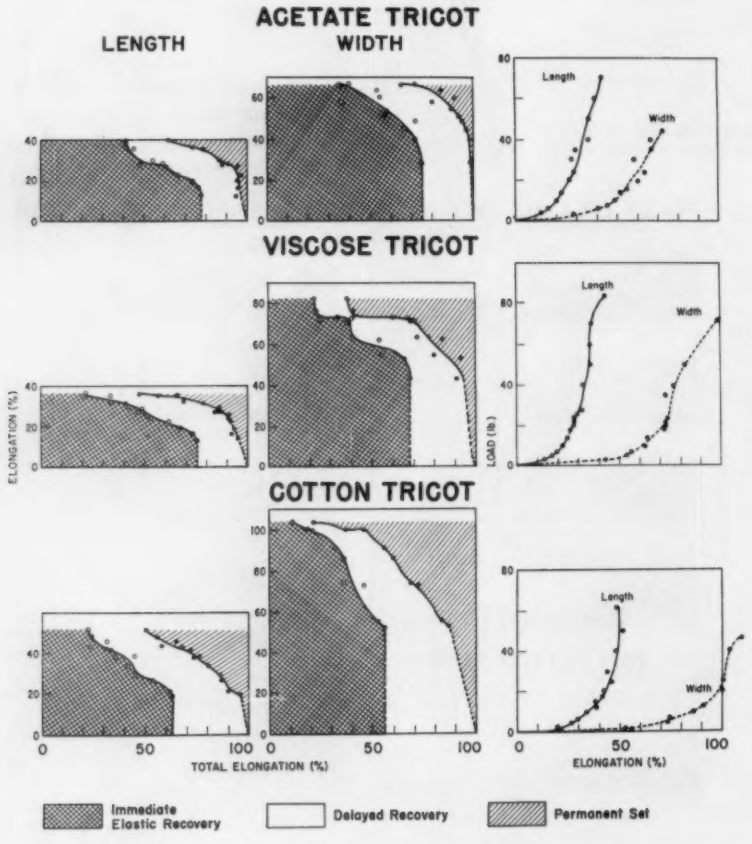

Fig. 5. Recovery behavior of acetate (No. 16), viscose (No. 36), and cotton (No. 9) tricot fabrics, all of 6/5 ratio and of 44 courses/in.

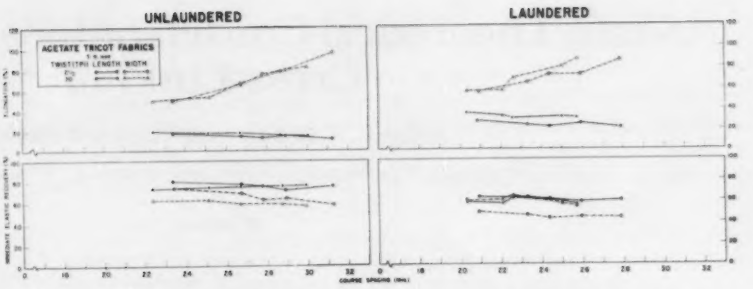

Fig. 6. Elongation and immediate elastic recovery of acetate tricot fabrics at 5-lb. load.

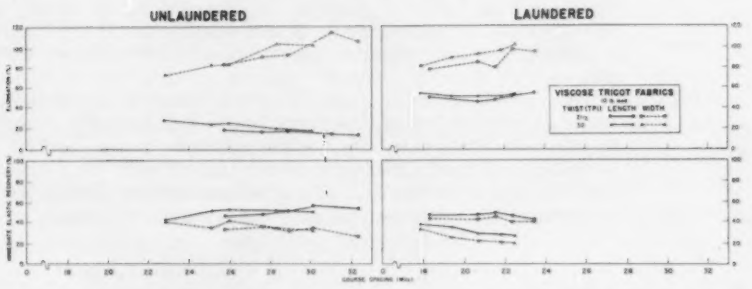

Fig. 7. Elongation and immediate elastic recovery of viscose tricot fabrics at 10-lb. load.

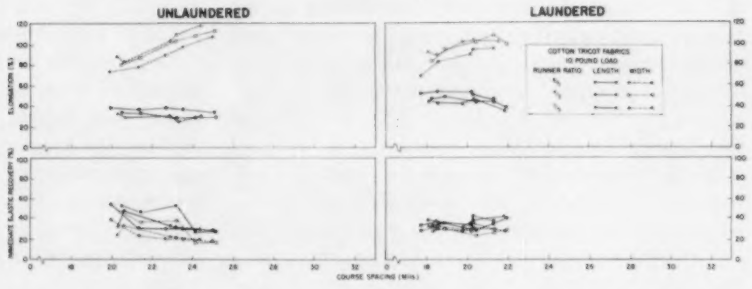

Fig. 8. Elongation and immediate elastic recovery of cotton tricot fabrics at 10-lb. load.

weaker than fabrics made with yarns of low twist ($2\frac{1}{2}$ turns/in.). The cotton fabrics with the higher runner ratios (4/3 and 7/5) were considerably weaker than those with the lower ratios (6/5 and 5/4). Twist had little influence on the elastic behavior of the yarns and fabrics.

The tricot fabrics differed in their elastic behavior. Those knit of the acetate yarns had the most immediate elastic recovery and the smallest permanent set; those knit of the cotton yarn had the smallest immediate elastic recovery and the largest permanent set. With increase in course spacing, elongation in width increased for all fabrics, but elongation in length did not change. The immediate elastic recovery changed little in either length or width with the change in course spacing.

Acknowledgment

Grateful acknowledgment is made to Elinora J. Sharpe for laboratory assistance.

Literature Cited

1. Fletcher, H. M. and Roberts, S. H., TEXTILE RESEARCH JOURNAL **26**, 11, 889–899 (1956).
2. Grosberg, P., *J. Textile Inst.* **51**, 1, T39–T48 (1960).
3. Hansen, A. M. and Fletcher, H. M., TEXTILE RESEARCH JOURNAL **16**, 11, 571–575 (1946).
4. Munden, D. L., *J. Textile Inst.* **50**, 7, T448–T471 (1959).
5. Susich, G. and Backer, S., TEXTILE RESEARCH JOURNAL **21**, 7, 482–509 (1951).

Manuscript received July 11, 1960.

Some Theoretical Considerations of Cellulose Cross-Linking[1]

John L. Gardon and Richard Steele

Textile Research Laboratory, Rohm and Haas Co., Philadelphia 37, Pa.

Abstract

Much available chemical evidence supports the hypothesis that covalent cross-linking is the best way to improve the resilience of cellulosic fabrics. This paper reviews the theories relating physical properties to cross-linking in rubbery polymers and shows that they apply in some qualitative aspects to cellulose. Particularly, the observed changes in swelling, solubility, modulus, tensile strength, and resilience are consistent with these theories.

On the basis of published data, the concentration of intermolecular cross links is estimated; it is found that at least every twenty-fifth accessible anhydroglucose unit has to be intermolecularly cross-linked when maximum crease recovery values are attained. In rubbery polymers, substantial changes in mechanical properties are obtained at much lower levels of cross-linking. This difference between cellulose and rubbers in response to cross-linking is probably due to the polar nature of cellulose.

IT IS widely accepted that cross-linking is the most efficient method to impart high resilience, good crease recovery, and dimensional stability to cellulose fabrics. The cross-linking hypothesis was first advanced by Meunier and Guyot [29] in 1929 for the formaldehyde–cellulose reaction. It obtained wider attention in 1948 through the work of Cameron and Morton [5], who based their conclusions on the lowered moisture regain, water imbibition, and solubility of rayon samples reacted either with urea-formaldehyde or melamine-formaldehyde precondensates or with formaldehyde or glyoxal alone. It had, however, been known [2, 8, 51] and has recently been confirmed by Reeves et al. [36] that wet state treatments of cellulose with formaldehyde increase the moisture regain and water imbibition. Furthermore, reduction in the solubility of cellulose may also be caused by simple single-ended substitution on the cellulosic hydroxyls. The evidence provided by Cameron and Morton was therefore not unequivocal.

A very powerful argument in favor of the cross-linking hypothesis is the general experience that only difunctional reactants are particularly efficient in improving the resilience of cellulosic fabrics. For example, Steele and Giddings [42, 43] found that monomethylol urea increased the crease recovery of cotton to a much lesser extent than dimethylol urea.

Most known cellulose cross-linkers are able to polymerize when reacted in the absence of cellulose. It has been argued that these compounds improve resilience by forming polymers within the fiber [25] and thus stabilizing the physical entanglements of the molecules [28]. One could imagine that complicated cross-linked structures are obtained by polymerizing difunctional reactants and that the resulting three-dimensional networks are more efficient in stabilizing the fabric than the linear polymers derived from monofunctional reactants. However, this argument is weakened by the available data indicating that certain reactants do form covalent links with cellulose. This has been shown by Wagner and Pacsu [49] by methylation of formaldehyde-treated cellulose, by Steele [40] through infrared studies on formaldehyde-treated cellulose, by Head [22], who studied the mechanism of the cellulose-glyoxal reaction, and finally by Cooke, Lineken, et al. [7, 26], who investigated the reaction product of cellulose and trimethylol melamine by means of infrared spectroscopy.

This paper is not intended to be a critical review of the cross-linking hypothesis. It must be admitted that the present evidence supporting it is largely circumstantial. Nevertheless, the evidence seems to us to be so strong that it is very reasonable to assume

[1] This is part of a paper presented at the Gordon Research Conference on Textiles, New London, N. H., on July 14, 1959.

that the major part of the physical changes produced when cellulose fabrics are treated with reactant crease-resistant finishes is due to covalent molecular cross-linking of the fibers. With this assumption in mind, we will review some of the theoretical work on the cross-linking of polymers in general and show, where possible, how it may be applied to rayon and cotton cellulose.

The Effect of Cross Links on Physical Properties

Theoretical work on the cross-linking of rubbers and synthetic polymers has developed a number of relationships between chemical structure and physical properties. For reasons to be discussed later, these cannot be expected to hold quantitatively for cellulose. Nevertheless, a review of the physical properties of cellulose treated with resins and certain other bifunctional reagents shows that the changes produced by the treatment often follow qualitatively the trends predicted by the theoretical work on cross-linking, and these parallels are instructive as we consider chemical processing of cellulose fibers.

Gelation and Swelling

The classical theory of the gelation of polymers was developed by Flory [9, 11] and Stockmayer [44] in 1941; it states that a polymer becomes insoluble, or gels, when it contains one cross-linked unit per weight average molecule or, assuming the "most probable" molecular weight distribution, one cross link per four number average molecules. Methods based on this theory are believed to be the most reliable ones available for the determination of permanent intermolecular cross links. In experimental work based on this theory, cross-linking has usually been varied by irradiation or by degradation until the incipient point of gelation is reached. By appropriately treating data from such experiments, the initial cross-link density can be calculated [6, 30, 38, 50]. The solubility of cellulose in cuprammonium hydroxide is widely used as a qualitative test for cross-linking. To use quantitative data from this test with gelation theory, the latter would have to be modified to include nonrandom distribution of cross links, since in cellulose the cross links are only in those less well ordered regions of the fiber which are accessible to the cross-linking reagent. No suitable modification of the theory is available which takes this into account.

The degree of intermolecular cross-linking in an insoluble polymer can be determined by measuring its swelling after it has been equilibrated with a liquid which is a good solvent for the uncross-linked polymer. The theoretical basis for this rests on the same assumptions and parameters as that for the solubility measurements and was worked out by Flory and Rehner in 1943 [13, 15, 17]. However, it is also doubtful whether this method can be applied to cellulose because it would be difficult to correct for the nonrandom distribution of cross links and for the cross links due to secondary valence bonds and crystallites. It must suffice here that, in general, ordinary cross-linked celluloses have reduced moisture regains and reduced imbibed water contents in qualitative agreement with the swelling theory. Many people have published data showing this effect, a well-known paper being that of Cameron and Morton [5]. Exceptions to this behavior will be discussed later.

Glass Transition Temperature

The glass transition temperature would appear to be important in the problem of creaseproofing and stabilizing cellulose fibers, since it has been shown [1, 3] that the resilience of synthetic fibers, as measured by elastic recovery, has a minimum at the glass transition temperature. This is probably due to the fact that below the glass transition temperature the recovery forces are due to deformation of valence bonds and decrease with increasing temperature, while above the glass transition temperature they are due to a rubberlike entropy mechanism and increase with temperature. The effect of cross-linking on the glass transition temperature of amorphous polymers has been considered from a theoretical basis by Fox and Loshaek [19] and experimental results appear to have confirmed their theory. For poly(methyl methacrylate) [27] and poly(styrene) [48], the glass transition temperature increased by about 60° C. as the cross-link density was increased to about 1 in 10 monomer units. However, Klein and Jenckel [24] studied the rebound of steel balls dropped on films of the same polymers and found that the resilience passed through a minimum near the glass transition temperature. Cross-linking with divinyl benzene did not change the position of the minimum as would have been expected from the results of Fox and

Loshaek. The absolute values of resilience, however, increased substantially on cross-linking.

The glass transition temperature of cellulose is uncertain and not enough is known about the transition temperature of the amorphous portions of crystalline polymers to be able to draw unequivocal conclusions from the available data. According to Ueberreiter [47], there is a change in slope for the volume–temperature relationship of dry rayon around 60°, but the resilience data of Bryant and Walter [3] give no indication of a glass transition in this region. Roseveare and Poore [37] suggested that the glass transition temperature for wet rayon was in the range of 40° to 60° C., based on their determination of the force–temperature relationship at constant elongation. However, Passaglia and Koppehele [35] have shown that the swelling effect cannot be neglected as it was by Roseveare and Poore and that the force–temperature relationship is strongly affected by the skin–core distribution in the rayon fiber. The resilience data [3] suggest that the wet rayon has a glass transition near 0° C.

None of the workers who have studied cellulose have given any data which would show how cross-linking affects the phenomenon which they observed. *A priori,* one might expect the transition temperature to be raised. On the other hand, the polar nature of the cellulose molecule and the polycrystalline structure of the fiber may make the observable effect much smaller than in amorphous or less polar polymers.

Modulus

One of the most fruitful hypotheses for correlating the mechanical properties of polymers with their molecular structure has been the kinetic theory of rubber elasticity. When a rubbery material is deformed, its molecular chains are moved from their random state to a more ordered, oriented state. The retractive force that arises in such deformation is due to the Brownian motion of the chain segments and can be calculated from the entropy changes involved. In contrast to this, Brownian motion in a glassy polymer is negligible, the retractive forces after deformation are caused by the changes in valence angles and can be calculated from the change in internal energy. Because of this difference, a rubbery polymer resists deformation to a greater extent as the temperature is increased and a glassy polymer does so to a lesser extent. This principle was the basis of the determination of the glass transition temperature of rayon by Roseveare and Poore [37], cited above.

In the theory of rubber elasticity it is assumed that the molecular chains are flexible, random, have a Gaussian distribution in space, and are noninteracting. Because of the latter property, such materials will not strongly resist deformation, but will flow because of chain slippage if the rate of deformation is slow enough. However, if there are chemical cross links between the chains, the material will resist deformation and its modulus will be, in the first approximation, proportional to the number of cross links. The modulus, G, is defined by the equation

$$f = G\,(\alpha - 1/\alpha^2)$$

where f is the retractive force and α is the strain. The modulus is given by the number of effective cross links, ν_e, times kT divided by the volume of the network:

$$G = \nu_e kT/V$$

This theory has been refined to account for non-Gaussian distribution and for chain entanglements that may be stabilized by the chemical cross links and act like them [10, 32]. The correlation between theory and experiment has been found to be very satisfactory for a number of polymers whose molecular properties are not too far from the assumptions made in the derivation.

The kinetic theory does not apply quantitatively to cellulose because of fundamental differences between the structure of cellulose and that of rubberlike polymers and between the methods of cross-linking them. The major problems arise from the following differences.

1. The cellulose molecule is relatively inflexible and stiff and is strongly hydrogen bonded to its neighbors.

2. For conventional cellulose cross-linkers, particularly for aminoplast resins, the length of the cross link introduced may not be negligible with respect to the cellulose chain segments between links as required by the theory.

3. The cellulose fiber is partially crystalline and only the less well ordered regions are accessible to the cross-linking reagent. There may also be a varying degree of order in the noncrystalline regions.

4. In industrial practice, cross-linking reagents are introduced into fabrics in aqueous solutions

which swell the cellulose. The impregnated swollen fabric is introduced into an oven, and the cross-linking reaction may begin while it is still swollen to some degree, which depends on the reagent and catalyst used. Laboratory procedures and patent examples have also been published where the reaction was carried out completely in the wet state.

5. In the usual practice, the wet, swollen fabric may be stretched to some degree during the reaction.

At present we have no way to take into account chain stiffness, molecular interaction, and cross-link length, but theories have been developed which help to bridge the other differences between cellulose and the rubber cross-linking model.

The effects of crystallinity and orientation were treated theoretically by Flory [14] and by Oosawa [34], who also considered swelling during cross-linking. Both authors were concerned with protein fibers and the explanation of muscle action. Flory's model was a partly crystalline polymer where the orientation in the amorphous portion was stabilized by crystallites. After the introduction of cross links into the amorphous portion, the crystallites were melted and the properties of the resulting structure were considered. According to Flory's results, orientation during cross-linking diminishes the effectiveness of cross links for increasing the modulus. In the extreme case, where the chains are perfectly oriented along the fiber axis, cross-linking should not affect the modulus at all.

In reviewing the available data for cellulose it must be kept in mind that the results are strongly dependent on the experimental methods, since under many of the conditions used it is difficult to eliminate the effects of the fiber's viscous behavior on the modulus being measured, particularly when the latter is the static modulus. The static modulus has been defined by various workers as the ratio of stress to strain at a particular strain (sometimes even the breaking point) or as the slope of the stress–strain curve at a given strain. Its value can be strongly affected by the mechanical history of the sample. It is believed that cyclic loading and unloading will eliminate most of the viscous effects in the fiber behavior and that measurements on a fiber mechanically conditioned in this way give a better value of the modulus. The dynamic modulus is generally determined by putting a high frequency sinusoidal stress on a prestrained sample and is greatly different from the static modulus for most viscoelastic bodies. Within these limitations the available data indicate that cross-linking cotton has very little effect on its modulus, while at sufficiently high cross-link concentration the modulus of rayon increases with the degree of cross-linking.

The elastic stiffness of cross-linked and uncross-linked cotton and rayon fabrics was determined by Steele and Giddings [42, 43], using the point of no relaxation technique [23] which is presumed to measure the modulus of a mechanically conditioned sample. Cotton containing 5.9% fixed dimethylol urea and rayon containing 7.5% were found to have the same elastic stiffness as the untreated fabrics when data were compared at equal initial stress. This level of treatment on cotton was sufficient to impart the maximum obtainable resilience, but the rayon treatment falls considerably short of the level required for substantial changes. Figure 1 gives the results of another experiment on cotton print cloth and rayon challis treated with dimethylol ethyleneurea. The precondensate was applied with 0.2 mmol. of NH_4Cl per gram as a catalyst and cured for 10 min. at 150° C. The treated cotton contained 5.5% fixed resin and the rayon, 18.5%. In the

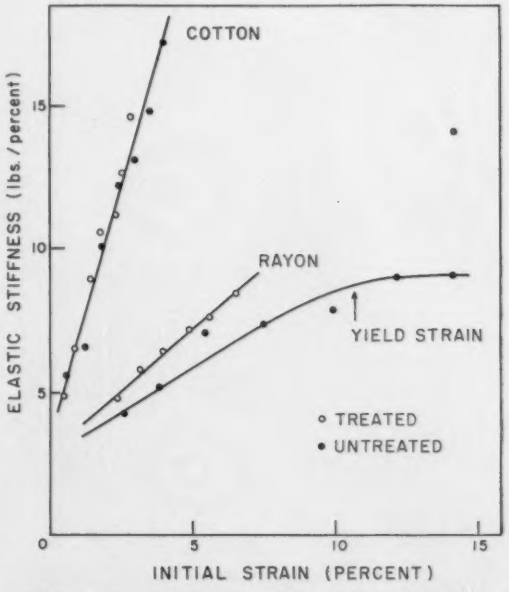

Fig. 1. Elastic stiffness of cotton print cloth and rayon challis untreated and treated to contain 5.5% and 18.5%, respectively, of fixed dimethylol ethyleneurea.

earlier work [42] the elastic stiffness of the treated and untreated fabrics was compared at equal initial stress. It would appear more reasonable to compare behavior at equal initial strain, as in Figure 1. In this case, the resin treatment again shows no effect on the elastic stiffness of cotton, but for rayon it has produced a significant increase in stiffness. The lack of effect on cotton may be explained in terms of Flory's theory by the high crystallinity and orientation of this fiber. The result on rayon is in line with that expected theoretically from a more amorphous polymer and with that obtained by other authors such as Gagliardi and Gruntfest [20] and Tokita and Kanamaru [46]. Gagliardi and Gruntfest found that the static modulus of rayon was increased by cross-linking with formaldehyde or with aminoplast resins. Tokita and Kanamaru used tetramethylene-bis-ethyleneurea as a cross-linking reagent and determined the dynamic moduli of the samples. As shown in Figure 2, the modulus first decreased, then passed through a minimum, and finally increased as the concentration of the cross-linker increased.

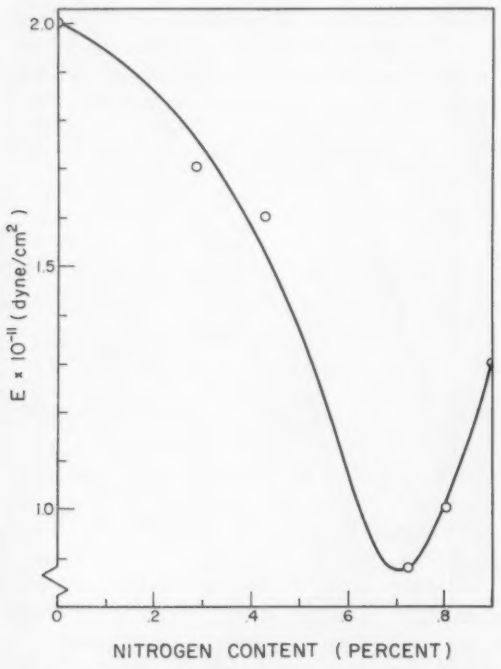

Fig. 2. Dynamic modulus of rayon fibers cross-linked with increasing amounts of tetramethylene-bis-ethyleneurea, from Tokita and Kanamaru [46].

The relation observed by Tokita and Kanamaru is strikingly similar to that found for the crease recovery of rayon fabrics treated with increasing amounts of a cross-linking resin. Figure 3 shows the crease recovery of two viscose fabrics with increasing levels of dimethylol ethyleneurea in the fabric. The minimum in the early part of this curve is very frequently, though not always, encountered. We have not observed it for cotton. It should be noted that the crease recovery is not greater than the original until more than 6 or 7% resin is introduced. This happens to be about the concentration used by Steele and Giddings in their modulus experiment and indicates that a higher level should have been examined.

A reasonable conclusion from the available data would be that in cotton the orientation is very high, so that cross links do not affect the modulus, and that in rayon, whose mechanical properties are controlled to a greater extent by the amorphous regions, there is more rubberlike behavior, and the modulus eventually goes up with cross-linking. This is complicated by an initial decrease in modulus, which is probably due to the disordering effect of the introduction of the reagent into the fiber during

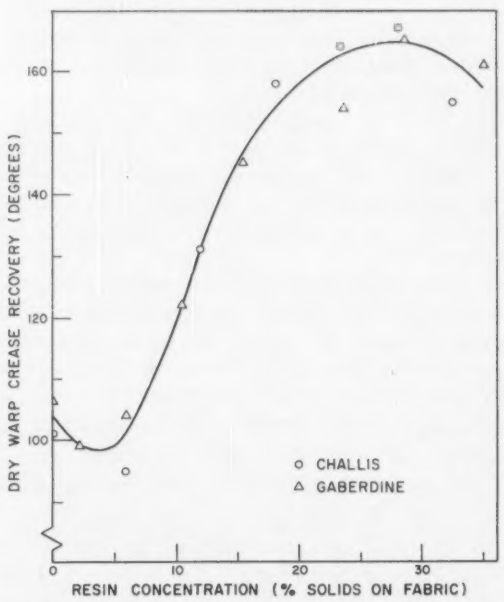

Fig. 3. Crease recovery of rayon fabrics treated with increasing levels of dimethylol ethyleneurea.

the swelling–deswelling operations of impregnating and curing.

Dimensional Stability

Shrinking of cellulose fabrics during washing may be due to relaxation of stresses in the fibers, to deformation in the fabrics due to fiber swelling, to irreversible crystalline–amorphous transitions, and finally, to feltinglike movements of individual fibers. Cross-linking can be expected to affect the first three mechanisms but probably not the felting. The effect of cross-linking on swelling has already been discussed; this is probably the major factor in dimensional stabilization. The remarks below relate to the shrinkage which may be due to crystalline–amorphous transitions and relaxation of stresses.

In his work on cross-linking partly crystalline polymers, Flory [14] concluded that, when the crystallites are melted, the length of an unrestrained fiber should vary linearly with the square root of the degree of cross-linking. This could be considered as part of a theoretical basis for the dimensional stabilization produced by resin finishes. When a fiber is wetted, some hydrogen bonds in the amorphous portion are broken and the fiber will tend to contract. This breakage of hydrogen bonds is to a degree analogous to Flory's "melting of crystallites," and it would be of great interest to correlate experimentally dimensional change with degree of cross-linking for cellulose.

The expected square-root relationship, however, may be obscured by other effects. Oosawa [34] showed that if an amorphous fiber is cross-linked in an extended state, its length, when the extending force is released, will vary in the first approximation linearly with the degree of cross-linking. Since in industrial practice the fabrics are frequently stretched in the curing oven, this linear relationship may be superimposed on Flory's square-root relationship.

There are other results of interest that arise from Flory's and Oosawa's theories. Flory showed that cross-linking in the amorphous portion increases the melting point of the crystallites. At present we do not really know if there is any crystalline–amorphous transition on stretching cotton or rayon fibers. If there is, cross-linking will affect it appreciably. It may also be of interest that, according to Flory, partially crystalline cross-linked polymers may have volume–temperature coefficients which are first positive and then negative with increasing temperature due to crystalline–amorphous transitions. Such transitions in cellulose may be involved in Roseveare and Poore's results as well as the postulated rubber–glass transition in the amorphous portion.

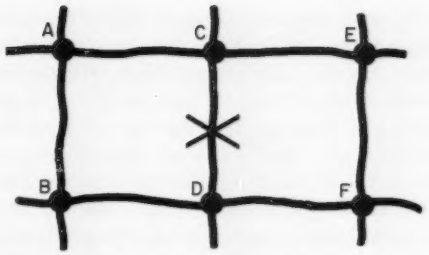

Fig. 4. The molecular model of Bueche [4] for explaining the effect of cross-linking on the tensile strength of polymers.

Tensile Strength

The theoretical basis of the effect of cross-linking on the strength of rubberlike polymers has been investigated by a number of workers, among them Morrell and Stern [31], Gee [21], Flory, Rabjohn, and Schaffer [16], and, more recently, Bueche [4]. In general, they have found that strength first rises, passes through a maximum, and then falls with increasing cross-linking.

The latest form of the theory, due to Bueche, may be outlined as follows. A cross-linked network like that in Figure 4 is assumed as a model. It is also assumed that the total force is unevenly distributed and that the broadness of the distribution of force per molecular chain segment between cross links increases with the number of such segments or with the degree of cross-linking. If the force acting on segment CD exceeds its tensile strength, the chain will break. When this happens the load on each of the two neighboring segments is increased by half the load formerly borne by CD. The sample will fail only if this new load on chain elements AB and EF exceeds their tensile strength. If the initial force distribution is known, or is assumed, the probability that a sequential process of this type will lead to failure of the sample can be calculated. The result expresses the tensile strength of the polymer in terms of the tensile strength of the individual chains, their molecular weight, the dimensions of the chain segments, and the degree of cross-linking. It predicts that the strength will pass through a maximum with increasing degree of cross-linking.

This result may be explained intuitively as follows. The increase in strength at low levels of cross-linking is due to the fact that cross-linking inhibits slippage of the molecular chains. However, as the degree of cross-linking increases and the relative movement of chains becomes more restricted, there is less opportunity for chain motion to help equalize the distribution of stress on individual chains. High local stress concentrations can then occur, and these increase the probability of rupture leading to failure.

Bueche also relates this idea to the effect of crystallinity or fillers in polymers on their tensile strength. If a chain breaks in a partly crystalline polymer, half of its load is not transmitted to the neighboring elements, but less than half, because the crystallites act as multifunctional cross links and distribute the new load over more than two molecular chains. The probability of a chain reaction leading to failure is thereby reduced. Fillers have a similar effect.

The behavior of cotton and rayon on cross-linking fits reasonably well with these ideas. Rayon is an amorphous material partly cross-linked by the presence of crystallites imbedded in the amorphous matrix. Introduction of additional cross links increases its tensile strength, then decreases it, as shown in Figure 5, which gives the tensile strength of viscose challis as a function of the amount of dimethylol ethyleneurea reacted in it. The tension on the samples during curing affects the results, but there is a maximum whether the fabric is relaxed or taut during curing.

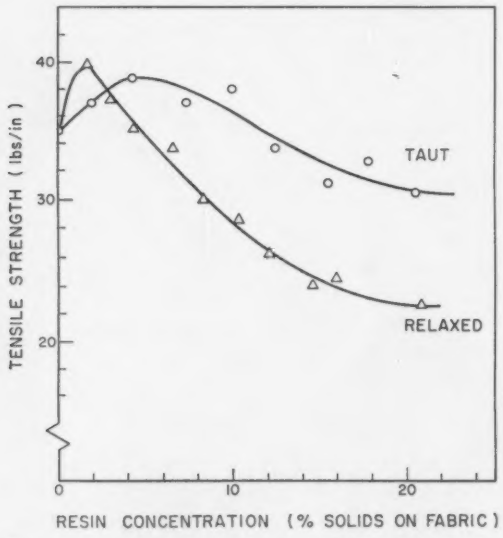

Fig. 5. Tensile strength of rayon challis treated with increasing levels of dimethylol ethyleneurea.

The general experience with cotton is that its tensile strength decreases on cross-linking, even when the catalysts used have no damaging effect. This has been demonstrated by Nickerson [33] and by Cooke et al. [7], who showed that the tensile strength of cotton cross-linked with trimethylol melamine increases to almost that of untreated cotton when the cross-linker is removed by hydrolysis in urea–phosphoric acid solution.

Cotton fibers are already relatively highly cross-linked by their high degree of crystallinity, and it appears that they have already passed the point of maximum strength obtainable by cross-linking. Adding more cross links always decreases their strength. This means that attainment of crease recovery by a cross-linking mechanism will always involve loss of strength in cotton and that elimination of all strength loss in this process is perhaps not attainable.

This extrapolation of cross-linking theory to cellulose is also reasonable in terms of the effect of moisture on tensile strength. Wetting cellulose fibers reduces molecular interactions, mostly hydrogen bonds, which act as cross links. This reduces the strength of rayon, since its original state corresponds to a point below the maximum of the strength–cross-linking curve. In cotton, taking out cross links by wetting improves the strength, since its original condition is beyond the maximum.

Resilience

The principal aim in cross-linking cellulose fibers is to improve their crease recovery or wash-wear properties. Gagliardi and Gruntfest [20] determined the elastic recovery of cross-linked rayon fibers by stretching them and comparing the length increment found after removing the load to that under load. These tensile elastic recovery values correlated well with crease recovery. Steele [41] presented data indicating that the wash-wear rating of cotton and rayon is a function of wet and dry crease recoveries. It is thus probable that all three tests (crease recovery, wash-wear rating, and elastic recovery) are related to the same fundamental property of cellulose.

From the rheological point of view, the elastic recovery test is well defined geometrically, and it is

convenient to discuss resilience in terms of this test. When a sample is extended under load, the extension is generally the sum of three components. The elastic deformation is time independent and is instantaneously recovered when the load is removed. The secondary creep is a time-dependent viscous and elastic deformation which slowly recovers after the load is removed. Finally, the permanent creep is a time-dependent, purely viscous deformation which cannot be recovered.

The kinetic theory of rubber elasticity does not apply to time-dependent deformation, since it deals only with equilibrium forces. We have no simple theory available quantitatively relating creep behavior to molecular structure. However, it is reasonable to assume that viscous deformation is due to chains slipping relative to each other and that cross links tend to stabilize the relative positions of chain segments and thus reduce creep. It is general experience that vulcanized rubbers do not show creep [39].

Wet and Dry State Cross-Linking

This subject has been recently discussed in detail by Steele [41] and Reeves et al. [36]. In contrast to conventional cross-linking, where the cellulose is essentially in a dry collapsed state during the reaction, wet cross-linking leads to higher wet than dry resilience and to increased moisture regain. Apparently wet cross-linking stabilizes the swollen, expanded state of cellulose and may even change the amorphous–crystalline ratio. The Flory-Rehner theory on swelling [13, 15, 17] does not apply at all to such systems.

Steele assumes that intermolecular cross links increase both wet and dry crease recovery but that the wet crease recovery can be enhanced by an additional mechanism. When a wet fiber is deformed by bending, there is likely to be a region in the strained area which is forced to deswell. The tendency of the fiber to reabsorb water when the deforming force is removed would provide an additional driving force tending to restore the unstrained form of the fiber. If the swelling of the fiber is increased by the finishing treatment, the available driving force for recovery from wet creasing would also increase. It is suggested that intramolecular cross links might act as structure-disrupting elements in cellulose so that its swelling would be increased (as it is, for instance by low levels of methylation) and that cross-linking carried out when the cellulose is swollen leads to a higher proportion of intramolecular cross links than reaction in the dry state.

The only investigator who has considered the cross-linking of swollen polymers in general is Oosawa [34]. This author showed that when an extended swollen polymer is cross-linked, the introduction of cross links may give rise under certain conditions to an increased retractive force, while the retractive force is unchanged when an extended unswollen polymer is cross-linked. Oosawa attempted to explain muscle action by this mechanism. More work is needed on both cellulose and other polymers before we can better understand the differences between wet and dry state cross-linking.

Cross Link Density in Resin-Treated Cellulose

It was shown above that certain analogies exist between cross-linked cellulose and cross-linked rubbery polymers and that the molecular theories developed for cross-linked rubbers qualitatively explain the behavior of cross-linked cellulose. One puzzling discrepancy between cross-linking rubbery polymers and cross-linking cellulose is that the presently available evidence indicates that the cross-link density required to give marked changes in the physical properties of cellulose is much higher than for rubbery polymers. No unequivocal work has yet been done to determine quantitatively the degree of intermolecular cross-linking in modified celluloses, and any picture that can be deduced from the available data cannot really be conclusive. Nevertheless, it is of interest to speculate on these matters on the basis of the available data, even though they are poorly suited to our purpose.

In practice it has been found that beyond about 5% dimethylol ethyleneurea add-on for cotton and beyond about 15% for rayon, further increments of reactant do not lead to improvements in resilience. These values are typical for nitrogenous finishes. If it is assumed that each dimethylol ethyleneurea molecule reacts to form a cross link and that cotton and rayon are 20% and 60% accessible to the reactant, respectively, it can be calculated that the treated cotton or rayon contains one cross link per two accessible glucose units, or that every accessible glucose unit is cross-linked. It is, however, very unlikely that this is so. The reactions that can compete with each other when cellulose and a nitrogenous

reagent are allowed to react are numerous, and lead to the following possibilities:

1. The cross link may contain more than one reactant molecule.
2. The cross link may be inter- or intramolecular with respect to the cellulose.
3. The reaction between the reactant and cellulose may be single-ended, giving rise to either a monomer residue or a polymer grafted to the cellulose.
4. Finally, the reactant may polymerize without forming chemical links with cellulose and be held simply by physical entrapment.

Steele and Giddings [42, 43] and Frick et al. [18] investigated the reaction of dimethylol urea and dimethylol ethyleneurea with cellulose. In separate experiments Frick established that the polymerization of dimethylol ethyleneurea in the absence of cellulose involves loss of formaldehyde. Thus the formaldehyde-to-urea ratio in a high-molecular-weight polymer would be about unity. Frick also assumed that free methylol end-groups would not survive the curing reaction. Thus in extreme cases a formaldehyde-to-urea ratio of two would correspond to monomolecular cross-link formation, while a ratio of unity would indicate either single-ended reaction, single-ended graft polymerization, or formation of a very-high-molecular-weight polymer not chemically linked with cellulose. The experimental formaldehyde–urea ratios were 1.5 for dimethylol urea and 1.4 for dimethylol ethyleneurea. From this it can be concluded that, regardless of what side reactions occurred, the actual number of cross links is not more than half the value calculated above. In other words, the ratio of accessible glucose units to cross links at the stated application levels is not two but four. In arriving at this figure we have not considered the possibility that intra- as well as intermolecular cross links could be formed.

It is striking that the amount of reactant required to reach the maximum effect on cotton and rayon is about proportional to their degree of accessibility. This suggests that the efficiency of cross links in the two materials is approximately equal, in spite of the fact that the DP of rayon is much lower than that of cotton. Flory, considering the effect of cross-linking on mechanical properties [12], reasoned that cross links near chain ends should be less effective in changing the modulus and suggested a correction for this effect to be introduced into the equation shown earlier. If ν is the actual number of intermolecular cross links, ν_e is the effective number of cross links, $(DP)_c$ is the number of monomer units between cross links, and $(DP)_n$ is the degree of polymerization before cross-linking, the correction may be calculated from the following relation:

$$\frac{\nu_e}{\nu} = 1 - 2\frac{(DP)_c}{(DP)_n}$$

If one assumes equal efficiency for cross links in cotton and rayon, this equation can be used to estimate roughly the frequency of cross links.

If we take the DP of cotton and rayon to be 3000 and 300, respectively, the ratio of effective cross links to total cross links is shown in Table I for various values of $(DP)_c$. The values for both materials are approaching unity and, in the range of 12 to 25 for $(DP)_c$, the cross-link efficiencies in the two fibers come within 15% of each other. Although these assumptions are rather tenuous, the results suggest that at least every twenty-fifth glucose unit must be intermolecularly cross-linked in resin-treated cellulose. It should be emphasized that it is not known with sufficient accuracy how accessible cotton and rayon are to the nitrogenous reactants or whether the 5% and 15% dimethylol ethyleneurea levels impart truly comparable changes in mechanical properties.

It was estimated above from the analytical evidence of Frick [18] and Steele [42] that one cross link per four accessible glucose units is the level of dimethylol ethyleneurea or dimethylol urea application where maximum crease recovery is attained. This includes both intra- and intermolecular cross links. The second estimate, from the chain-end correction, gave an intermolecular cross-link density of at least one out of 25 accessible glucose units. These figures might be reconciled if the proportion of cross links which are intermolecular could be estimated for the first case. In this respect a recent Japanese paper is of interest. Zyo and Kamiya [52]

TABLE I. Ratio of Effective to Total Cross Links for Cotton and Rayon at Various Cross-Link Densities

	ν_e/ν	
$(DP)_c$	Cotton	Rayon
100	.934	.333
50	.967	.667
25	.983	.834
12.5	.992	.917

cross-linked secondary cellulose acetate with tetramethylene-bis-ethyleneurea and determined the actual number of intermolecular cross links by swelling the insoluble product in a solvent and treating the data by the Flory-Rehner theory. Recalculation of their data shows that, at application levels corresponding to 1 cross link per 5.5–3.5 glucose units, the actual number of intermolecular cross links was four times less. As already shown, the total number of cross links at the saturation level of dimethylol ethyleneurea application corresponds to 1 in 4 accessible glucose units. This figure is in the application range of Zyo and Kamiya. If it could be assumed that for cotton and rayon, as for cellulose acetate, 25% of the total cross links are intermolecular, this correction applied to the analytical estimate would indicate that every sixteenth accessible glucose unit is intermolecularly cross-linked. This figure is consistent with the end-effect calculation which indicated that at least every twenty-fifth glucose unit is intermolecularly cross-linked.

It must be emphasized that these estimates are based on poor circumstantial evidence. Recent work by Tesoro [45] suggests that if these estimates are in error, then this error involves underestimation rather than overestimation of the actual cross-link densities. Tesoro found the total number of cross links to be higher than the estimate reached above. In her work, cotton was cross-linked with pyridine salts of bischloromethyl ethers of ethylene glycol homologues and at the highest level of crease recovery attained one cross link was attached to each accessible anhydroglucose unit.

All of these results seem to indicate that cellulose needs considerably more cross-linking to produce large changes in mechanical properties than rubbery polymers. For example, in rubber, an increase in cross-linking density from 1 in 300 to 1 in 100 monomer units raises the modulus threefold. This difference between cellulose and rubbery polymers can be best understood in relation to other rheological problems.

The primary aim of reactant finishes is to improve the resilience of cellulose by affecting the viscous portion of the deformation process. Increasing the modulus probably has little practical effect. In uncross-linked polymers the occurrence of creep or irrecoverable deformation is due to chain slippage. If, however, the condition for an infinite molecular network is fulfilled, i.e., the polymer contains one cross link per number average molecule, chain slippage is normally completely inhibited. In rubbers, striking changes in the rheological properties do indeed start to occur in the region where the degree of cross-linking reaches the postulated level. In cellulose this level would correspond to 1 intermolecular cross link per 3000 glucose units in cotton and 1 per 300 or 400 in rayon if crystallinity were neglected, and even lower levels if it were not.

The case of cotton is perhaps the simpler. It is general experience that the crease recovery of cotton gradually increases at low levels of resin application and then levels out. Generally even at the highest degree of application the warp crease-recovery angle does not exceed $\sim 150°$. Thus two interrelated facts must be explained:

1. Even at very low reactant application levels, the degree of cross-linking probably exceeds that theoretically required to inhibit chain slippage. Nevertheless, the elastic recovery of the samples is improved only gradually at these low levels of cross-linking.
2. Even at the highest levels of reactant applications the elastic recovery of cotton is not complete.

It is possible that these complications are partly due to the fabric structure. The movement of individual fibers in the fabric is very little controlled by the reactant resins. Friction and mechanical entanglement involved in the slippage of fibers in the fabric may be the reason that the crease recovery levels off at values lower than 180°. The importance of this cannot be decided until we have better data on the relation between single fiber and fabric properties for cross-linked celluloses.

Regardless of how important the fabric structure is in limiting crease recovery, it does not account for the results obtained in the intermediate resin application range, where the crease recovery angle does not reach the leveling-off value while the degree of intermolecular cross-linking is already much higher than that theoretically required to inhibit slippage of the individual molecules. It seems likely therefore that, in spite of the stiffness of the cellulose chain, a high degree of cross-linking is necessary to attain the necessary degree of inhibition of segmental motion in the chain. To obtain crease recovery, not only must large-scale chain slippage be prevented when the cross-linked network is deformed, but also the readjustment of relatively short chain segments.

In cross-linked rubbers, this deformation is resisted only by very weak interchain forces. When a high degree of molecular interaction is involved, as it is in cellulose, segmental slippage and creep are more important in the mechanical behavior and a much higher cross-linking density is required to prevent them. Molecular interaction in cellulose through hydrogen bonds and other polar forces makes segmental motion more time dependent than in rubber and important in determining crease recovery.

At high levels of cross-linking the arguments put forward for cotton also apply to rayon. At low levels of resin application, for example, at 0–3% dimethylol ethyleneurea or dimethylol urea, the crease recovery does not increase, but decreases, as shown in Figure 3. It was estimated that at the 15% application level about every sixteenth to twenty-fifth glucose unit in rayon is intermolecularly cross-linked. It would be very difficult to estimate the number of effective cross links at the low reactant application levels, especially because the chain-end correction at these levels becomes extremely high due to the low molecular weight of rayon. In fact, at these very low degrees of cross-linking, Flory's formula can hardly be applicable, because it may even lead to theoretically impossible negative values of the effective cross-link density. It should suffice to say that it is very probable that in the range of 0–3% reactant add-on the condition for the formation of an infinite molecular network is not fulfilled and chain slippage may occur. As soon as chain slippage is inhibited by the increasing concentration of reactant, the crease recovery rises by the same mechanism as described for cotton.

Conclusion

Cross-linking insolubilizes cellulose and reduces its swelling as in other polymers, but swelling and gelation data on cross-linked cellulose cannot be treated quantitatively to determine cross-link density because the theoretical treatment cannot take into account the nonrandom distribution of cross links which results from the polycrystalline structure of the polymer. The glass transition temperature for cellulose is uncertain, and no information on the effect of cross-linking on it is available. The dynamic modulus of rayon is first decreased, then increased by cross-linking. The modulus of cotton is unchanged by cross-linking because of its high molecular orientation. The effect of cross-linking on the tensile strength of cellulose is apparently analogous to the usual effect in other polymers, which shows a maximum as the cross-link density goes up. The maximum is observable in rayon but not in cotton, since the latter is already highly cross-linked in the native state by crystalline regions.

Rayon and cotton celluloses appear to require very high degrees of cross-linking to modify their properties to the point where wash-wear behavior is obtained.

Literature Cited

1. Brown, A., TEXTILE RESEARCH JOURNAL **25**, 891–901 (1955).
2. Bruckhaus, W., *Oesterr. Chem.-Ztg.* **29**, 156–157 (1926).
3. Bryant, G. M. and Walter, A. T., TEXTILE RESEARCH JOURNAL **29**, 211–219 (1959).
4. Bueche, F., *J. Polymer Sci.* **24**, 189–200 (1957); **33**, 259–271 (1958).
5. Cameron, W. G. and Morton, T. H., *J. Soc. Dyers Colourists* **64**, 329–336 (1948).
6. Charlesby, A., *J. Polymer Sci.* **11**, 513–520 (1953); *Proc. Roy. Soc., London* **215A**, 187–214 (1952); **222A**, 60–74, 542–557 (1954); **224A**, 120–128 (1954).
7. Cooke, T. F., Dusenbury, J. H., Kienle, R. H., and Lineken, E. E., TEXTILE RESEARCH JOURNAL **24**, 1015–1036 (1954).
8. Eschalier, X., French Patent 347,724 (1906) and additions 8122 (1906) and 9904 (1908); *c.f.* Hall, A. J., *Can. Textile J.* **58**, No. 6, 34–36, 50 (1941).
9. Flory, P. J., *J. Am. Chem. Soc.* **63**, 3083–3090 (1941); *J. Phys. Chem.* **46**, 132–140 (1942).
10. Flory, P. J., *Chem. Revs.* **35**, 51–75 (1944).
11. Flory, P. J., "Principles of Polymer Chemistry," Ithaca, Cornell 360 (1953).
12. Flory, P. J., "Principles of Polymer Chemistry," Ithaca, Cornell 461 (1953).
13. Flory, P. J., "Principles of Polymer Chemistry," Ithaca, Cornell 580 (1953).
14. Flory, P. J., *J. Am. Chem. Soc.* **78**, 5222–5235 (1956); *Science* **124**, 53–60 (1956).
15. Flory, P. J. and Krigbaum, W. R., *J. Chem. Phys.* **18**, 1086–1094 (1950).
16. Flory, P. J., Rabjohn, N., and Schaffer, M. C., *J. Polymer Sci.* **4**, 435–455 (1949).
17. Flory, P. J. and Rehner, J., Jr., *J. Chem. Phys.* **11**, 521–526 (1943).
18. Frick, J. G., Jr., Kottes, B. A., and Reid, J. D., TEXTILE RESEARCH JOURNAL **29**, 314–322 (1959).
19. Fox, T. G. and Loshaek, S., *J. Polymer Sci.* **15**, 371–390 (1955).
20. Gagliardi, D. D. and Gruntfest, I. J., TEXTILE RESEARCH JOURNAL **20**, 180–188 (1950).
21. Gee, G., *J. Polymer Sci.* **2**, 451–462 (1947).

22. Head, F. S. H., *J. Textile Inst.* **49**, T345–T356 (1958).
23. Hindman, H. and Burr, G. S., *Trans. Am. Soc. Mech. Engrs.* **71**, 789–796 (1949).
24. Klein, E. and Jenckel, E., *Z. Naturforsch.* **7a**, 800–807 (1952).
25. Landels, G., *J. Soc. Dyers Colourists* **72**, 137–146 (1956).
26. Lineken, E. E., Davis, S. M., and Jorgensen, C. M., TEXTILE RESEARCH JOURNAL **26**, 940–947 (1956).
27. Loshaek, S., *J. Polymer Sci.* **15**, 391–404 (1955).
28. Marsh, J. T., *Textile Mfr.* **85**, 294–295 (1959).
29. Meunier, L. and Guyot, R., *Rev. gén. colloides* **7**, 53–66 (1929).
30. Minnema, L. and Staverman, A. J., *J. Polymer Sci.* **29**, 281–306 (1958).
31. Morrell, S. H. and Stern, J., *Trans. Inst. Rubber Ind.* **28**, 269–277 (1953).
32. Mullins, L., *J. Appl. Polymer Sci.* **2**, 1–7 (1959).
33. Nickerson, R. F., *Am. Dyestuff Reptr.* **39**, P46–P50, P62 (1950).
34. Oosawa, F., *J. Polymer Sci.* **32**, 229–246 (1958).
35. Passaglia, E. and Koppehele, H. P., *J. Appl. Polymer Sci.* **1**, 28–36 (1959).
36. Reeves, W. A., Perkins, R. M., and Chance, L. A., TEXTILE RESEARCH JOURNAL **30**, 179–192 (1960).
37. Roseveare, W. E. and Poore, L., *J. Polymer Sci.* **14**, 341–354 (1954).
38. Schultz, A. P., *J. Am. Chem. Soc.* **80**, 1854–1860 (1958).
39. Staverman, A. J. and Schwarzl, F., in "Die Physik der Hochpolymeren," Vol. IV, H. A. Stuart, ed., Springer Verlag, 14 (1956).
40. Steele, R., TEXTILE RESEARCH JOURNAL **25**, 545–548 (1955).
41. Steele, R., TEXTILE RESEARCH JOURNAL **30**, 37–46 (1960).
42. Steele, R. and Giddings, L. E., Jr., *Ind. Eng. Chem.* **48**, 110–114 (1956).
43. Steele, R. and Giddings, L. E., Jr., TEXTILE RESEARCH JOURNAL **26**, 116–123 (1956).
44. Stockmayer, W. H., *J. Chem. Phys.* **11**, 45–55 (1943); **12**, 125–134 (1944).
45. Tesoro, G. C., TEXTILE RESEARCH JOURNAL **30**, 192–201 (1960).
46. Tokita, N. and Kanamaru, K., *Kogyo Kaguku Zasshi* **59**, 824–830 (1956); *J. Polymer Sci.* **27**, 255–267 (1958).
47. Ueberreiter, K., *Z. physik. Chem.* **B48**, 197–218 (1941).
48. Ueberreiter, K. and Kanig, G., *J. Chem. Phys.* **18**, 399–406 (1950).
49. Wagner, R. E. and Pacsu, E., TEXTILE RESEARCH JOURNAL **22**, 12–20 (1952).
50. Wall, F. T., *J. Chem. Phys.* **11**, 67–71 (1943).
51. Wood, F. C., *J. Soc. Chem. Ind.* **50**, 411T–418T (1931).
52. Zyo, N. and Kamiya, M., *Bull. Textile Res. Inst., Japan* **45**, 79–86 (1959).

Manuscript received July 6, 1960.

On Changes in the Weight Distribution Function of Artificial Fibers Due to Random Fiber Breakage

W. J. Byatt

Sandia Corporation, Albuquerque, New Mexico

Abstract

It is possible to prepare artificial fibers so that each of them has, initially, the same length. This possibility simplifies the mathematical treatment of the subsequent random time breakage, as in ginning. Upper and lower bounds to an exact expression for the time-dependent weight distribution function, $W(l, t)$, are found. Under certain conditions, the bounds coalesce to the exact solution $W(l, t)$.

The usefulness of the approximations found for testing the theory and in finding certain transition probabilities associated with fiber decay is discussed.

Introduction

In an earlier paper [1] dealing with cotton, there was derived an integro-differential equation which governed the time-dependent changes of the weight distribution function (WDF) of fibers subjected to random breakage.

The present paper will discuss artificial fibers. It turns out that this is a decided advantage from

one point of view because of the fact that man-made fibers can be prepared in such a way that their initial WDF is a delta function. That is, if the total fiber weight is assumed to be unity, the initial WDF is characterized by

$$\delta(l - l_0) \tag{1}$$

Then, the total weight

$$W_T = \int_0^\infty \delta(l - l_0)dl = 1 \tag{2a}$$

Further, as is known,

$$f(l_0) = \int_0^\infty \delta(l - l_0)f(l)dl \tag{2b}$$

The familiar properties 2(a, b) of the delta function make considerable generalization of earlier results of [1] possible. The same Boltzmann transport equation derived there is applicable. It is

$$W_t + \sigma(l)W = \int_l^{l_0} p(l' \to l)W(l', t)dl' \tag{3}$$

where subscripts indicate differentiation with respect to the variable indicated; $W(l, t)$ is the time-dependent WDF, $\sigma(l)$ is the probability per unit time of decay of a fiber of length l, and $p(l' \to l)$ is the probability per unit length per unit time that a fiber of length l' decays such that one of its segments is of length l. In Reference 1, Equation 3 was solved subject to the conditions that

$$\lim_{t \to 0} W(l, t) \equiv W(l, 0) \tag{4}$$

was arbitrary, but known or measurable, and that

$$\left.\begin{aligned} \sigma(l) &= kl \\ p(l' \to l) &= k \end{aligned}\right\} \tag{5}$$

With Conditions 4 and 5, the solution to Equation 3 is

$$W(l, t) = e^{-\mu l}\left\{W(l, 0) + \mu \int_l^\infty W(l', 0)dl'\right\} \tag{6}$$

where $\mu = kt$ is a parameter having dimensions of reciprocal length. If Condition 1 is now placed into Equation 6, the expression for $W(l, t)$ becomes

$$\begin{aligned} W(l, t) &= e^{-\mu l}\{\delta(l - l_0) + \mu\}; \quad (l \leq l_0) \\ &= 0 \quad (l > l_0) \end{aligned} \tag{7}$$

It is easily shown that Solution 7 satisfies the "conservation" condition

$$\int_0^{l_0} W(l, t)dl = \int_0^{l_0} \delta(l - l_0)dl = 1 \quad (l \leq l_0)$$

Development of Equation for Study of Bounds

The present note will be concerned with the establishment of bounds on the solution to Equation 3 for more general forms of the functions $\sigma(l)$ and $p(l' \to l)$. In particular, results of the work to follow will show that one can find two functions, W_1 and W_2, such that

$$W_1 \leq W(l, t) \leq W_2$$

where W is the exact solution to Equation 3. It develops that Equation 7 is related to the lower bound W_1. The first aim will be to recast Equation 3 in a form more suitable for a study of bounds.

To come to details, consider Equation 3 with initial data

$$\lim_{t \to 0} W(l, t) = \delta(l - l_0)$$

Put

$$W(l, t) = e^{-\sigma t}\delta(l - l_0) + X(l, t) \tag{8}$$

Henceforth, it is to be understood that $\sigma \equiv \sigma(l)$; $\sigma_0 \equiv \sigma(l_0)$. The quantity $X(l, t)$ is, then, the representation of broken fibers. The first term of the right-hand of Equation 8 satisfies the equation

$$W_t + \sigma W = 0$$

so that X satisfies

$$X_t + \sigma X = p(l_0 \to l)e^{-\sigma_0 t} + \int_l^{l_0} p(l' \to l)X(l', t)dl' \tag{9}$$

The initial condition on X is, of course,

$$X(l, 0) = 0$$

since no fibers have been broken at $t = 0$. To continue with the transformation of Equation 9, observe that

$$X_t + \sigma X = e^{-\sigma t}\frac{\partial}{\partial t}(e^{\sigma t}X)$$

so that X satisfies the integral equation

$$X = p(l_0 \to l)e^{-\sigma t}\left[\frac{e^{-(\sigma_0 - \sigma)t} - 1}{\sigma - \sigma_0}\right] + \int_0^t e^{-\sigma(t-\tau)}\int_l^{l_0} p(l' \to l)Xdl'd\tau \tag{10}$$

A transformation

$$Y = e^{\sigma t}X$$

casts Equation 10 into the more simple form

$$Y = p(l_0 \to l)\left[\frac{e^{-(\sigma_0-\sigma)t}-1}{\sigma-\sigma_0}\right] + \int_0^t\int_t^{l_0} p(l' \to l)\,Y(l',\tau)dl'd\tau \quad (11)$$

It is Equation 11 which will be discussed.

A Lower Bound for Y *and* W(l, t)

Each term in Equation 11 is positive. An iterative scheme will produce a sequence of functions Y_n such that

$$Y = \sum_{n=0}^{\infty} Y_n \quad (12)$$

where

$$\left.\begin{aligned} Y_0 &= p(l_0 \to l)\left[\frac{e^{-(\sigma_0-\sigma)t}-1}{\sigma-\sigma_0}\right] \\ \text{and} \quad Y_{n+1} &= \int_0^t\int_t^{l_0} p(l' \to l)\,Y_n(l',\tau)dl'd\tau \end{aligned}\right\} \quad (13)$$

It follows that the truncated series $\sum_{n=0}^{N} Y_n$ satisfies the inequality

$$Y \geq \sum_{n=0}^{N} Y_n$$

Then, a lower bound will be determined by an iterative procedure. Consequently, there exists a function

$$W(l,t) \geq e^{-\sigma t}\{\delta(l-l_0) + \sum_{n=0}^{N} Y_n\} \quad (14)$$

In particular, taking only the term $n = 0$,

$$W(l,t) \geq e^{-\sigma_0 t}\left\{\delta(l-l_0) + p(l_0 \to l)\left(\frac{e^{\sigma t}-e^{\sigma_0 t}}{\sigma-\sigma_0}\right)\right\} \quad (15a)$$

Now, as $l \to l_0$, $\sigma \to \sigma_0$ in which case Equation 15a approaches

$$W(l,t) \geq e^{-\sigma t}\{\delta(l-l_0) + p(l_0 \to l_0)t\} \quad (15b)$$

But Equation 15b is precisely Equation 7. This proves the assertion made earlier that one can find a lower bound W_1 (related to the Equation 6) for the solution to Equation 3. It is noteworthy that no restrictions whatever on the choice of either σ or $p(l_0 \to l)$ have been used in deriving 15(a, b).

Further terms in the iteration scheme cannot be evaluated unless some form for the probability p is assumed. Since such assumptions were to be avoided, apart from the fact that the p's are bounded, the iterative scheme will be pursued no further.

An Upper Bound for Y *and* W(l, t)

An upper bound is easily established by invoking the assumption that the probabilities $p(l_0 - l)$ and $p(l' \to l)$ are bounded. Although this assumption might appear trivial, it is to be recalled that the p's are probability *densities*. There is no guarantee that these densities may not greatly exceed unity and become, even, infinite in the range $0 \leq l \leq l_0$[1] Let the maximum of the p's be called p_1, a constant. Then there exists a function Z, satisfying

$$Z = p_1 t + p_1 \int_0^t\int_t^{l_0} Z(l',\tau)dl'd\tau \quad (16)$$

related to Y through the inequality

$$Y \leq Z$$

To show this, it is only necessary to observe that, if p_1 is the maximum of $p(l_0 \to l)$,

$$p(l_0 \to l)\left(\frac{e^{+(\sigma-\sigma_0)t}-1}{\sigma-\sigma_0}\right) \leq p_1\int_0^t e^{-a\tau}d\tau$$

where $a = \sigma_0 - \sigma$. Then, since $e^{-at} \leq 1$, it follows that $\int_0^t e^{-a\tau}d\tau \leq t$. The inequality $Y \leq Z$ then follows. When the solution to Equation 16 is obtained, there will correspond to Z a function W_2 such that $W(l,t) \leq W_2$.

To find the solution to Equation 16, differentiate with respect to t and take the Laplace transform of the expression obtained on differentiation. The result is

$$s\hat{Z} = p_1/s + p_1\int_t^{l_0} \hat{Z}dl' \quad (17)$$

where $\hat{Z}$ is the Laplace transform of Z. As $l \to l_0$,

[1] An example is the following: If $p(l' \to l)$ were given by a Gaussian distribution with very small deviation from the mean, its maximum might be huge, although the integral of p would be unity. A delta function probability density would become infinite at some point in $0 \leq l \leq l_0$.

$\hat{Z} \to p_1/s^2$. Differentiating Equation 17 with respect to l produces the equation

$$\hat{Z}_l = -\frac{p_1}{s}\hat{Z}$$

the solution to which is

$$\hat{Z} = \frac{p_1}{s^2} e^{\frac{p_1}{s}(l-l_0)} \tag{18}$$

The inversion of Equation 18 gives the expression for Z; it is

$$Z = \left(\frac{p_1 t}{l_0 - l}\right)^{\frac{1}{2}} I_1(2\sqrt{p_1(l_0 - l)t}) \tag{19}$$

where $I_1(x)$ is the Bessel function of order unity and imaginary argument. Then, there exists a function

$$W_2 = e^{-\sigma t}\left\{\delta(l-l_0) + \left(\frac{p_1 t}{l_0 - l}\right)^{\frac{1}{2}} I_1(2\sqrt{p_1(l_0-l)t})\right\} \tag{20}$$

such that $W(l, t) \leq W_2$.

Finally, then, the assertion made at the outset of this section is verified: one can find two bounds to the solution $W(l, t)$ of Equation 3 such that

$$e^{-\sigma t}\left\{\delta(l-l_0) + p(l_0 \to l)\left[\frac{e^{(\sigma-\sigma_0)t}-1}{\sigma-\sigma_0}\right]\right\} \leq W(l, t)$$

$$\leq e^{-\sigma t}\left\{\delta(l-l_0) + \left(\frac{p_1 t}{l_0 - l}\right)^{\frac{1}{2}} I_1(2\sqrt{p_1(l_0-l)t})\right\} \tag{21a}$$

If $l_0 - l$ is small, and if the σ's vary slowly with l, the inequality reduces to the form

$$e^{-\sigma t}\{\delta(l - l_0) + p(l_0 \to l)t\} \leq W(l, t)$$
$$\leq e^{-\sigma t}\{\delta(l - l_0) + p_1 t\} \tag{21b}$$

Remembering that p_1 is the assumed maximum of $p(l_0 \to l)$, it is seen that, if the value of $p_1 \approx p(l_0 \to l)$, the two bounds are indeed rather close to one another. If $p(l_0 \to l)$ is a constant, it can be called p_1; the bounds coalesce so that the exact solution to $W(l, t)$ is given by Equation 21b for $p(l_0 \to l) = p_1$.

Discussion

Earlier [1] it was seen that a solution of the form of Equation 6 was, in general, in fair to good agreement with the observed time-dependent changes in the WDF of cotton. In general, the range of the parameter $\mu = kt$, where k was the assumed constant value of $p(l' \to l)$, was from $0.1 \leq \mu \leq 0.2$ in.$^{-1}$ Examples discussed [1] indicate that, as fiber length increased, μ had to increase in order that theory agree with observation. Such an increase of μ with length is contrary to the assumption made earlier [1]: $p(l' \to l) = k$, a constant. It was also pointed out that this was a defect in the theory. Such an objection is no longer valid in the present paper. For example, in Equation 15, there are no restrictions whatever placed on $\sigma(l)$ and on $p(l_0 \to l)$. But it is known, too, from experiment, that the usual range of $p(l_0 \to l)t$ is in the neighborhood of 0.1 to 0.2. This suggests immediately that Equation 15 will be a good approximation to $W(l, t)$, since further iterates will contain terms in higher powers of p. If all $p(l_0 \to l)t$ are of the same order of magnitude, then higher order terms will make a negligible contribution.

It is the understanding of the author that the idea of using artificial fibers in a cotton gin to test the theory developed here and to find explicit forms for $\sigma(l)$ and $p(l_0 \to l)$ is being actively pursued by Kendall Company Research Laboratories, Paw Creek, N. C., under the direction of J. P. Elting and J. C. Barnes.

Acknowledgments

Readers familiar with the mathematics of the transport Equation 3 will immediately note the obvious debt which the author owes to the well-developed literature of the so-called straight-ahead approximation of gamma-ray transport theory [2]. Discussions with Professor I. Kolodner of the University of New Mexico, a consultant to Sandia Corporation, and with Dr. G. M. Wing, Mathematics Division of Sandia Corporation, on the gamma transport problem have materially aided in the preparation of this paper. Finally, work of this kind was first proposed to the author by J. P. Elting of Kendall Company Research Laboratories, in collaboration with whom Reference 1 was written.

Literature Cited

1. Byatt, W. J. and Elting, J. P., TEXTILE RESEARCH JOURNAL **28**, 417 (1958).
2. Goldstein, H., "Fundamental Aspects of Reactor Shielding," Addison-Wesley Co., Chapter 5 (1959).

Manuscript received July 25, 1960.

Letters to the Editor

Cotton Fiber Weight Distribution

The September 1959 issue of TEXTILE RESEARCH JOURNAL included an article entitled "Blending Cottons Differing Widely in Maturity, Part I" by Messrs. Fiori, Louis, and Sands in which there was a discussion of fiber fineness distribution according to fiber length group. In the August 1960 issue of the JOURNAL correspondence relative to this discussion was published. Since the appearance of these letters, we have received three other communications pertaining to the topic. The authors of the original paper have reviewed the comments of two of these letters, and have prepared a reply. The four contributions have been brought together in this special section of Letters to the Editor. We appreciate the interest shown in this topic, and we hope that the presentation of divergent points of view has been helpful, but in view of the space already devoted to it, we propose to complete the discussion with these letters.—EDITOR

Hellenic Cotton Board
Technological Laboratory
5a Stadium Street
Athens, Greece
November 8, 1960

To the Editor
TEXTILE RESEARCH JOURNAL

Dear Sir:

Cotton fiber weight distribution was recently discussed in this Journal [2]; it was shown that short fibers are finer than the long ones, varying by fiber length group. On this two letters [3] were written, one expressing the opposite view and the other supporting the original.

As the correlation between fiber length and fineness is of basic importance, hereunder are given some test results that may be useful to this end. In these tests, cotton of *Gossypium hirsutum*, American Upland type, grown in Greece, of different Micronaire index and fibers from seed cotton were examined for length and weight fineness. The length is expressed in millimeters and the fineness in micro-

TABLE I. Weight Fineness of Fibers per Group of Length from Cotton of Different Micronaire Index

Micronaire 3.6		Micronaire 4.8		Micronaire 5.7	
Group length, mm.	Fineness, μg./cm.	Group length, mm.	Fineness, μg./cm.	Group length, mm.	Fineness, μg./cm.
34	1.43	36	1.49	—	—
32	1.47	32	1.55	32	1.89
30	1.48	30	1.60	30	2.05
28	1.51	—	—	28	2.24
26	1.55	26	1.62	26	2.38
24	1.56	—	—	24	2.50
22	1.62	22	1.72	22	2.68
20	1.63	20	1.81	20	2.66
16	1.69	18	1.82	18	2.39
12	1.64	16	1.93	16	2.07
10	1.57	12	1.69	14	1.76
8	1.51	—	—	—	—

grams per centimeter. For fineness the cut fiber technique was used.

From the table and the figure it is shown that the shorter and the longer fibers are fine, yet the longer are the finest. There are many indications that several short fibers are not "real" short fibers but rather parts of longer fine fibers that were broken during ginning and other processes.

After that, whole fibers from seed cotton were tested. The results verified those of another publication [1]; that is, fibers from the micropylar tip are shorter and coarser and become longer and finer in the chalazal cap. This was also easily proved by the differential dyeing method. Shorter and coarser fibers in the micropylar tip dye red, while the longer and finer in the chalazal cap dye green.

From the table and the figure it is fairly evident that in the same seed, strain, or variety the shorter fibers are generally coarser and the longer are finer; long and fine varieties are much more uniform in their fiber weight distribution than the shorter and coarser ones; and the natural fiber fineness distribution is modified and even changed through ginning, mixing, and other processes that break some of the longer and finer fibers.

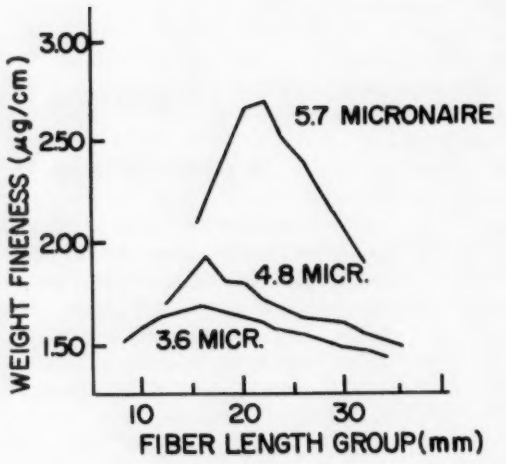

Literature Cited

1. Anon., "Better Cottons," U.S.D.A., Beltsville, Md., U.S.A. (September 1947).
2. Fiori, Louis A., Gain, L., and Sands, Jack E., TEXTILE RESEARCH JOURNAL **29**, 706–716 (1959).
3. Shah, Jamnadas; and Sands, J. E., Louis, G. L., and Tallant, J. D., TEXTILE RESEARCH JOURNAL **30**, 618–620 (1960).

TEL. CHYTIRIS

United States Rubber Company
Winnsboro, South Carolina
September 7, 1960

To the Editor
TEXTILE RESEARCH JOURNAL

Dear Sir:

With reference to the difference in opinion on cotton fiber weight distribution in the Letters section of the August issue of TEXTILE RESEARCH JOURNAL, there is a matter of technique that should be taken into consideration.

Sorting, by either the Suter-Webb or the Baer Sorter, is never perfect. If enough arrays are combined to provide a 75-mg. sample of each length group, and these are resorted, a frequency distribution is obtained which in some cases is not greatly different from arrays on raw cotton of similar length. There is a much greater chance of longer fibers being found in the short groups and shorter fibers in the long groups than the other way around, and the actual mean length of the fibers in any length group is often closer to the mean length of the sample than to the nominal midpoint of the length group in which they are found.

If the technician who counts out the fibers for weighing is not aware of this, or does not check the length of every fiber selected, this mixing has the effect of giving a higher weight per fiber for the short groups than would have been the case if they had all been the right length, and when this weight per fiber is divided by the nominal length instead of the actual mean length of the fibers, the calculated weight per inch of the shortest groups may be as much as two to three times the true value. Similarly, the apparent weight per inch of the longest groups is lowered by the admixture of shorter fibers.

When I was working on weight per inch in the U.S.D.A. Laboratory in Washington, in the early 1930's, we at first obtained curves similar to those accompanying Mr. Shah's letter, but after we learned to select and weigh only fibers of the correct length,

there was little or no evidence of any difference in weight per inch among different length groups. It was shown that the differences that had been found could be accounted for entirely by the amount of mixing of different fiber lengths that had been found in the arrays.

In the table accompanying the letter from Messrs. Sands, Louis, and Tallant, the weight per inch of the 5/16-in. group varies from 65% to 134% of that of the 13/16-in. group, and the 21/16-in. varies from 67% to 110% of the weight per inch of the 13/16-in. group. Among the 42 cottons listed, examples can be found where any one of the length groups has the highest weight per inch of those shown for a particular sample and others where each is the lowest. Also, in Figure 1 of the original paper (TEXTILE RESEARCH JOURNAL, September 1959, Page 709) by Fiori, Louis, and Sands, the 7/16-in. group from the blend has a lower weight per inch than the same length group from the fine cotton used in the blend, and there are several other points at which the weight per inch of the blend differs considerably from the average of $\frac{1}{3}$ coarse and $\frac{2}{3}$ fine cottons forming the blend. Furthermore, a comparison of Figures 1 and 2 suggests that there is very little correlation between weight per inch and maturity, except that the coarse cotton is always the highest in both properties. There seems to be plenty of evidence here to suggest that the weight per inch of individual length groups cannot be (or, at least, is not usually) measured more accurately than to within about one microgram of the true value.

It may well be that whatever relationship really exists between fiber length and weight per inch is masked by imperfect sorting and by random variations in sampling and testing.

EDWARD W. S. CALKINS

Technological Laboratory
Indian Central Cotton Committee
Adenwala Road, Matunga,
Bombay-19, India
January 4, 1961

The Editor
TEXTILE RESEARCH JOURNAL

Dear Sir:

I have read with interest the letters by Jamradas Shah [3] and by Jack E. Sands et al. [2] in the August 1960 issue of your JOURNAL. While Shah's results support the earlier findings of Dr. Turner and myself [1], those of Sands et al. are not in complete agreement with them.

It is observed from the results for 42 cottons given by Sands et al., that the value of the linear density for the lowest length group of 5/16 in. is in most cases very much lower than that for the other length groups. Presumably these samples have been obtained from commercial bales. Hence they may be derived from seed cotton picked by machines, then precleaned at several cleaning points to remove all the embedded trash, and thereafter ginned in the saw gin. The picking machine does not make any distinction between fully-mature and immature bolls. Furthermore, before picking, the plants are often defoliated so that some of the bolls do not attain complete maturity. Consequently, the picked seed cotton may contain an appreciable quantity of immature or under-developed seeds with immature fibers. During the process of cleaning and ginning it is likely that these weak immature fibers may break. The broken fibers may form a considerable proportion of the 5/16-in. length group and part of the 9/16-in. length group of the sample. Thus the immature element may be responsible for the very much lower linear density shown by the 5/16-in. length group in the investigation of Sands et al. It may also account for lowering the value of their next higher length group of 9/16 in. Determination of the fiber maturity of these samples might have thrown some light on this point.

The influence of this factor was not present in the samples examined by us. The produce obtained was from fully-developed bolls, picked by hand mostly from State farms. It was, therefore, representative of well-developed and carefully picked cotton. However, the results of the shorter length group of 5/16 in. were not determined, and furthermore the linear density was determined from cut lengths from the middle of the fiber, as remarked by Sands et al. In order to eliminate these factors, another set of eight samples was studied. These were carefully ginned and whole fibers of length groups of 1 in., 12/16 in. and 6/16 in. were weighed

TABLE I. Linear Density of Cotton Fibers of Different Length Groups in Millitex.

No.	Species	Variety	Length group, in. 1	12/16	6/16
1.	*G. hirsutum*	MCU-1 (Laboratory produce)	166	175	205
2.	*G. hirsutum*	MCU-1 (Avanashi)	164	180	166
3.	*G. hirsutum*	MCU-1 (Dharapuram)	159	163	169
4.	*G. hirsutum*	MCU-2	178	198	217
5.	*G. hirsutum*	134-Co2	168	176	194
6.	*G. hirsutum*	170-Co2	166	180	201
7.	*G. hirsutum*	Laxmi	154	166	184
8.	*G. herbaceum*	Digvijay	128	139	163
	Mean		160	172	187

and the linear density calculated. The results obtained are given below (Table I).

It will be observed that in all cases the linear density is lowest for the 1-in. length group and higher for the 12/16-in. one. It is highest for the 6/16-in. length group except in one case. The mean values are 160, 172 and 187 for 1 in., 12/16 in. and 6/16 in., respectively. Thus linear density is found to increase as the length of the fiber decreases and to be highest for the shortest length group, not lowest as observed by Sands et al. The above findings are in close agreement with our earlier findings.

It would, therefore, appear that in normally developed *hirsutum* cottons, the linear density of the fiber generally decreases with the increase of length group. However, in the bulk samples of these cottons, this trend may be modified due to presence of a large quantity of broken immature fibers in the shorter lengths.

Literature Cited

1. Iyengar, R. L. N. and Turner, A. J., *J. Textile Inst.* **21**, T417–440 (1930).
2. Sands, J. E., Louis, G. L., and Tallant, J. D., TEXTILE RESEARCH JOURNAL **30**, 619–620 (1960).
3. Shah, J., TEXTILE RESEARCH JOURNAL **30**, 618 (1960).

R. L. N. IYENGAR

Southern Utilization Research
and Development Division
1100 Robert E. Lee Boulevard
New Orleans 19, Louisiana
October 25, 1960

To the Editor
TEXTILE RESEARCH JOURNAL

Dear Sir:

The Letter to the Editor by Mr. Calkins [2] raises several distinct and provocative questions germane to linear density distribution data published by the authors [3, 6]. First, the precision of segregating cotton fibers by length groups is questioned. Taking Mr. Calkins' suggestion, the authors assembled from many previous arrays sufficient fibers of the same specified length to permit rearraying by standard methods [1a]. The results of rearraying for five selected length groups are shown in Table I. The mean lengths of these rearrays were only about $\frac{1}{32}$ in. longer than the lengths of the original arrays, with at least 60% of the weight being in the specified length groups. Furthermore, over 90% of the weight was concentrated in the specified length group and its adjacent length groups. The consistent increase of about $\frac{1}{32}$ in. may be partially explained by the possible removal of residual crimp during rearraying and by slight stretching as the fibers were placed on velvet boards, which had not been done for the parent arrays. The above data indicate that the errors in linear density determinations resulting from faulty arraying should be relatively small. Errors in determining linear density should be further minimized because with each tuft of about 100 fibers, before microscopic examination and counting, the operator must "Comb carefully to form well-dressed tufts containing fibers of essentially the same length" [1b].

TABLE I. Variability Within Length Groups (Suter-Webb)

	Length group sorted 5/16 in.	9/16 in.	13/16 in.	17/16 in.	21/16 in.
Specified length, in. (midpoint of cell)	0.31	0.56	0.81	1.06	1.31
Mean, in.	0.33	0.59	0.84	1.10	1.33
Coefficient of variation, %	27	18	15	9	9
Weight in specified cell, %	72	64	61	63	67
Wt. in next higher cell, %	16	23	26	32	22
Wt. in next lower cell, %	6	6	4	2	6
Total wt. of specified and adjacent cells, %	94	93	91	97	95
Remaining wt. above next higher cell, %	4	4	5	2	3
Remaining wt. below next lower cell, %	2	3	4	1	2

Second, it is implied that linear density does not vary with length group within a cotton. It is true, as Mr. Calkins points out, that isolated instances can be found among the 42 cottons [6] to support this view; however, a statistical analysis should demonstrate any dominant trend. Table II shows the algebraic average of differences in linear density between pairs of length groups and significant differences between length group means computed on the data reported by the authors [6]. The data indicate that all differences were either significant or highly significant except for three of the ten comparisons. The three nonsignificant differences were between the extremes, 5–21/16 in. and 7–19/16 in., and between the pair near the peak of the curve, the 13–17/16 in. comparison. This would seem to confirm the generally curvilinear relationship between length group and linear density mentioned by the authors [3]. This relationship was recognized by Morlier et al. [5], who, using a cut fiber technique, reported "weight fineness of the center section varied with length and with variety; in general, it increased with fiber length to a maximum value at the length slightly shorter than the modal-length group, and then decreased."

Third, Mr. Calkins states that usually the precision of individual linear density values is about 1 μg./in. The mean absolute difference between paired observations for each length group of each of the first 35 cottons (for which pairs of observations were available) reported [6] and the standard deviations of these differences are presented in Table III. These data show that the average difference between pairs of observations is far less than 1 μg./in. for all length groups. In view of the standard deviations found for these data, the chances are less than 1 in 100 that operators would diverge by 1 μg./in. even in the least accurate determination, the 5/16-in. length group. The increased precision with increasing length, as shown by the decreases in standard deviations, is to be expected, since the relative error by the operator in measuring each length would be expected to decrease with increasing length. With reference to the accuracy of the more useful over-all average linear density of a cotton, it should be realized that this average is a weighted average which necessarily gives greater importance to the longer groups which normally contain the greater proportion by weight of the fibers in the samples. Thus, the over-all average linear density is influenced to a large degree by the operator determinations in length groups which inherently provide for obtaining the greater accuracy. Furthermore, useful information on the linear density vs. length relationship within a cotton can be obtained through use of the standard ASTM method for measuring linear density [1b].

TABLE II. Mean Algebraic Differences in Linear Density Among Selected Length Groups for 42 Domestic and Foreign Cottons

Length group	Length group			
	5/16 in.	9/16 in.	13/16 in.	17/16 in.
	Mean differences in linear density, μg./in.*			
9/16 in.	0.42†	—	—	—
13/16 in.	0.68†	0.26†	—	—
17/16 in.	0.54†	0.12	−0.14	—
21/16 in.	0.13	−0.17‡	−0.44‡	−0.48†

* Mean differences based on the shorter length group subtracted from the longer group.

† Differences between length groups are highly significant at the 99% probability level.

‡ Differences between length groups are significant at the 95% probability level.

TABLE III. Mean Absolute Difference Between Pairs of Linear Density Observations for 35 Cottons

	Length group				
	5/16 in.	9/16 in.	13/16 in.	17/16 in.	21/16 in.
Mean absolute difference between pairs of observations, μg./in.	0.24	0.18	0.17	0.11	0.09
Standard deviation of differences, μg./in.	0.32	0.24	0.21	0.15	0.12

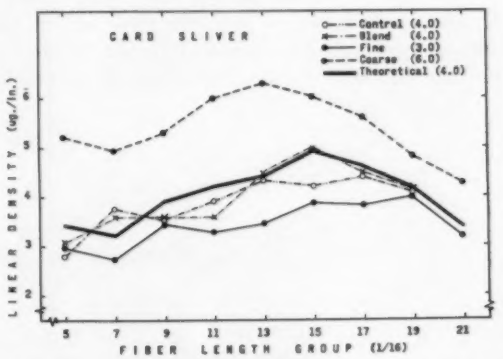

Fig. 1. Fiber linear density distributions of the control, blended, theoretical, fine, and coarse cottons by fiber length groups.

Mr. Calkins also implies that the linear density of the blend shown in Figure 1 of the original article [3] differed from a theoretical blend based on 60:40 blend of very fine- and very coarse-fibered cottons. Such an observation did not consider that there might be differences in the weight–length distributions. Actually, the low linear density cotton contained more short fibers than the high linear density cotton. Therefore, when an over-all 60:40 blend was made, the proportions varied from this ratio in each length group. Figure 1 shows the relationship between actual and computed theoretical blends for card sliver based on the actual weights in the corresponding length groups of the high and low linear density cottons. Agreement is very good, particularly for the 13/16-in. and longer length groups. The authors regret that the original paper [3] did not include both figures, one for card sliver and one for picker lap, since the linear density data for card sliver are more representative due to the greater degree of cotton fiber blending and homogeneity.

The authors also regret the discrepancy pointed out by Mr. Calkins in the picker lap graph [3] for the 7/16-in. length group and can only offer "experimental error" as the source. However, by combining the 3.0 and 6.0 Micronaire Reading cottons in a 60:40 proportion and considering the length frequency distributions for the respective parent cottons a theoretical value of 3.39 μg./in. is arrived at in contrast to the experimentally determined 2.65 μg./in. This difference of 0.74 μg./in. was the largest encountered between the theoretical and experimental values.

Interjecting a philosophical note, the authors wonder whether the contradictory findings of recent linear density determinations with those in the past, such as reported by Iyengar and Turner [4] and by Calkins [2] are due to differences in technique, variety, or to real changes over the decades in the linear density–length distribution of cotton.

In spite of Dr. Iyengar's letter contradicting the general length–linear density relationship reported by Sands et al. [6], the authors, using irrigated Acala cotton, hand picked and hand ginned, found the following length–linear density (μg./in.)–maturity (%) values: 5/16—4.08–73; 9/16—3.98–78; 13/16—4.95–93; 17/16—4.58–94; 21/16—3.86–92; 23/16—3.50–90. Hence for this sample Iyengar's postulate of fiber breakage is inapplicable and the relationship found still agrees with authors' original findings.

Acknowledgments

The authors express appreciation to Miss D. C. Legendre for performing the special arrays and to Mr. H. W. Little, Statistician, for assistance in interpretation of the linear density values.

Literature Cited

1. Am. Soc. Testing Materials, Committee D-13, ASTM Standards on Textile Materials, Philadelphia, 1959. (1a) ASTM Designation D1440-55; (1b) ASTM Designation D1442-54.
2. Calkins, E. W. S., TEXTILE RESEARCH JOURNAL **31**, 176 (1961).
3. Fiori, L. A., Louis, G. L., and Sands, J. E., TEXTILE RESEARCH JOURNAL **29**, 706–716 (1959).
4. Iyengar, R. L. N. and Turner, A. J., *J. Textile Inst.* **21**, T417–440 (1930).
5. Morlier, O. W., Orr, R. S., and Grant, J. N., TEXTILE RESEARCH JOURNAL **21**, 6–13 (1951).
6. Sands, J. E., Louis, G. L., and Tallant, J. D., TEXTILE RESEARCH JOURNAL **30**, 619–620 (1960).

LOUIS A. FIORI
JACK E. SANDS
GAIN L. LOUIS
JOHN D. TALLANT

Acid Hydrolysis of Dimethylol Urea Polymerized in Cotton

The Ahmedabad Textile Industry's
Research Association
Ahmedabad, India
October 4, 1960

To the Editor
TEXTILE RESEARCH JOURNAL

Dear Sir:

The activation energy for the hydrolysis of dimethylol urea (DMU) in solution at different pH has been reported by Landqvist [2] and deJong and deJonge [1]. Steele [4] has studied the acid hydrolysis of DMU polymerized in a cotton fabric in the presence of ammonium chloride catalyst and has obtained a value of activation energy ranging from 20.4 to 21.2 kcal./mole. According to him, this represents the hydrolysis of the N—CH_2O—Cell bond at one end of the cross link between the DMU polymer and cellulose, the other end being then hydrolyzed rapidly.

Removal of the "resin" from the fabric depends not only on the hydrolysis of the terminal N—CH_2O—Cell bonds but also of the N—CH_2—N bonds in the DMU polymer. It has been shown that the former bond is hydrolyzed faster than the latter during acid hydrolysis of dimethylol ethylene urea [3] and alkaline hydrolysis of DMU [5] applied to cotton under usual conditions. Data are presented here of the acid hydrolysis of DMU (polymerized in cotton) under sufficiently mild conditions to distinguish between the rupture of the two types of bonds. Steele did not observe this distinction, probably because of the more severe conditions of hydrolysis used by him.

Fabric samples were treated with a dimethylol urea solution and $MgCl_2 \cdot 6H_2O$ catalyst, 30% on the weight of the resin. Resin concentration in the bath was adjusted to give approximately 7% add-on on the fabric. After padding, the samples were dried at 110° C. for 8 min., cured at 150° C. for 5 min., and washed with soap and soda ash. The samples were then hydrolyzed under reflux with a mixture

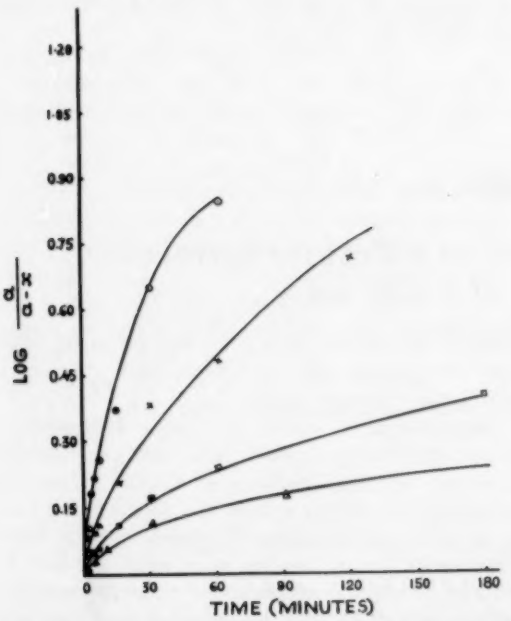

Fig. 1. Rate of nitrogen loss vs. time of hydrolysis of DMU-treated cotton with 0.1 *M* acetic acid + 0.1 *M* sodium acetate at 94° C. (○), 84° C. (×), 74° C. (□), and 64° C. (△).

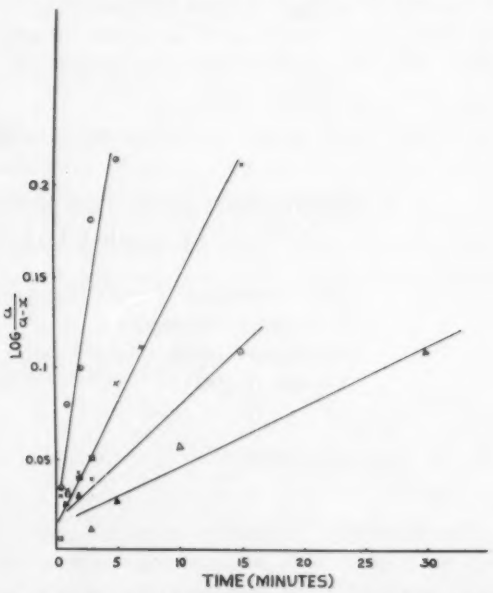

Fig. 2. Rate of hydrolysis of N-CH_2OR bonds in DMU-treated cotton at 94° C. (○), 84° C. (×), 74° C. (□), and 64° C. (△).

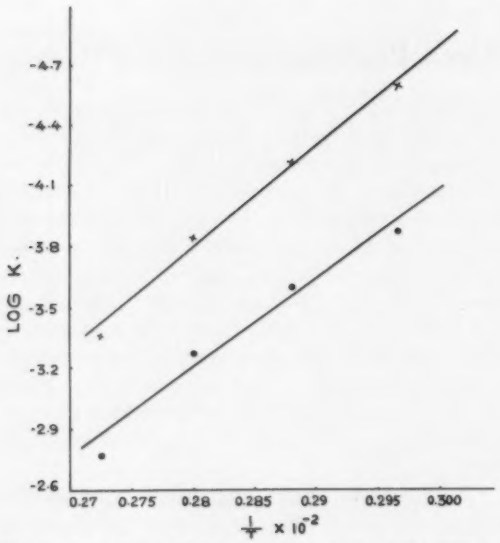

Fig. 3. Log K vs. $1/T$ for the hydrolysis of N—CH_2O—Cell and N—CH_2—N bonds.

of 0.1 M acetic acid and 0.1 M sodium acetate solutions (pH 4.7) at 94°, 84°, 74°, and 64° C. for various lengths of time. Percent nitrogen was estimated on these hydrolyzed samples.

The data of residual nitrogen are plotted against time of hydrolysis in Figure 1 as a first order reaction. The curves show the typical pattern of a fast and a slow reaction occurring simultaneously. The initial portion of Figure 1 has been replotted in Figure 2, which also shows straight lines fitted statistically to the experimental points. Similarly, straight lines could be fitted to the latter portions of Figure 1 also, though these have not been shown here. The rate constants for the faster hydrolysis of N—CH_2O—Cell are 16.62, 5.18, 2.46, and 1.26×10^{-4} sec.$^{-1}$ respectively at 94°, 84°, 74°, and 64° C., whereas for the slower hydrolysis of N—CH_2—N they are 4.31, 1.42, 0.58, and 0.22×10^{-4} sec.$^{-1}$ at the four temperatures.

In Figure 3, log K has been plotted against $1/T$ according to the Arrhenius equation to give activation energies of 20.3 and 23.6 kcal./mole respectively for the hydrolysis of N—CH_2O—Cell and N—CH_2—N bonds.

Literature Cited

1. deJong, J. I. and deJonge, J., *Rec. Trav. Chim.* **71**, 661 (1952).
2. Landqvist, N., *Acta Chem. Scand.* **10**, 244 (1956).
3. Reid, J. D., Reinhardt, R. M., and Kullman, R. M. H., TEXTILE RESEARCH JOURNAL **28**, 242 (1958).
4. Steele, R., private communication.
5. Steele, R. and Giddings, L. E., *Ind. Eng. Chem.* **48**, 110 (1956).

K. C. EAPEN
J. R. MODI
P. C. MEHTA

Cuprammonium Insolubility as a Test for Covalent Cross-Linking of Cellulose

The Ahmedabad Textile Industry's Research Association
Ahmedabad, India
October 4, 1960

To the Editor
TEXTILE RESEARCH JOURNAL

Dear Sir:

The insolubility in cuprammonium hydroxide of cellulose treated with creaseproofing resins under certain conditions has been generally regarded as evidence for the cross-linking of cellulose with the resin. In an earlier paper [3] we had given some data to question the validity of this test in the case of DMU-treated cellulose. More data in support of this are presented here.

Recent work has shown that cotton dyed with H brand Procion dyes, which have only one reactive chlorine, becomes insoluble in CuAm at certain concentrations of the dye in the fiber [5]. Similarly, when cotton cellulose is reacted with acrylonitrile under certain conditions, a graft polymer is formed which is insoluble in the usual solvents for either reactant [1, 2]. No cross-linking is possible in either of these treatments. Thus, insolubility in CuAm is not invariably the result of a cross-linking of cellulose.

TABLE I. Nitrogen Content and CuAm Insolubility of DMU-Treated Fabrics with Different Catalysts

No.	Treatment*	% Nigrogen content	% CuAm insolubility
1	DMU alone—dried, cured, and washed	1.63	49.7
2	DMU + tartaric acid—dried	1.86	96.6
3	DMU + tartaric acid—dried and washed	1.82	97.9
4	DMU + tartaric acid—dried, cured, and washed	1.75	100.5
5	DMU + $MgCl_2$—dried	1.85	Swelled (soluble when stirred for 48 hr.)
6	DMU + $MgCl_2$—dried and washed	1.36	Soluble
7	DMU + $MgCl_2$—dried, cured, and washed	1.83	101.2
8	DMU + $NaHCO_3$—dried, cured, and washed	1.69	94.2

* Drying—110° C., 8 min.; curing—150° C., 5 min.; washing—with a neutral detergent.

Table I gives values of CuAm insolubility of cotton treated with DMU under various conditions. Details of the test method have been described elsewhere; washing of the insoluble residue with acetic acid was omitted here [3]. It can be seen that, even after treatment with DMU without catalyst or with $NaHCO_3$ catalyst at 150° C., and with tartaric acid catalyst at 110° C., about 50–95% of the treated cellulose remains insoluble in CuAm. It is generally accepted that cross-linking of cellulose is unlikely to occur under such conditions of treatment.

The use of CuAm insolubility as an index of cross-linking is particularly fallacious in the case of DMU treatments. Treatment with 0.5 *N* NaOH at 20° C. has been shown to hydrolyze off any cross links formed between the $—N\cdot CH_2OH$ of the resin and —OH of cellulose. In fact, this method has been used to estimate formaldehyde present as $—N\cdot CH_2OR$. Similar hydrolysis can conceivably occur during treatment with the highly alkaline CuAm reagent as well. In the case of DMU treatments, therefore, insolubility of the treated cellulose in CuAm cannot be ascribed to presence of cross links which would have been already ruptured during the test.

To confirm that such a hydrolysis does, in fact, occur, nitrogen and formaldehyde were estimated in the CuAm-insoluble portions of some of the samples. The data given in Table II show that there is a large decrease in both nitrogen and formaldehyde content of the fabric after treatment with CuAm, indicating extensive hydrolysis and partial removal of the resin.

For further confirmation, these five fabrics were hydrolyzed in 0.5 *N* NaOH at 20° C. for 48 hr. and their insolubility in CuAm determined before and after the alkaline hydrolysis. These data show conclusively that, even after the hydrolysis by alkali of any cross links that may have been present initially in the DMU-treated fabrics, their insolubility in CuAm is hardly affected. In the light of these results, conclusions about the cross-linking of DMU-

TABLE II. Nitrogen and Formaldehyde Contents of DMU-Treated Samples with Different Catalysts Before and After CuAm Test

Treatment no.*	Initial N on fabric, %	N content of CuAm-insol. portion, %	N loss, %	Initial HCHO on fabric, %	HCHO content of CuAm-insol. portion, %	Loss of HCHO, %
1	1.87	—	—	2.596	0.636	75.5
2	1.86	1.25	32.8	2.92	1.59	45.2
4	1.75	1.38	21.1	2.68	1.83	31.9
7	1.83	1.25	31.5	2.989	2.00	32.7
8	1.69	1.02	31.6	2.557	1.489	41.7

* Refer to Table I.

TABLE III. CuAm Insolubility Before and After Alkaline Hydrolysis

Treatment No.†	% CuAm insolubility	
	Before alkaline hydrolysis	After alkaline hydrolysis
1	49.7	60.4
		28.4*
		36.2*
2	96.6	91.6
4	100.5	101.4
7	101.2	102.2
8	94.1	93.6
		85.7*

* Alkaline hydrolysis was carried out for six days.
† Refer to Table I.

treated celluloses based on their insolubility in CuAm appear very questionable.

The mechanism of solution of cellulose in CuAm involves as an intermediate step the formation of a coordination compound between the $Cu(NH_3)_4$ complex and the four hydroxyls in the 2 and 3 positions of adjacent cellulose chains [4]. Nonavailability of such hydroxyls in cellulose due to cross-linking with the resin, presence of methylene cross links, strong H-bond formation, or mechanical hindrance may prevent the formation of the intermediate coordination compound and decrease solubility of the cellulose in CuAm. It has already been shown [3] that samples treated with DMU and cured in the presence of acid (or latent acid) catalysts are not fully soluble in CuAm even after the resin is completely removed by hydrolysis. These hydrolyzed samples also show a small amount of formaldehyde, probably present as methylene cross links and responsible for insolubilizing the cellulose.

It was expected that measures such as moisture regain and water imbibition for the accessibility of the DMU-treated celluloses may show a relation with the CuAm insolubility of the latter. No such relation was found between CuAm insolubility and moisture regain, while water imbibition data, though following the expected pattern more closely, showed some marked discrepancies. The possibility of H-bond formation of water with the NH groups of the DMU polymer may be a source of error.

Literature Cited

1. Chitale, A. G., private communication.
2. Geacintov, N., Stannet, V., Abrahamson, E. W., and Hermans, J. J., *J. Appl. Polymer Sci.* **3**, 54 (1960).
3. Mehta, P. C. and Mehta, R. D., TEXTILE RESEARCH JOURNAL **30**, 524 (1960).
4. Ott, E. and Spurlin, H., "Cellulose and Cellulose Derivatives Part II," New York, Interscience Publishers, 878 (1954).
5. Vickerstaff, T., *Hexagon Digest* **27**, 6 (December 1958).

R. D. MEHTA
P. C. MEHTA